Cross-Calibration Comparisons using Galaxy Cluster Emission from *NuSTAR*, *Chandra*, *XMM-Newton*, *Suzaku*, and *XRISM*

X-RAY ASTROPHYSICS
DEPARTMENT OF PHYSICS & ASTRONOMY

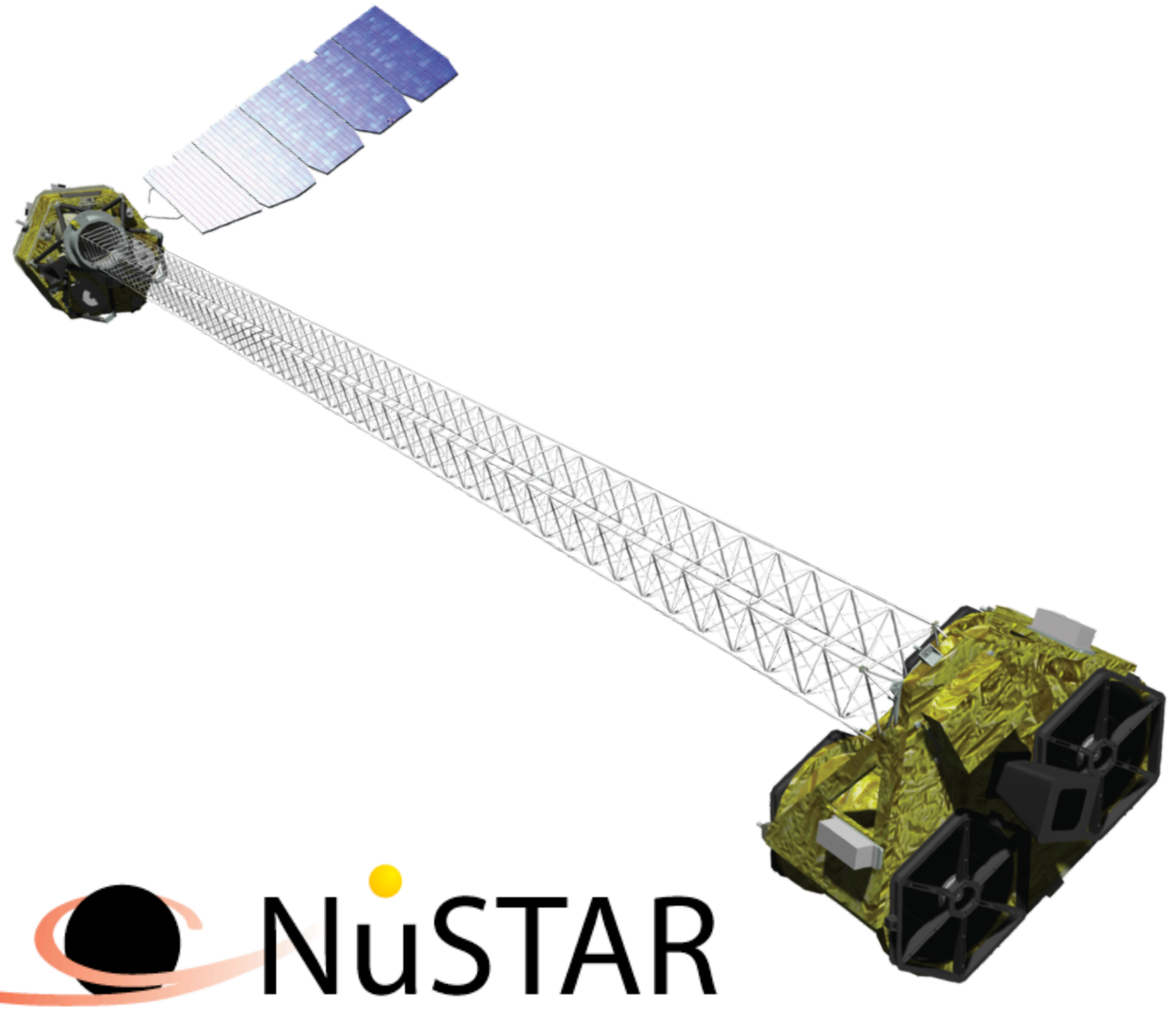

NuSTAR

CHANDRA X-RAY OBSERVATORY

Daniel R. Wik
(University of Utah)

Based mostly on work from
Cicely Potter
(Utah)
and
Fiona Lopez
(Texas A&M)

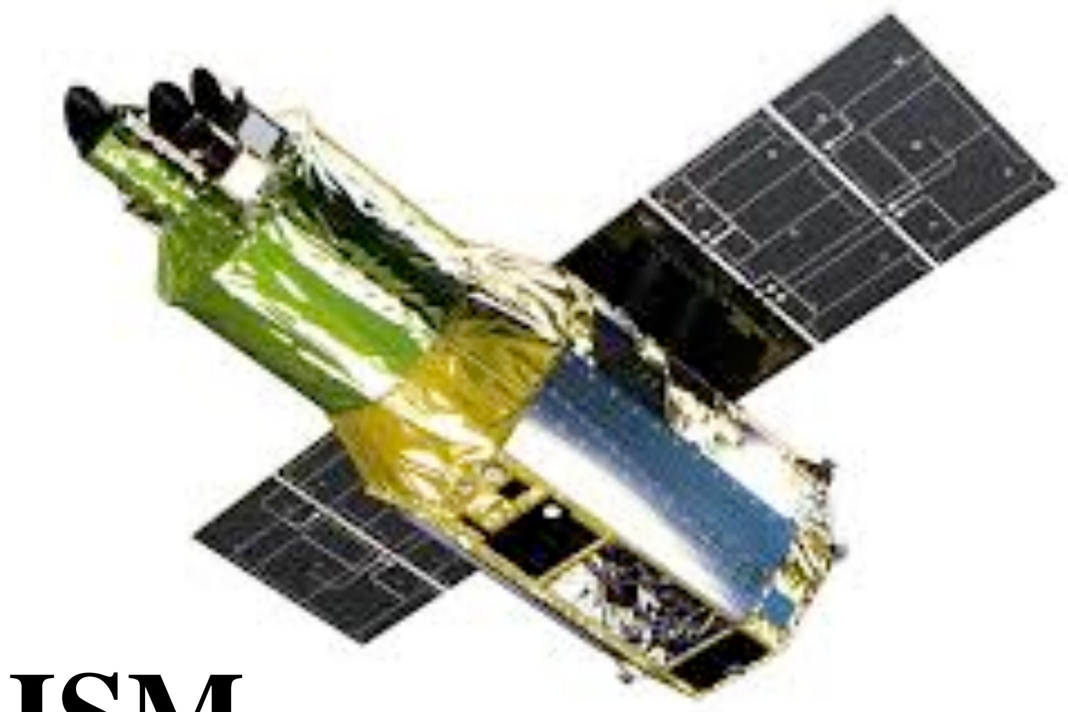

XRISM

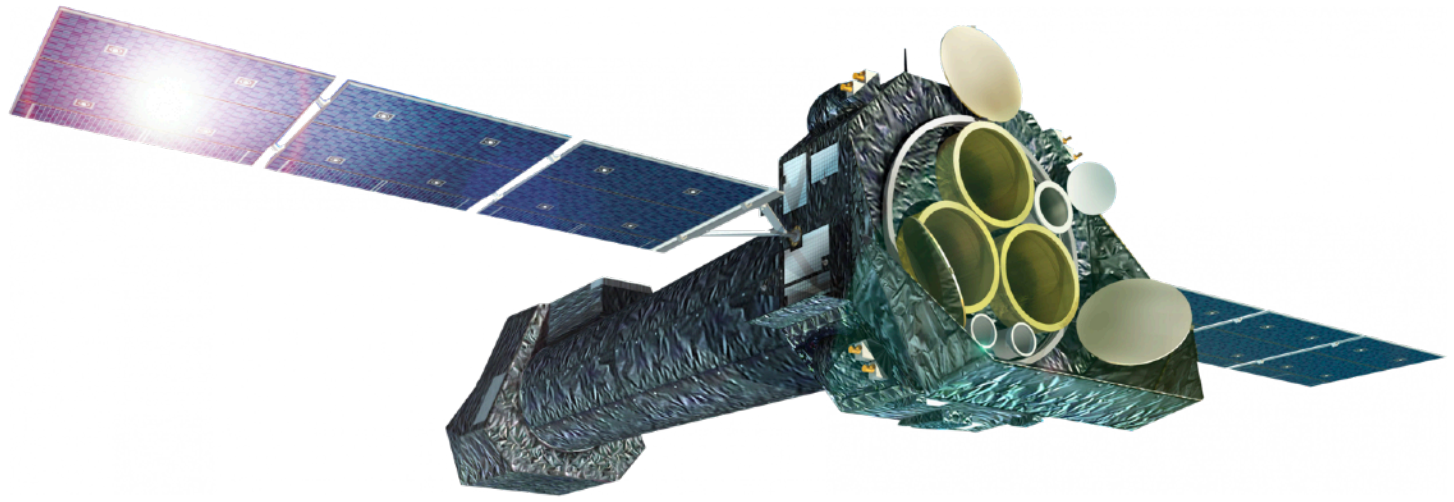

XMM-NEWTON

Galaxy Clusters: Temperature Discrepancy

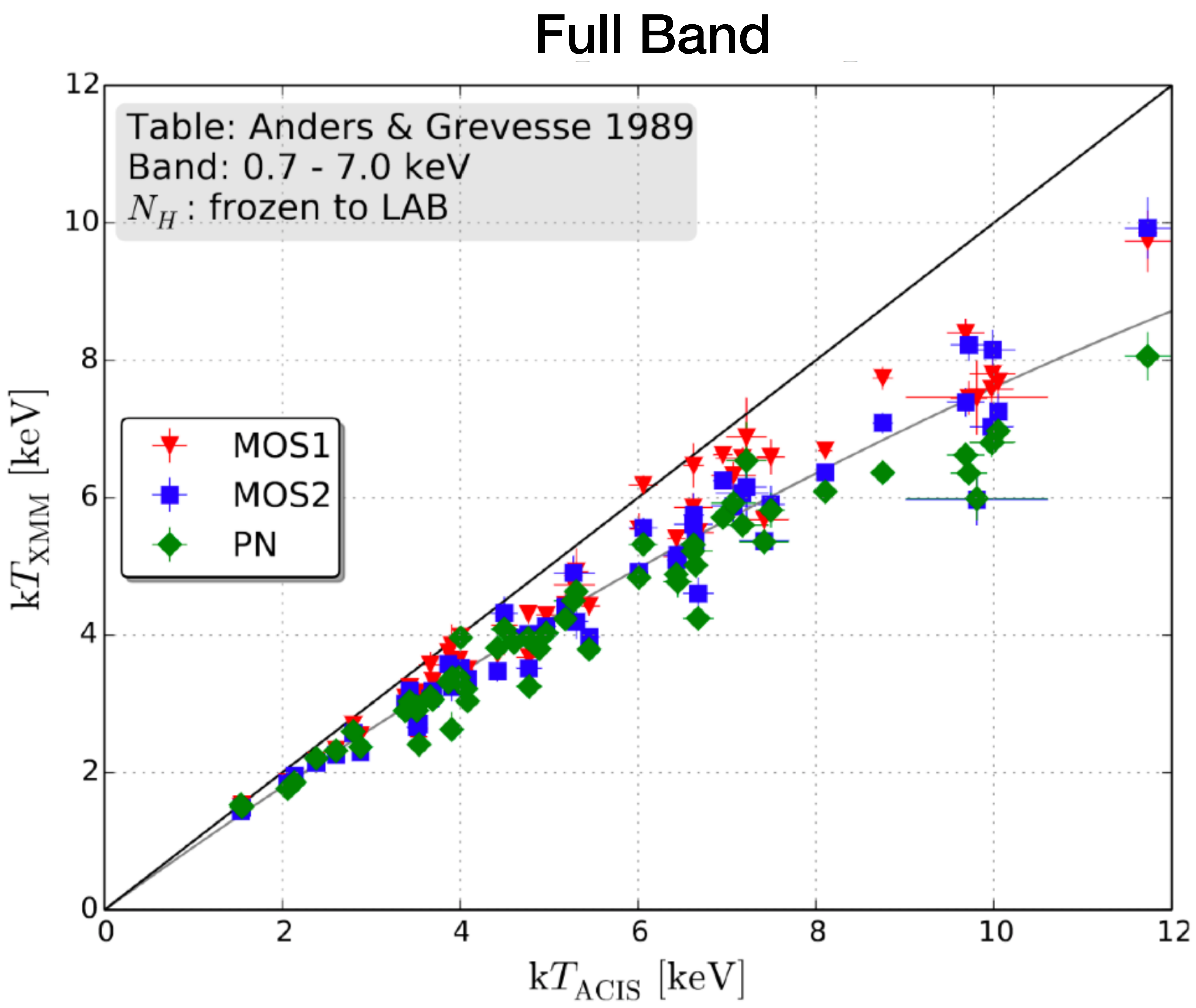

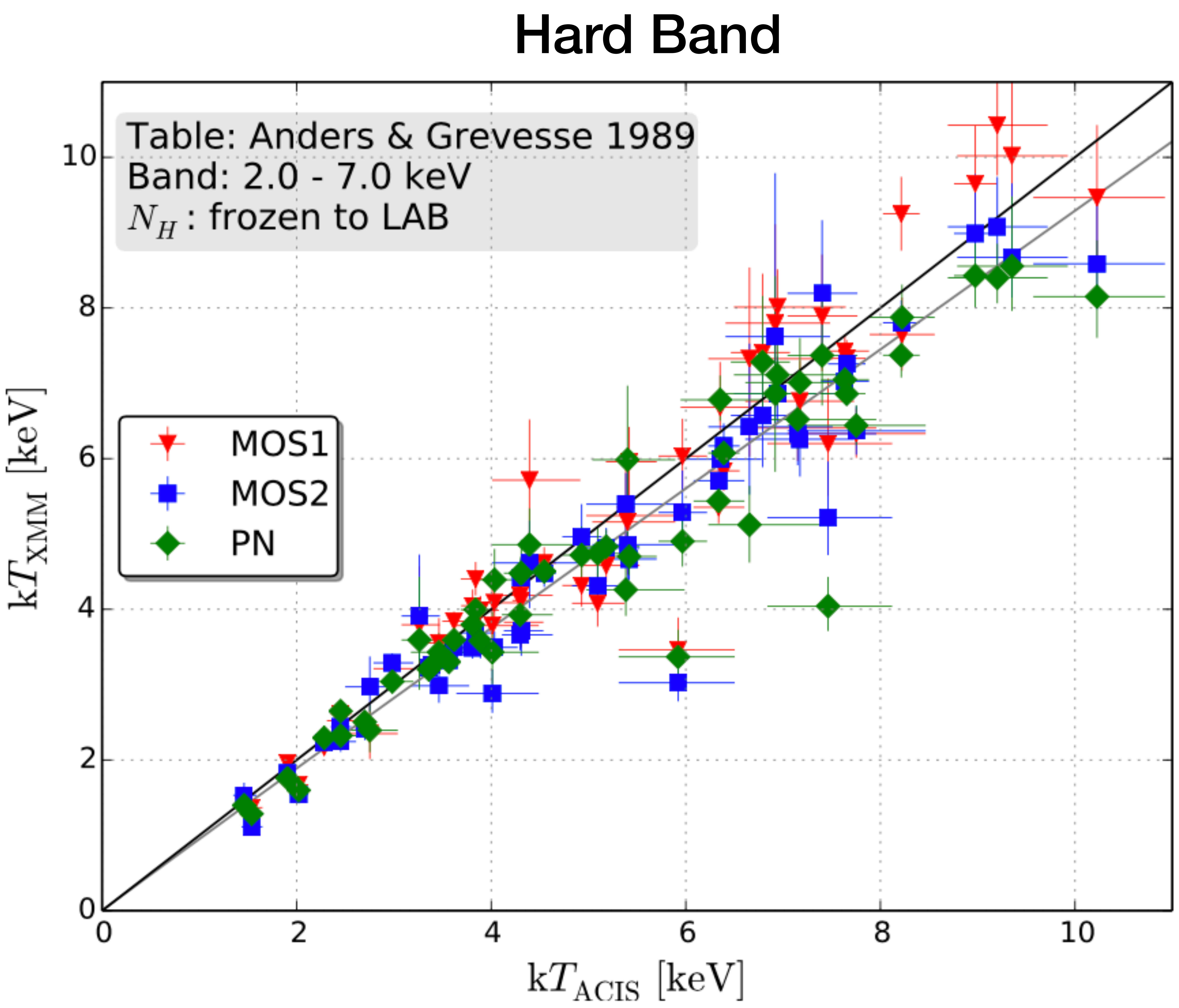

Schellenberger+ 2015

Crucial for Cluster Cosmology

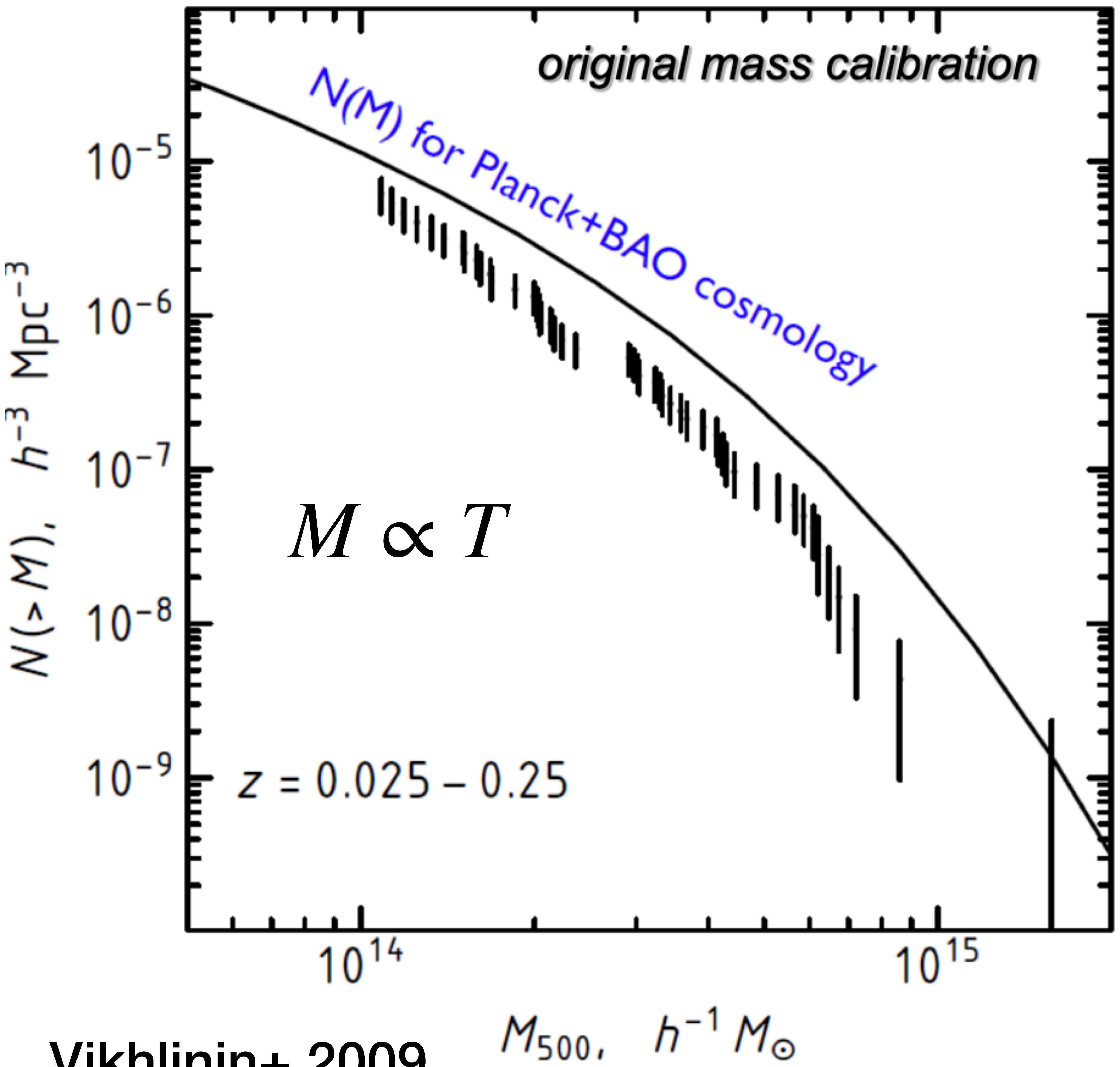

Vikhlinin+ 2009

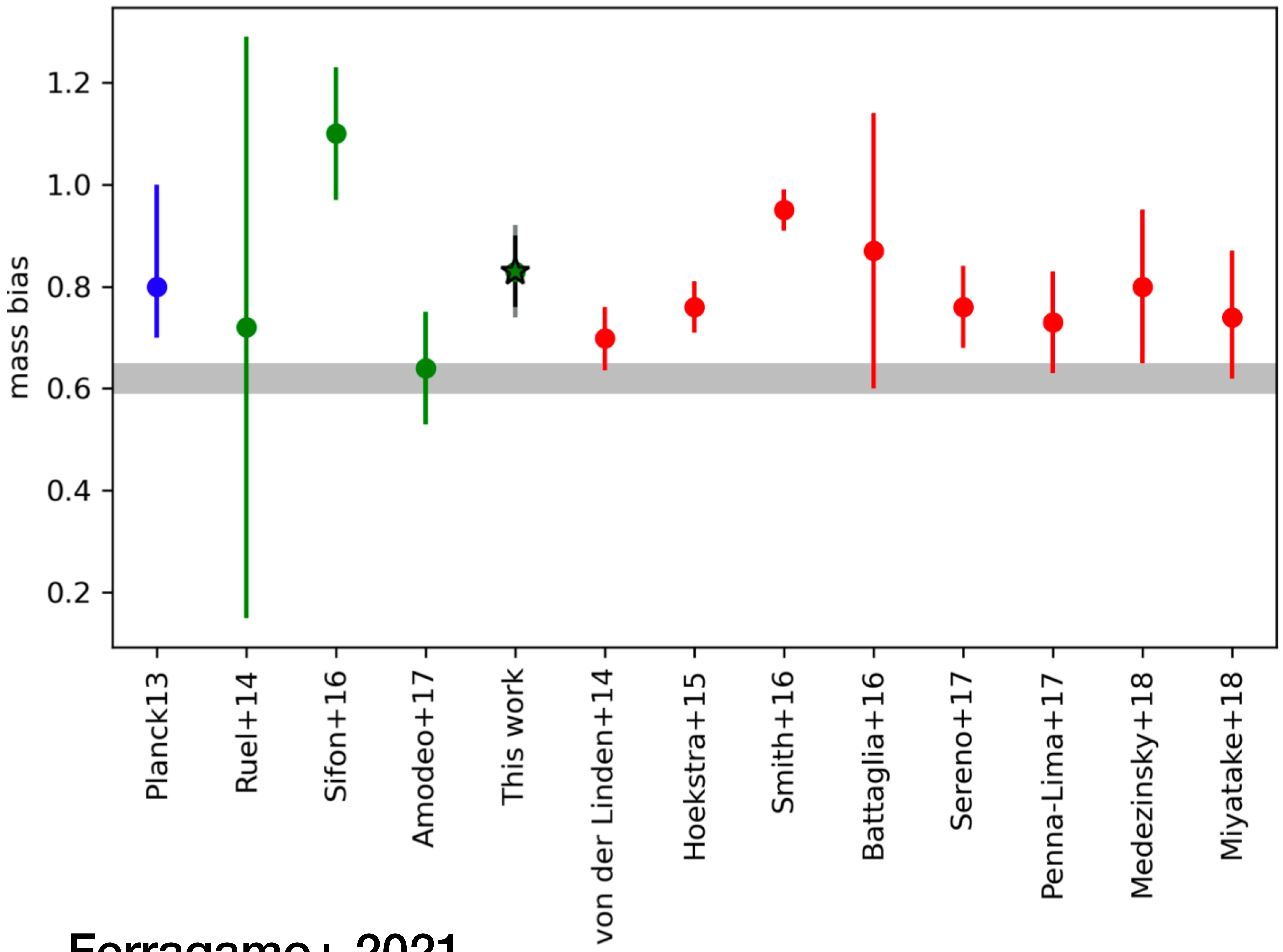

Ferragamo+ 2021

NuSTAR's Advantages

- Discrepancy worst at high *kT*s
- At low *kT*s, *NuSTAR* can make precise measurements
  - Exponential turnover stronger
  - But emission fainter
- Galactic foreground absorption (often) negligible
- Background low and stable
- Unresolved lines have less impact on the continuum (below bandpass)
- In-orbit verification of effective area (Madsen+ 22)

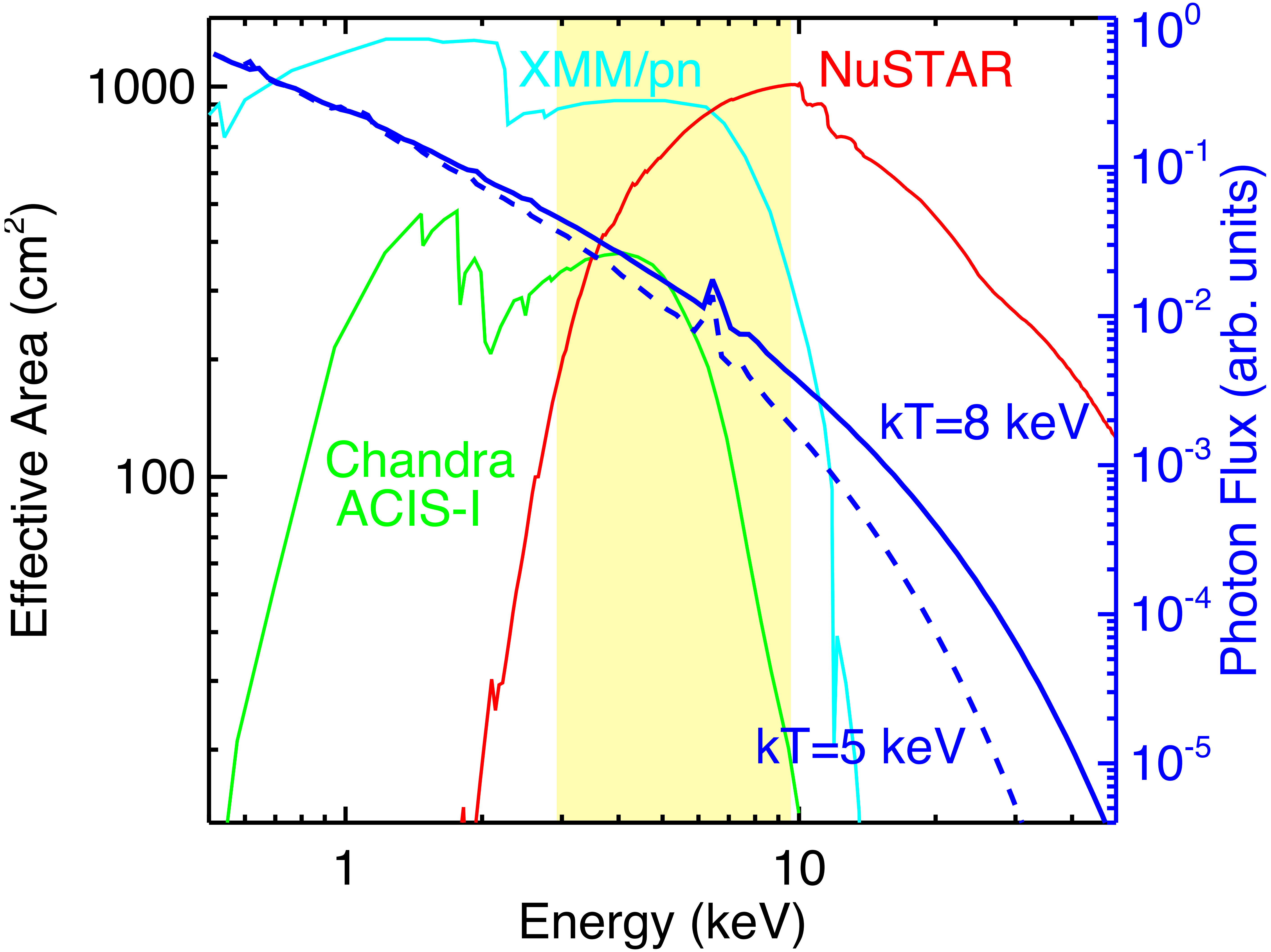

NuSTAR's Disadvantages

NuCrossARF

- Large PSF (~1' HPD)
    - Fit spectra with cross-ARFs
    - Mitigates crosstalk but precision lost
- Hard-to-model effects
    - Scattered light (no pre-collimators)
    - Stray light (open optical path)
    - Mostly rare/avoidable
- Low spectral resolution

Systematic uncertainty of point source reconstruction is 3.4% (Creech+ 2024)

Intrinsic Emission | Scattered Emission

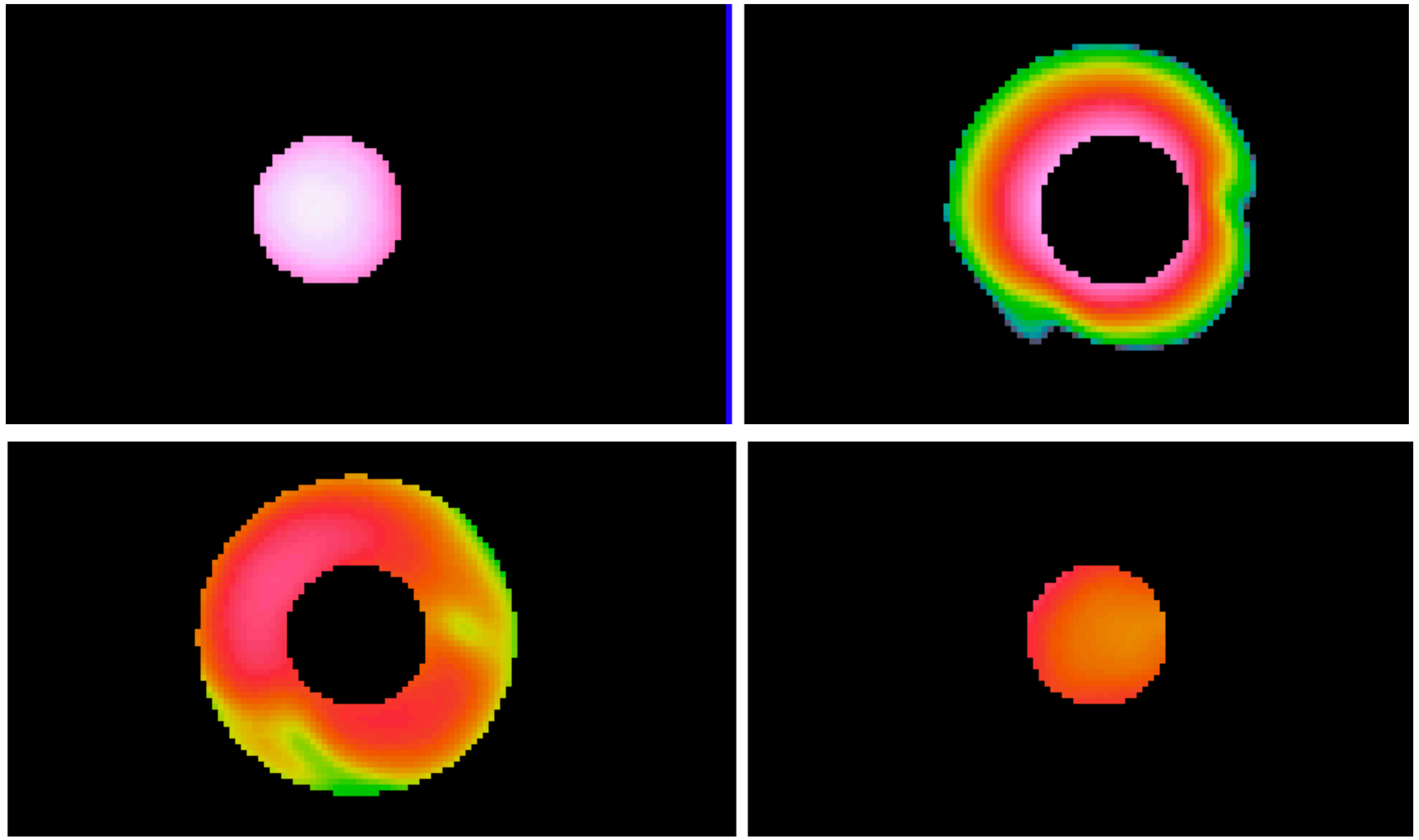

Global *kT* Measurements (*Chandra* vs. *NuSTAR*)

Wallbank+ 22

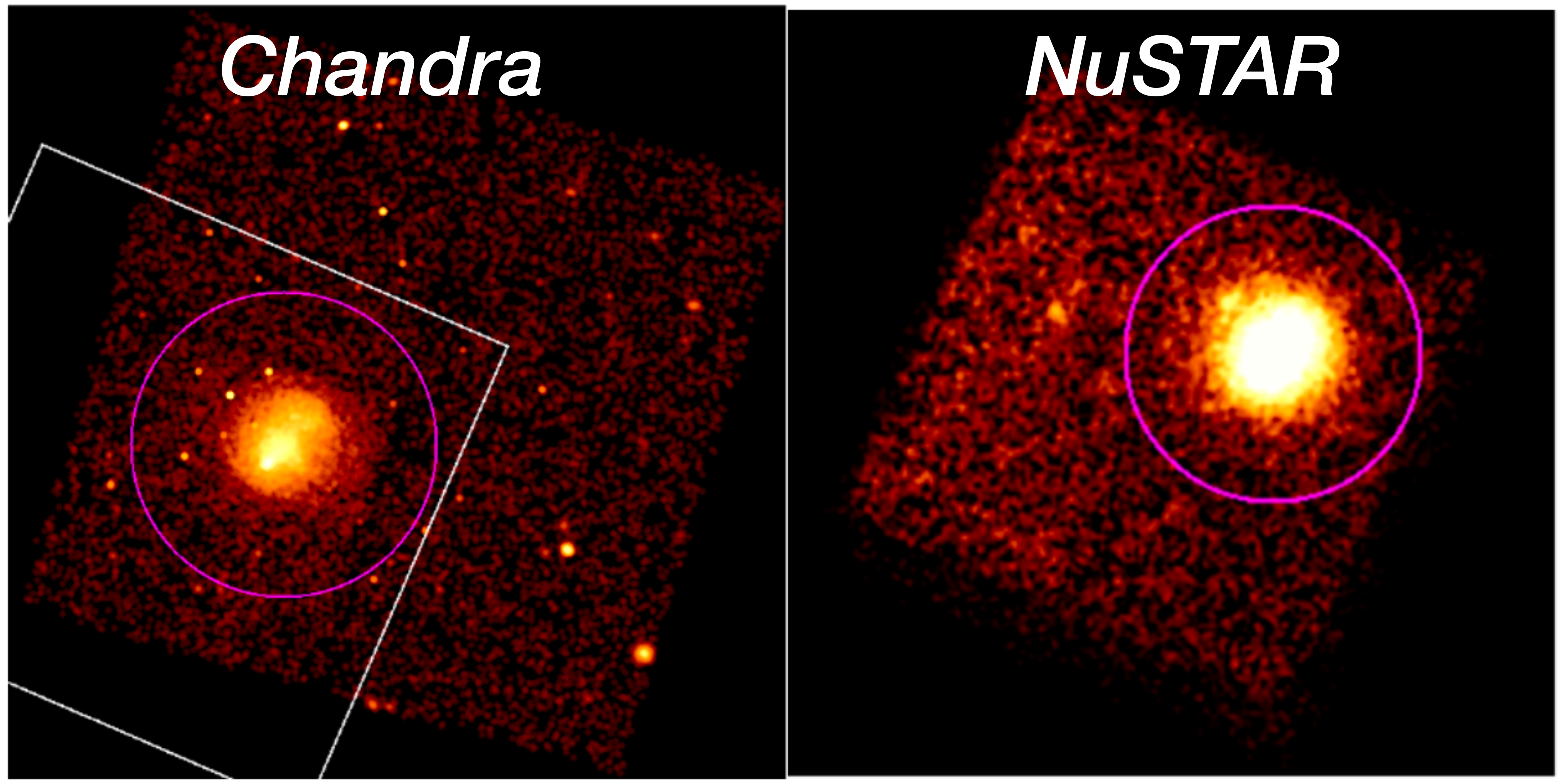

A2146

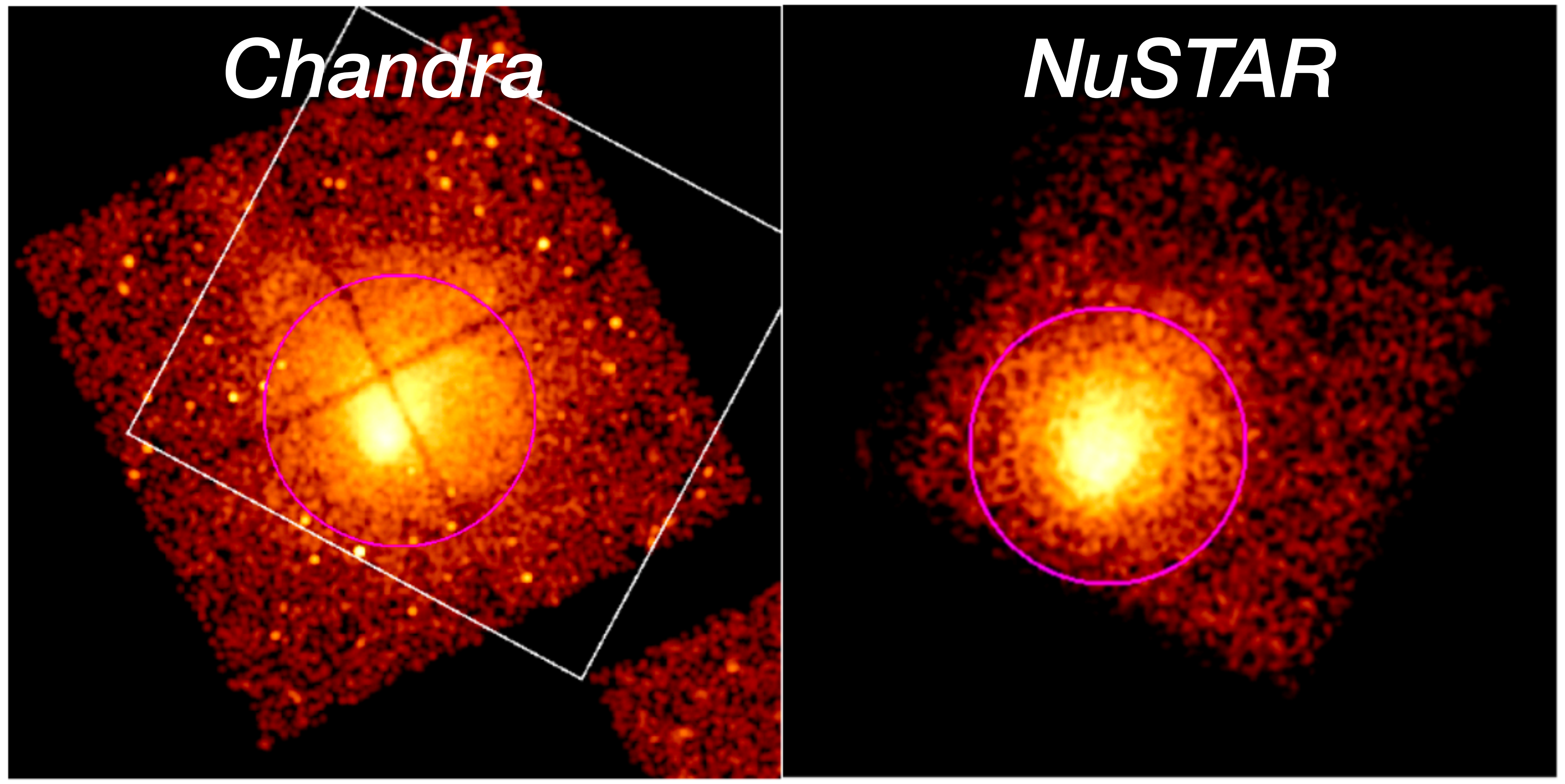

A665

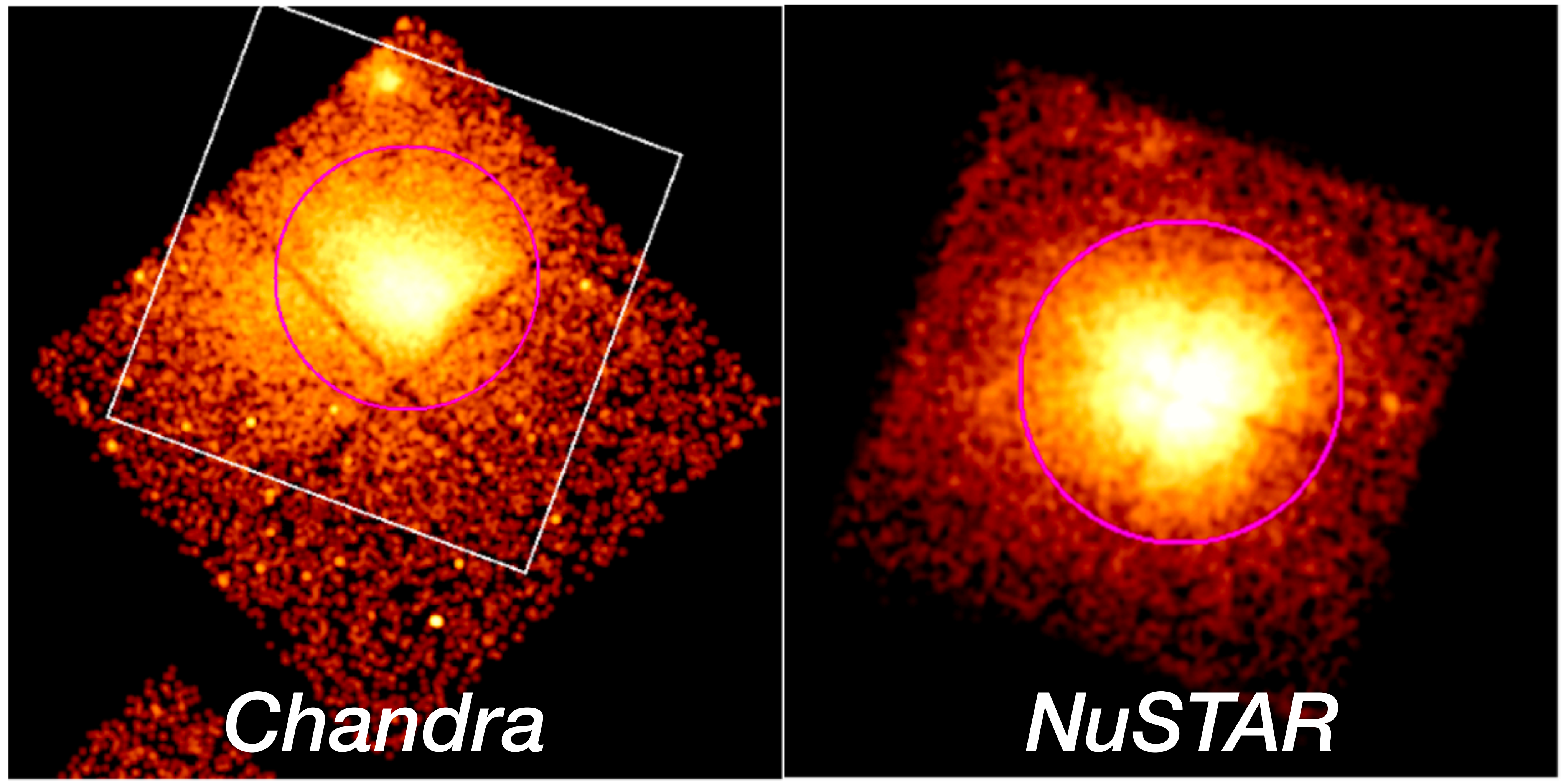

A2163

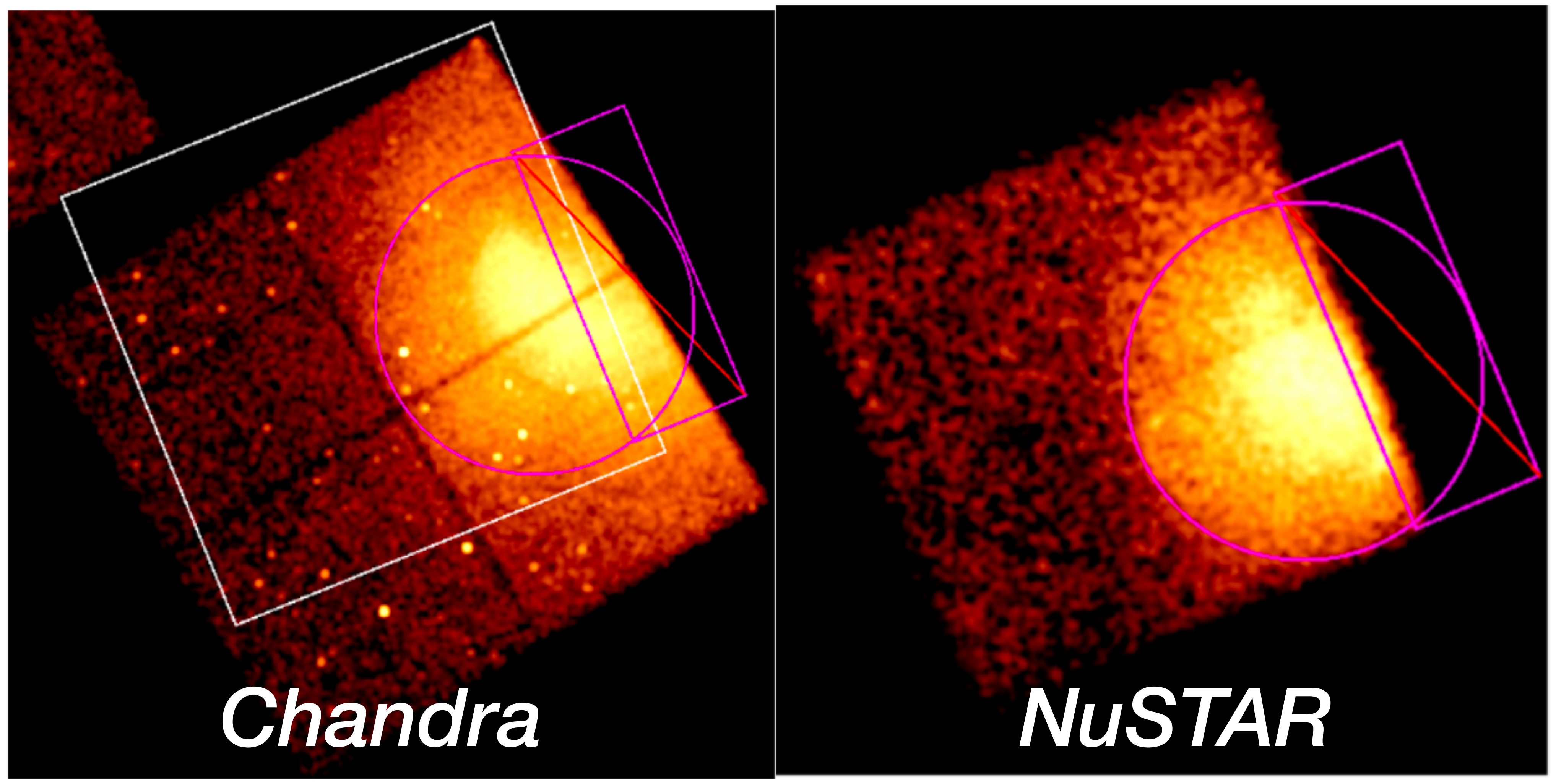

A754

Global *kT* Measurements (*Chandra* vs. *NuSTAR*)

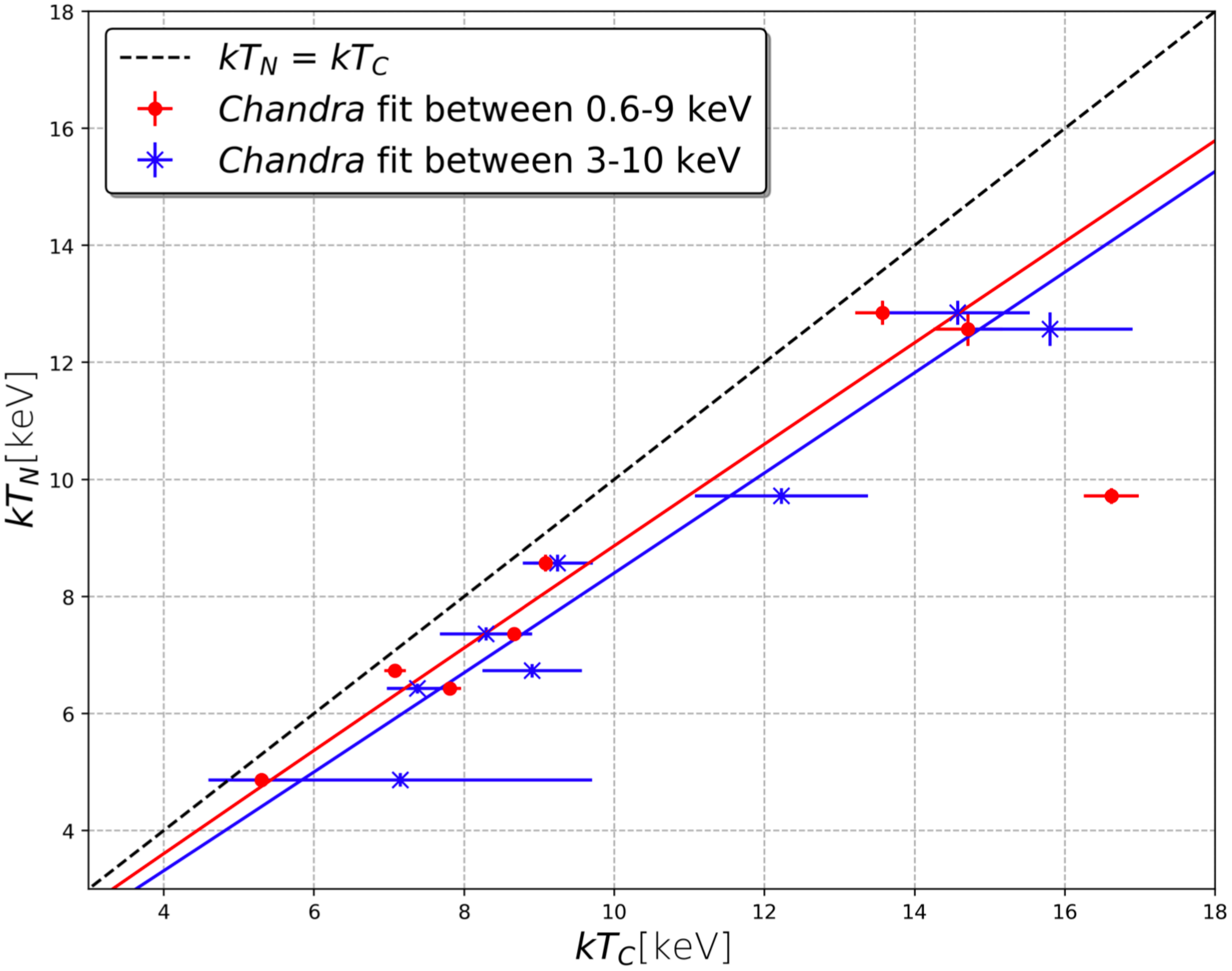

Cluster Name	$kT_{C,(0.6-9)}$ keV	kT_C keV	kT_N keV
Abell 2146	7.08 ± 0.14	8.9 ± 0.66	6.72 ± 0.11
Abell 2163	$16.36 \pm 0.70^{\dagger}$	12.23 ± 1.15	9.72 ± 0.13
Abell 2256	7.81 ± 0.15	7.38 ± 0.41	6.43 ± 0.085
Abell 523	5.30 ± 0.36	7.15 ± 2.55	4.87 ± 0.12
Abell 665	8.66 ± 0.23	8.29 ± 0.62	7.36 ± 0.11
Abell 754	9.09 ± 0.17	9.25 ± 0.47	8.57 ± 0.14
1E 0657-56	13.57 ± 0.36	14.57 ± 0.96	12.85 ± 0.20
RX J1347.5-1145	14.71 ± 0.46	15.80 ± 1.09	12.57 ± 0.29

For a *Chandra kT* of 10 keV, the *NuSTAR kT* is 11% or 16% lower

Physically, *NuSTAR* should be biased to *higher kT*s —> must be due to differences in calibration

Wallbank+ 22

Global *kT* Measurements (*Chandra* vs. *NuSTAR*)

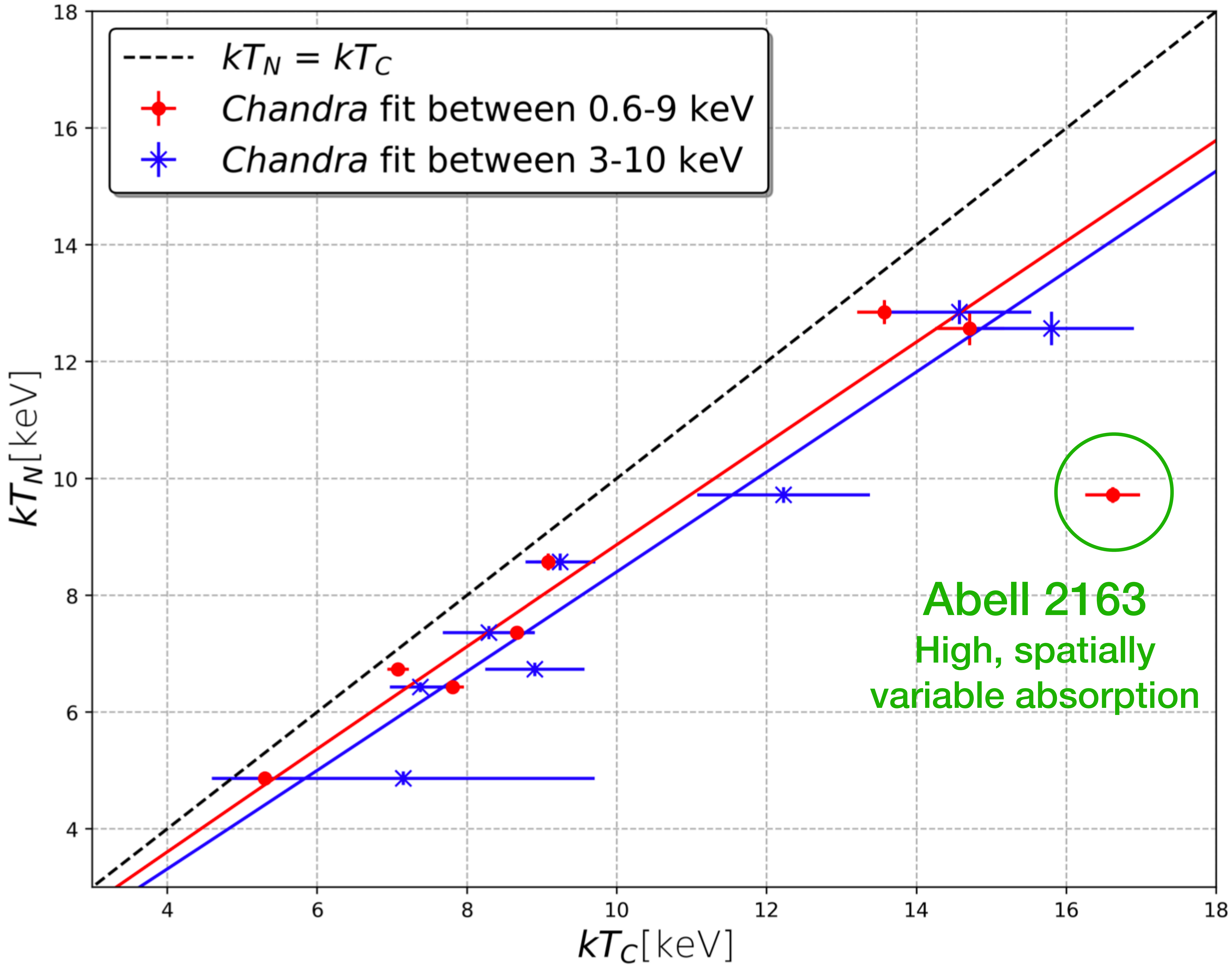

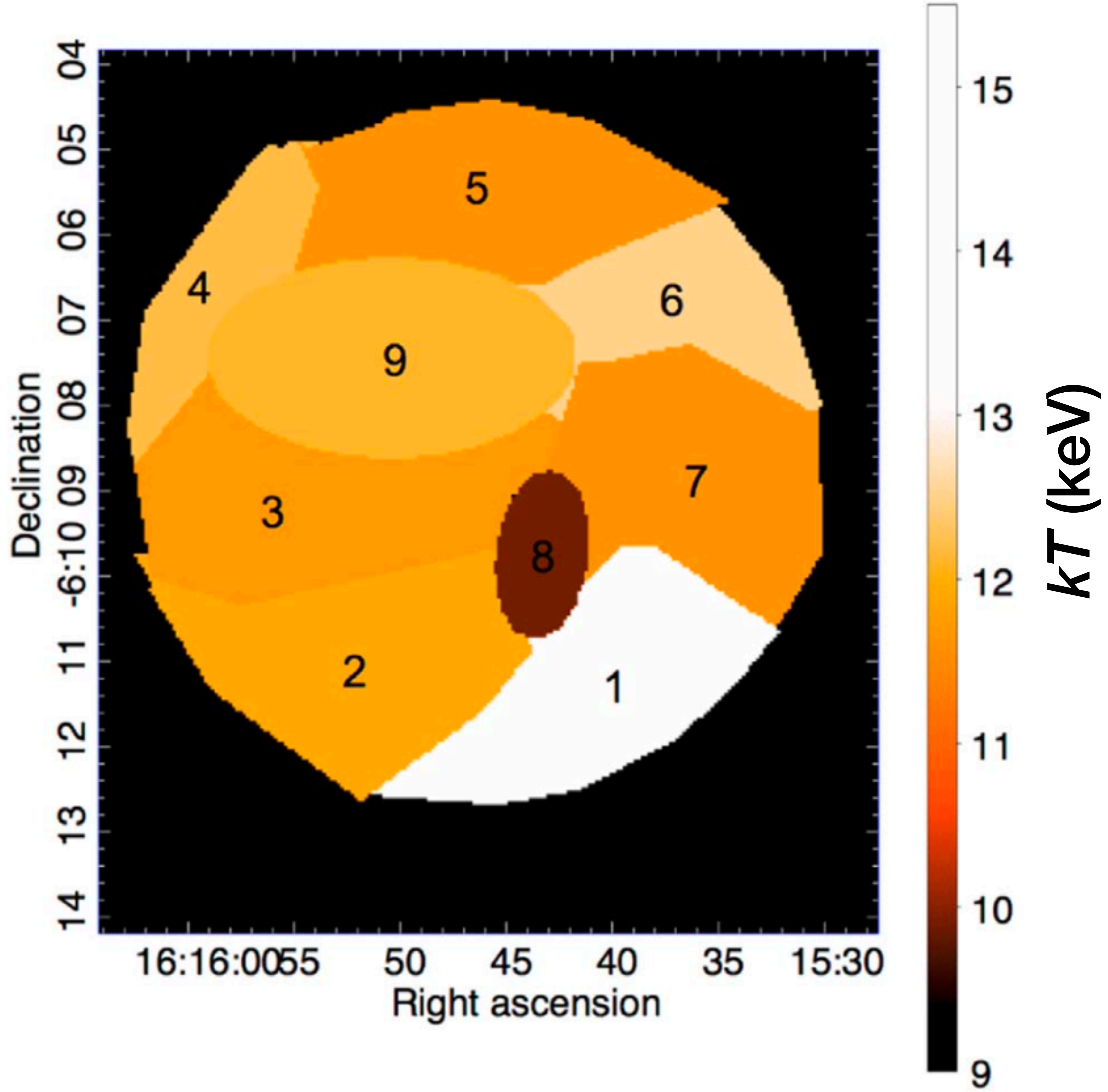

Rojas Bolivar+ 21

Wallbank+ 22

NuSTAR - *Chandra* Comparison

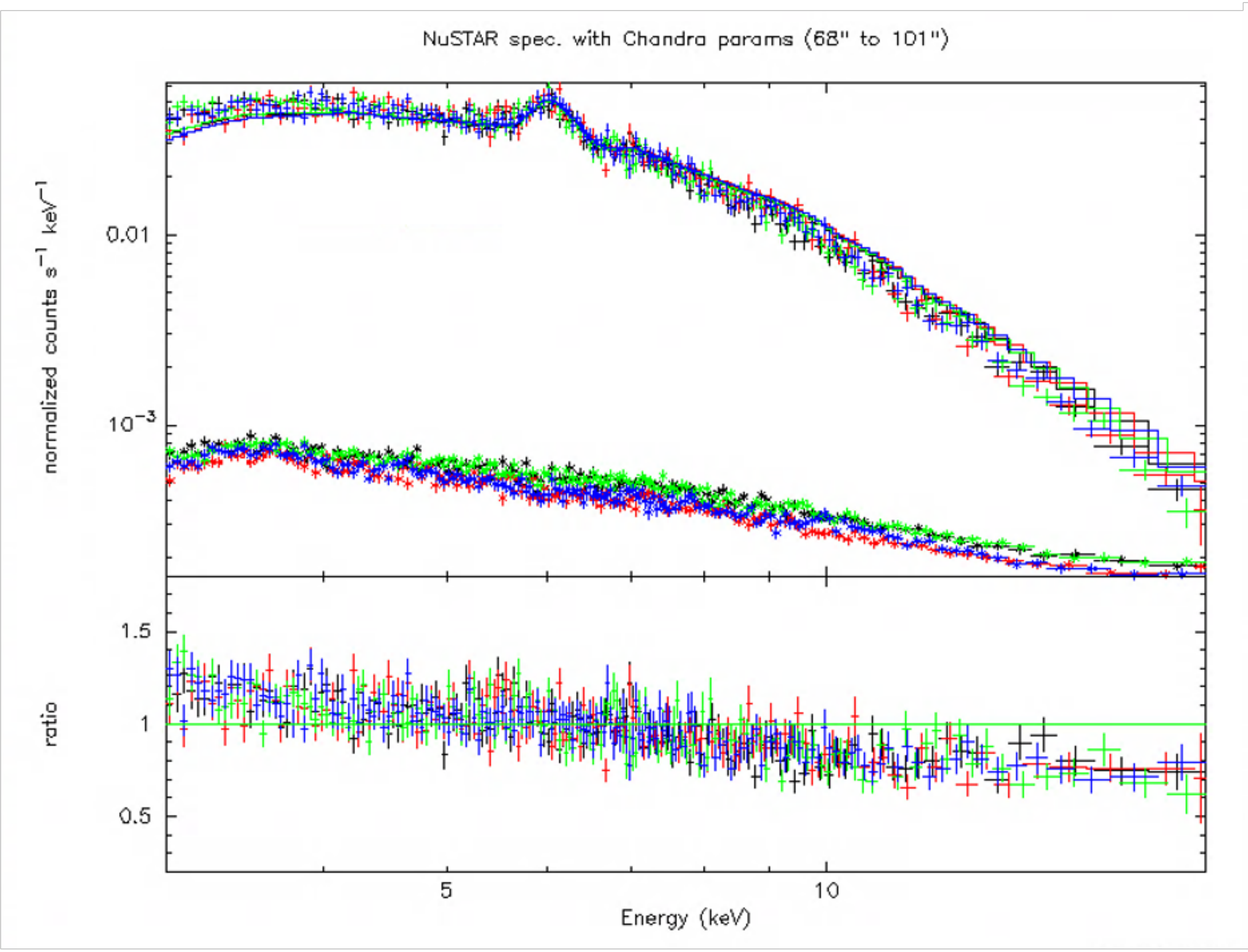

NuSTAR data with *Chandra* best-fit model
C-stat/dof: 3006/1567

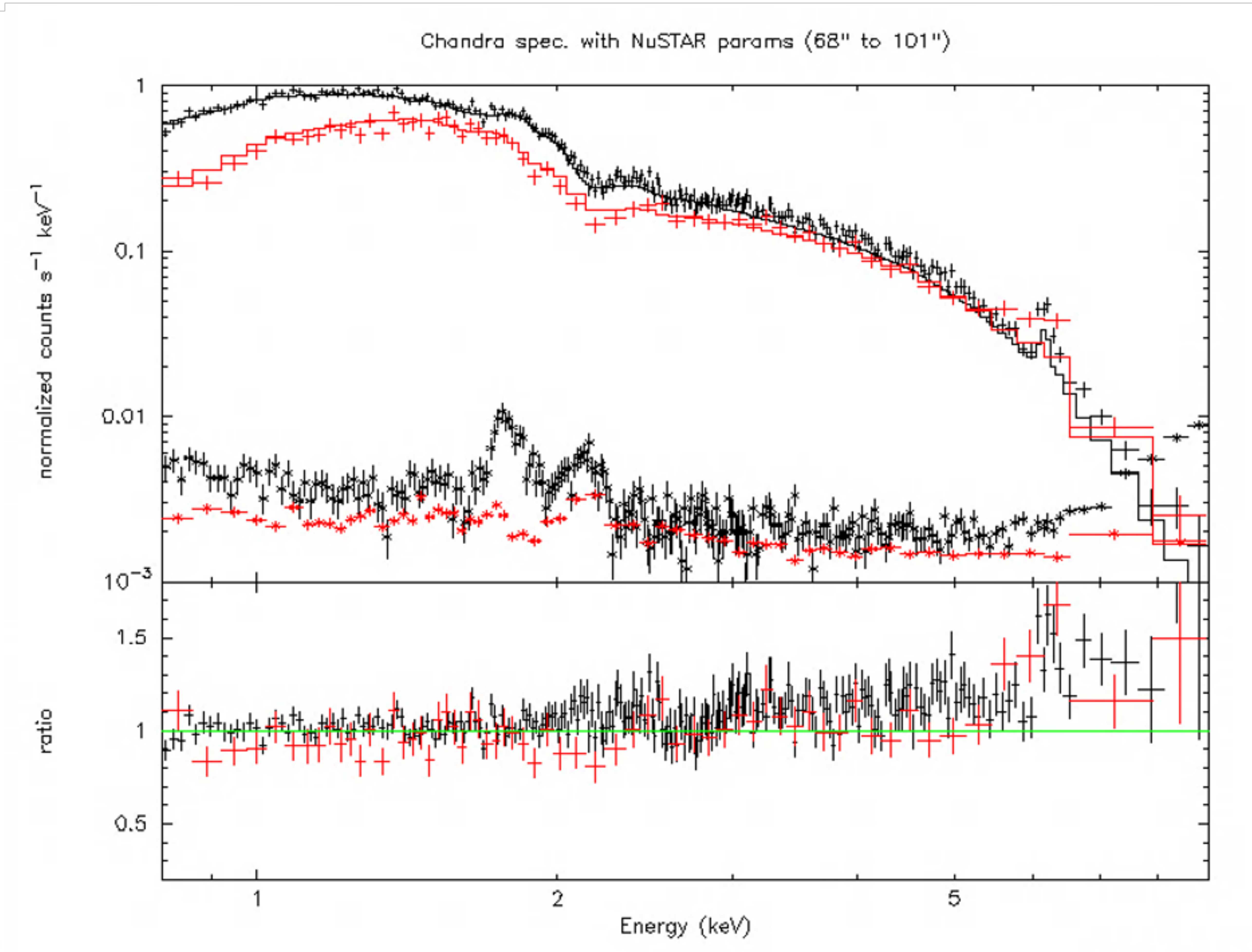

Chandra data with *NuSTAR* best-fit model
C-stat/dof: 1105/964

NuSTAR Stray Light CXB Measurement

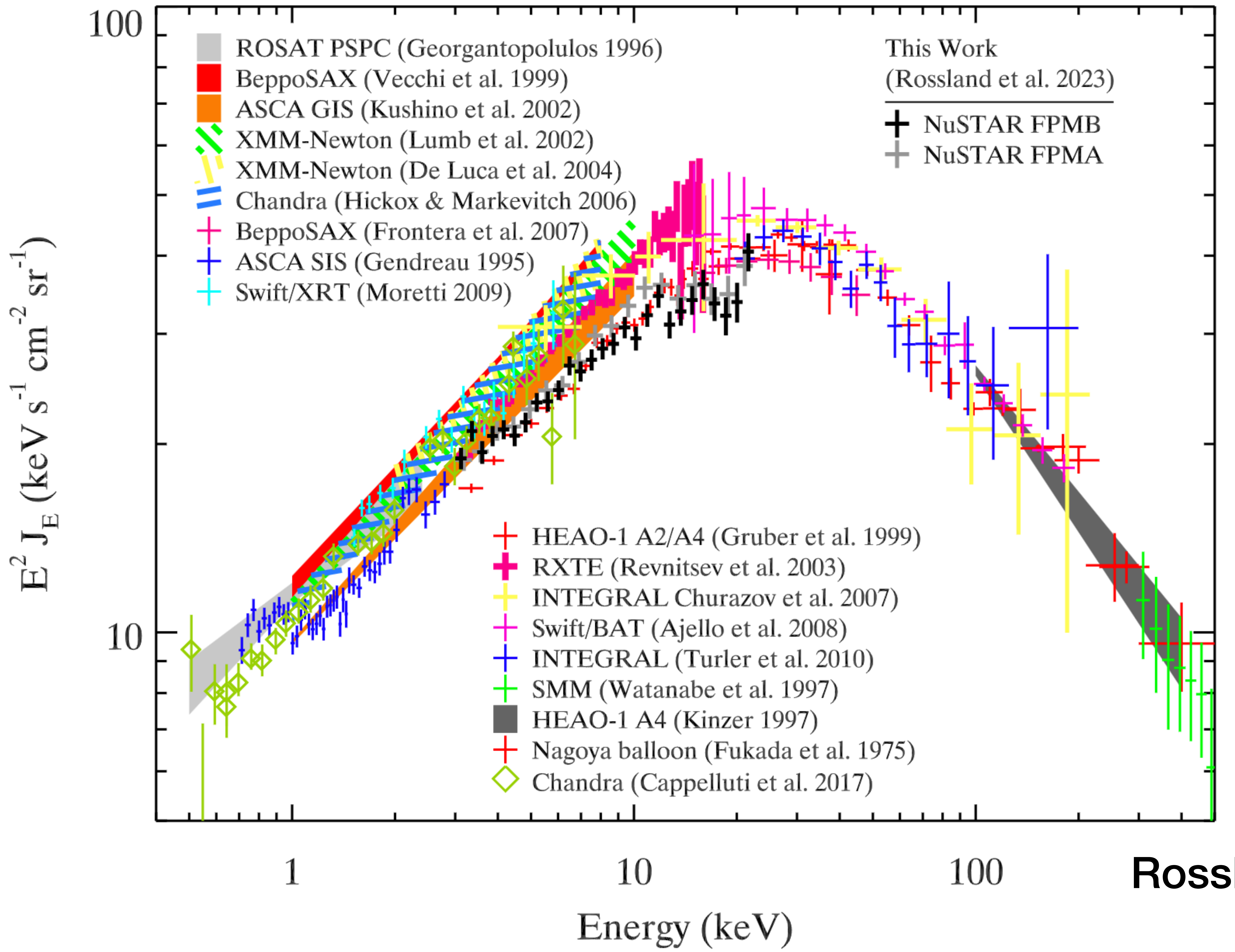

Rossland+ 2023

NuSTAR Stray Light CXB Measurement

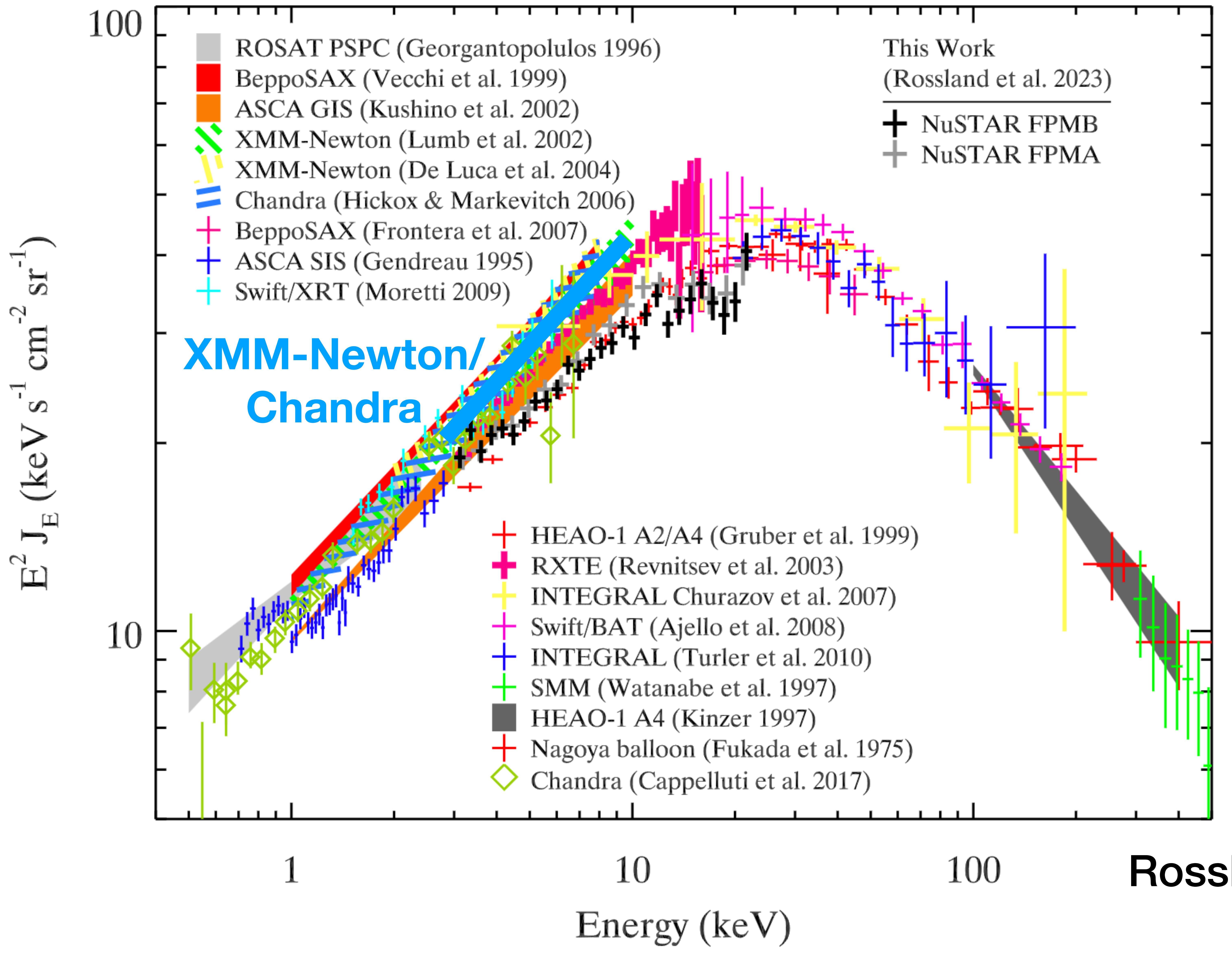

Rossland+ 2023

NuSTAR Stray Light CXB Measurement

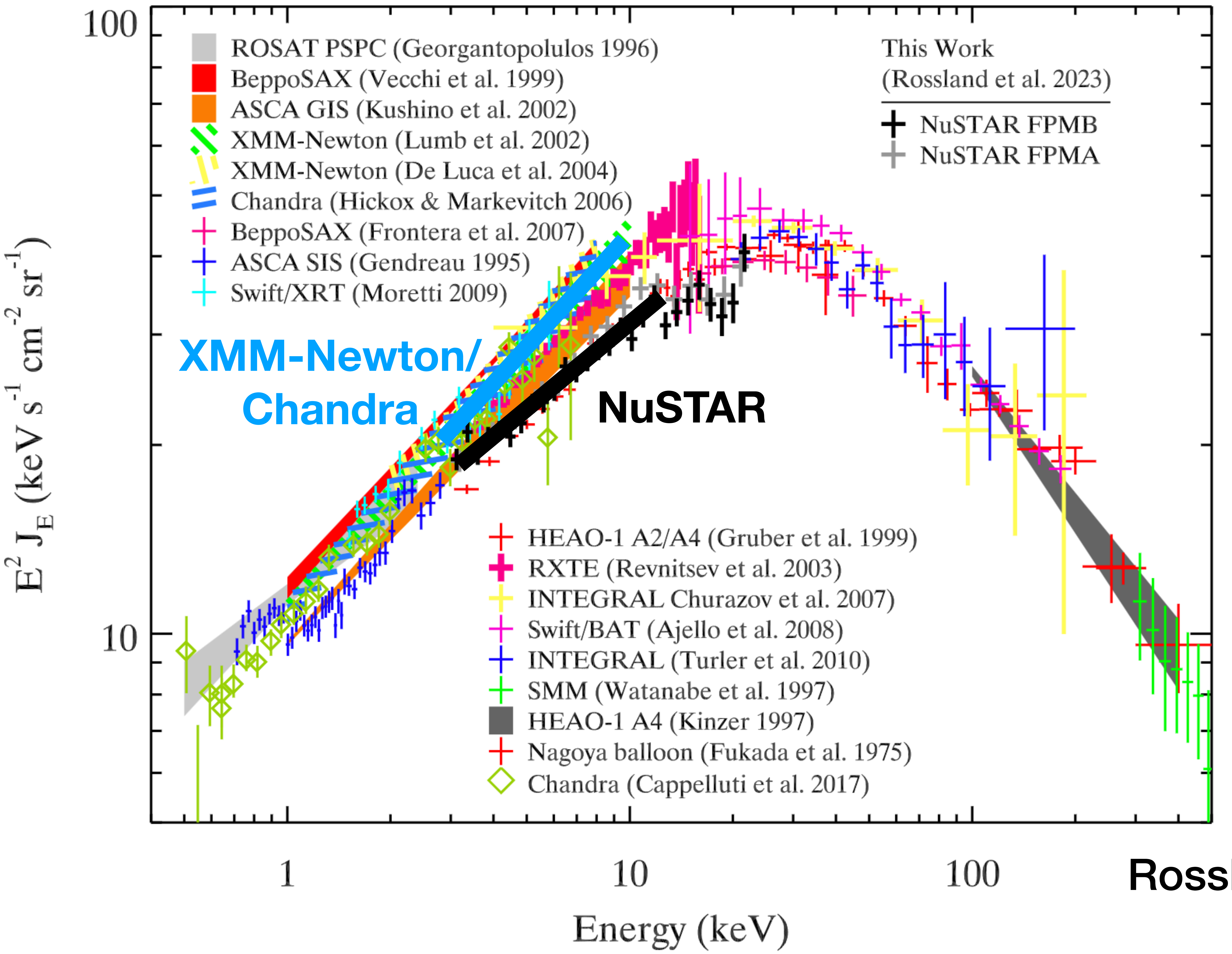

Rossland+ 2023

Cross-calibration with Relaxed Clusters

Dr. Cicely Potter
(Defended a week ago)

NuSTAR Large Program (>100 ks each)

Cluster	kT (keV)	z
Abell 2029	8.5	0.077
Abell 478	7.3	0.088
Abell 1795	6.1	0.062
Abell 2199	4.4	0.030

Reanalysis of *Chandra/XMM-Newton* data in exact same regions

Fiona Lopez
(REU student, incoming NMSU grad)

NuSTAR Cluster Snapshot C Program (20 ks each)

Cluster	kT_C (keV)	ΔkT_X (keV)	$\frac{T_C - T_X}{T_X}$	ΔkT_N (keV)
RXC J1504	9.8 ± 0.8	0.2	0.53	0.8
Abell 3571	8.1 ± 0.1	0.1	0.27	0.1
Abell 3558	7.4 ± 0.3	0.1	0.35	0.2
Abell 1651	7.1 ± 0.3	0.1	0.16	0.1
Abell 3391	6.6 ± 0.2	0.1	0.19	0.2
Abell 1650	6.4 ± 0.1	0.1	0.25	0.2
Abell 3158	6.0 ± 0.1	0.1	0.18	0.1
Abell 3112	5.5 ± 0.1	0.1	0.36	0.2
Abell 1644	5.3 ± 0.1	0.2	0.15	0.2
Abell 496	5.2 ± 0.1	0.1	0.18	0.2
~~Abell 3562~~	~~5.0 ± 0.3~~	~~0.1~~	~~0.19~~	~~0.1~~

Extract same regions as in Schellenberger+ 2015
($r < 3.5'$, excising cores)

NuSTAR FPMA+B combined
(Bgd-sub, exp-corrected)

4-25 keV

Potter+ in prep

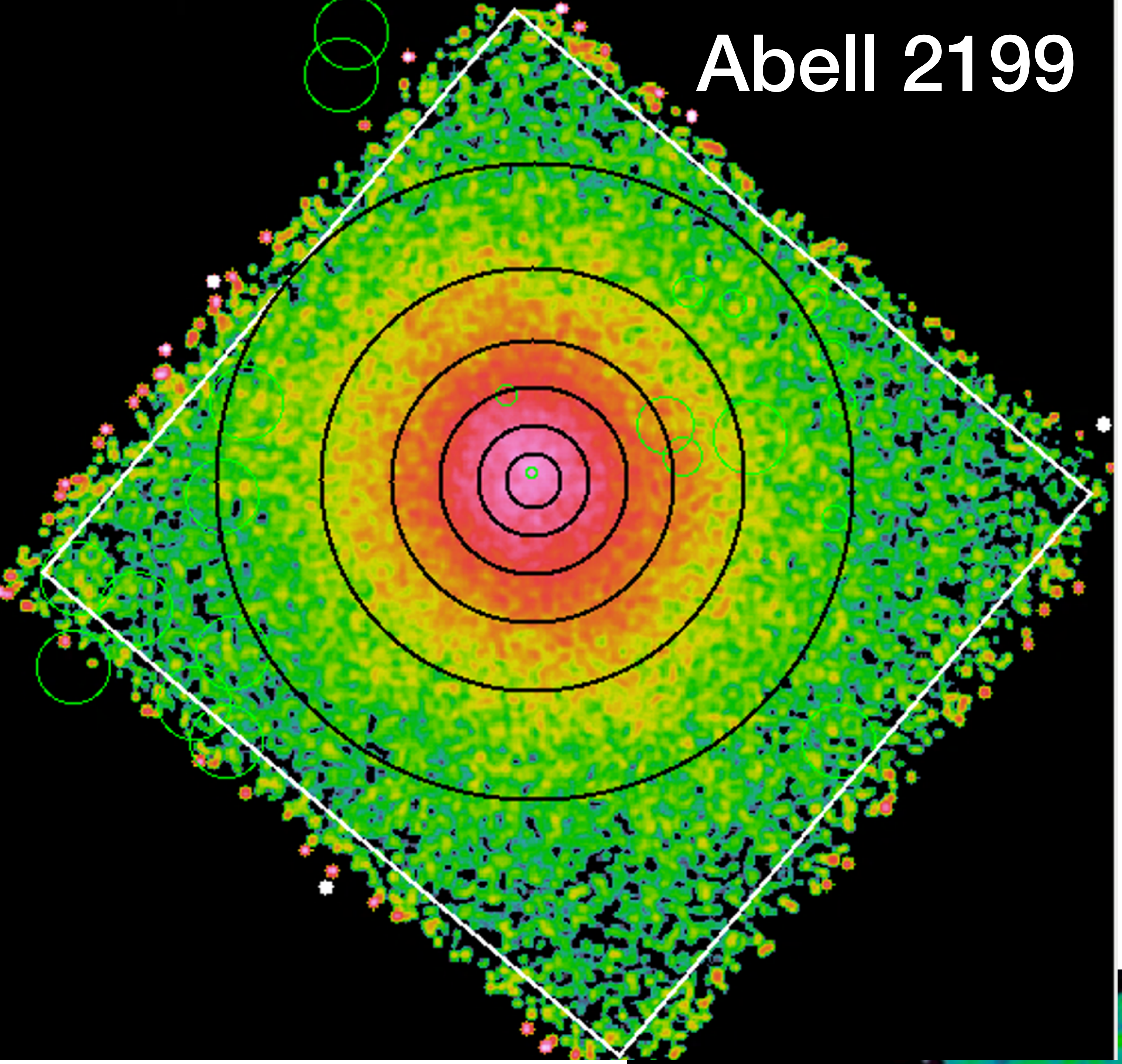

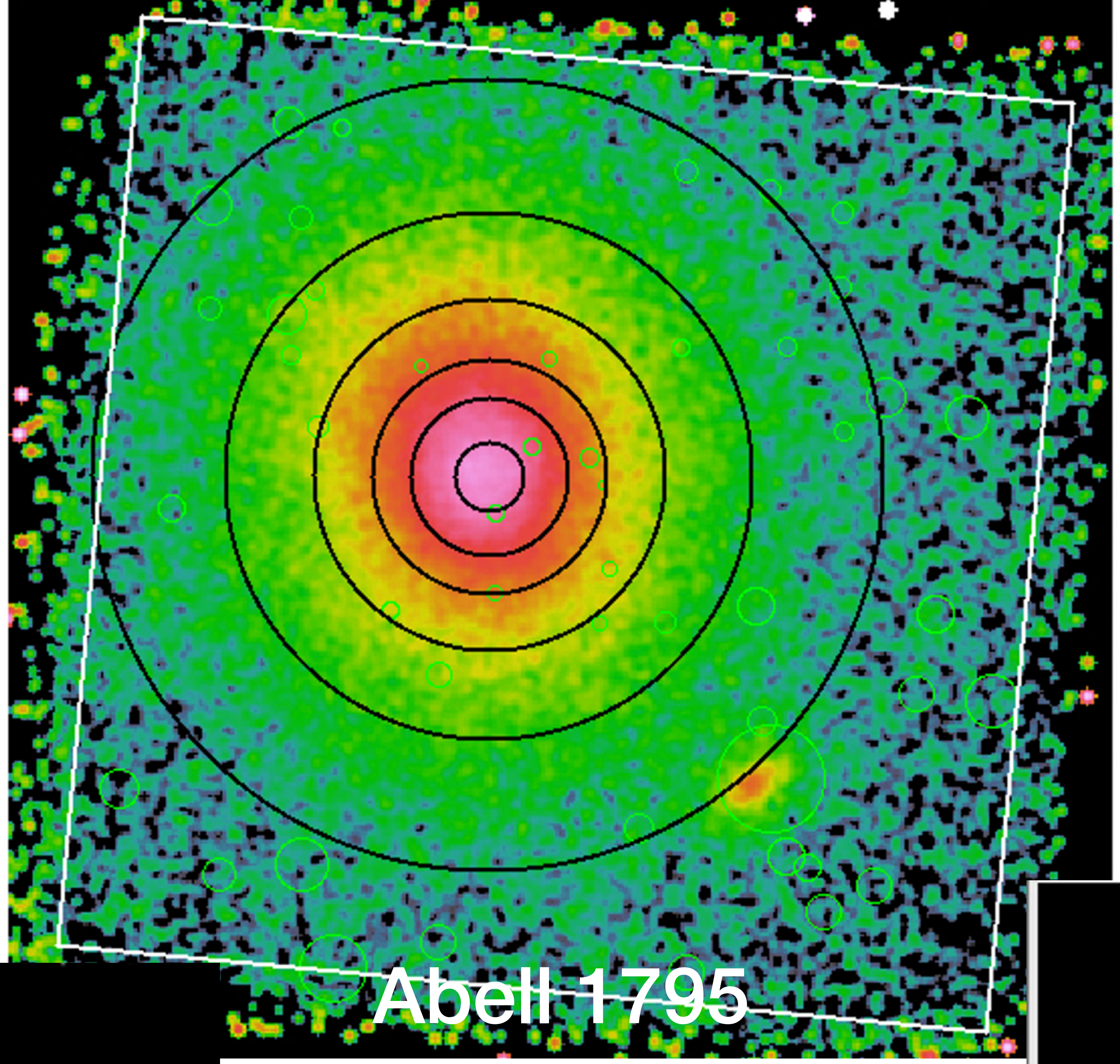

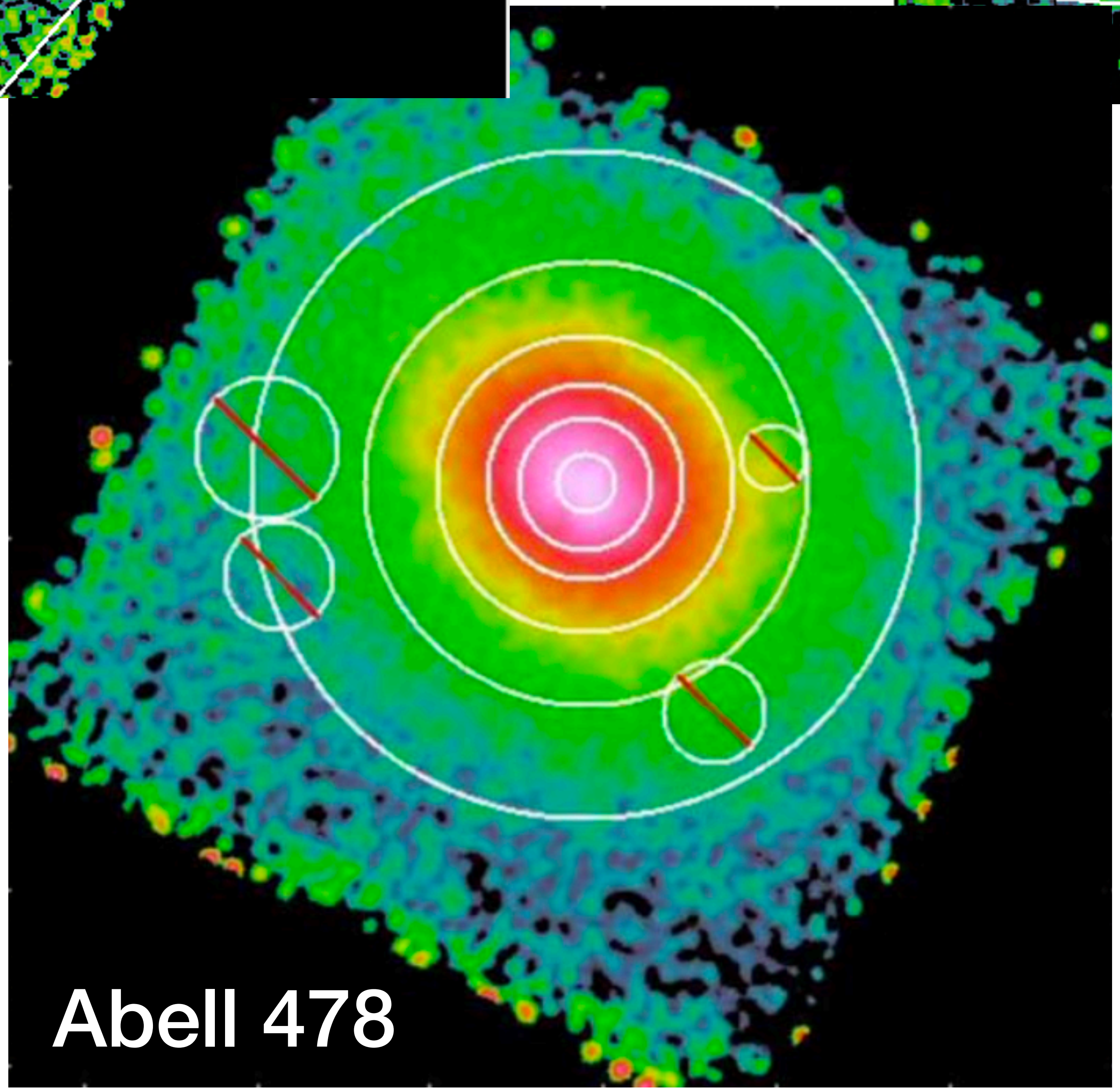

Potter+ 2023

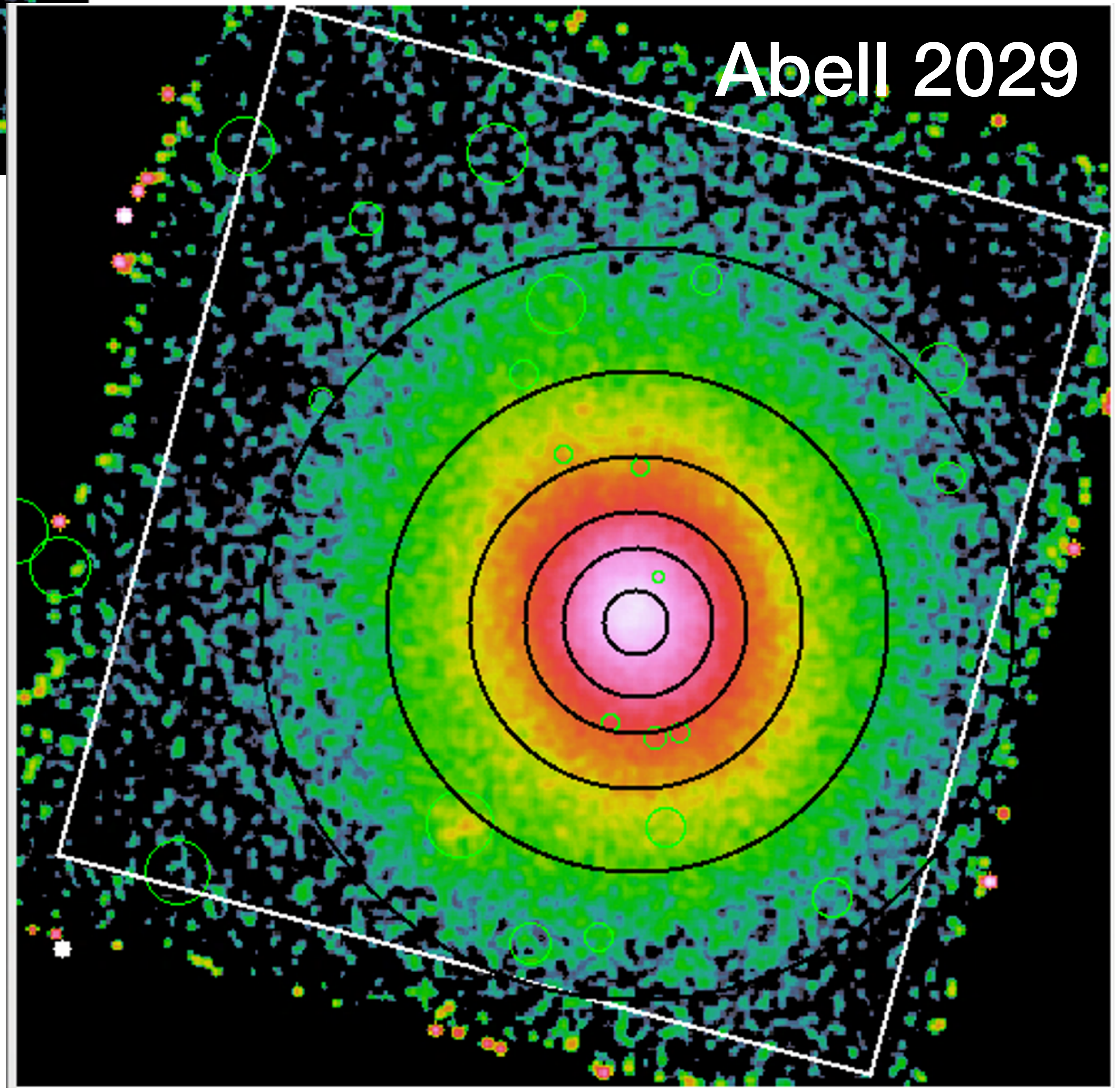

Deep Sample: Temperature Profiles

Abell 478

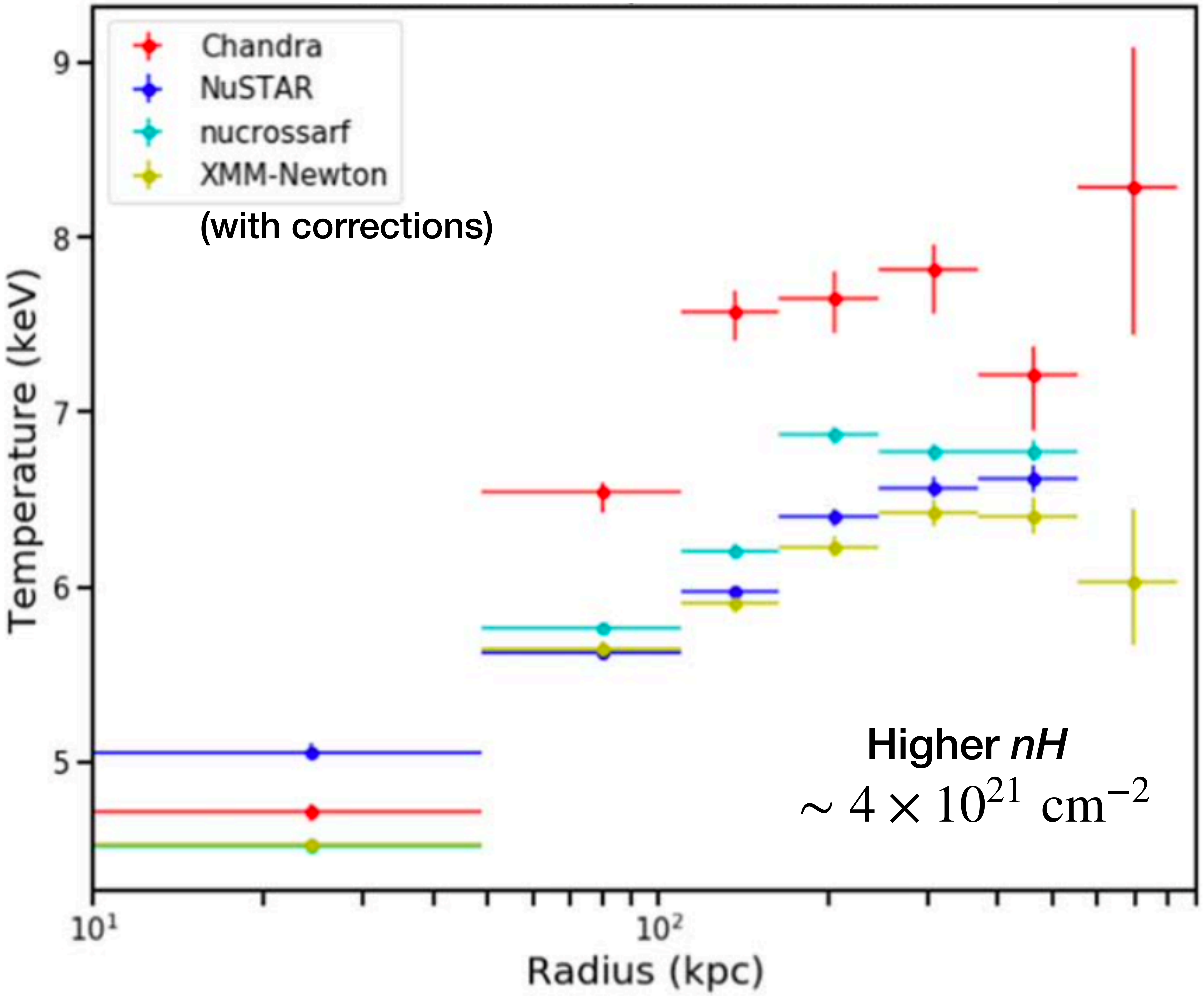

Potter+ 2023

Abell 2029

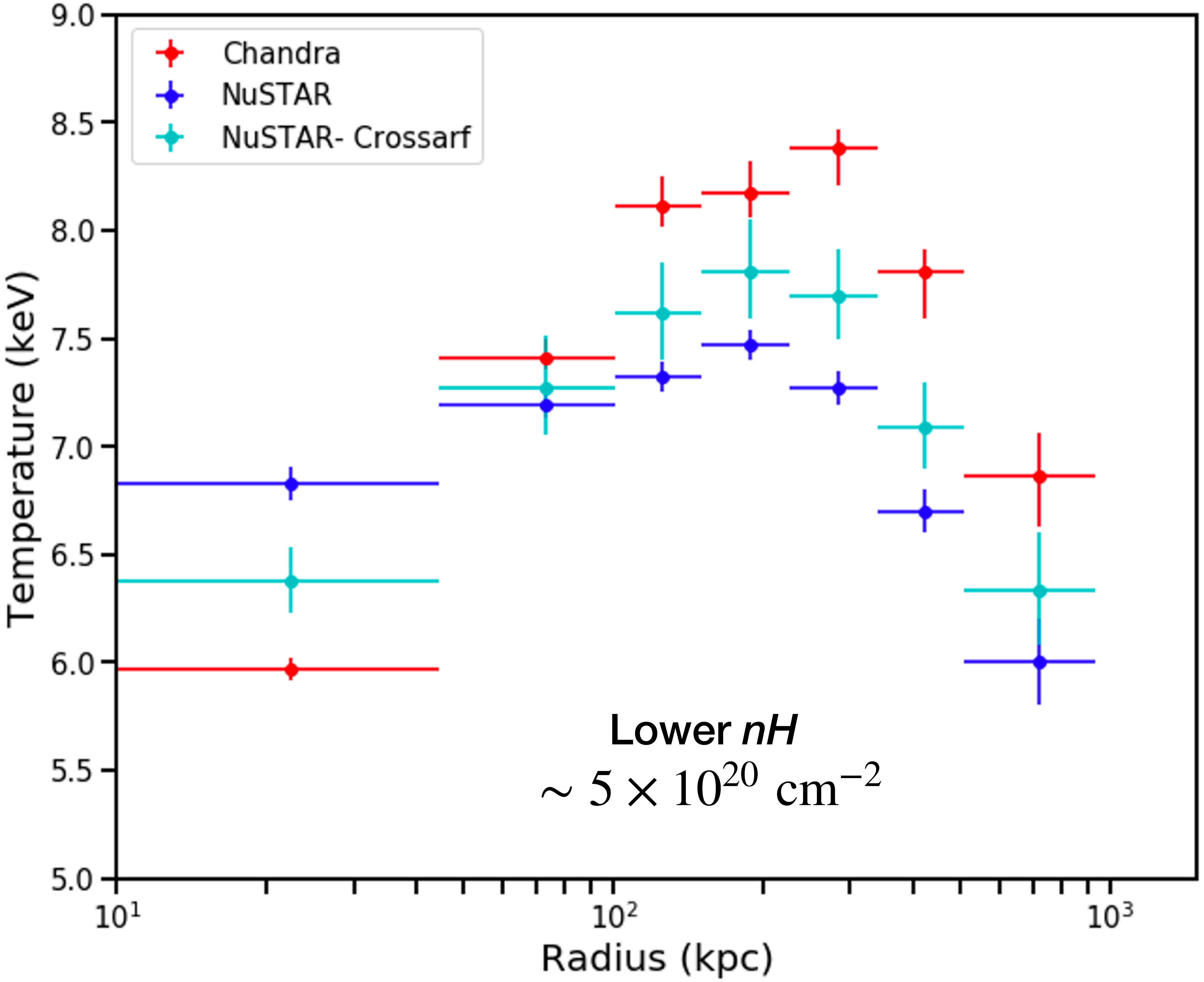

Potter+ in prep

Deep Sample: Temperature Profiles

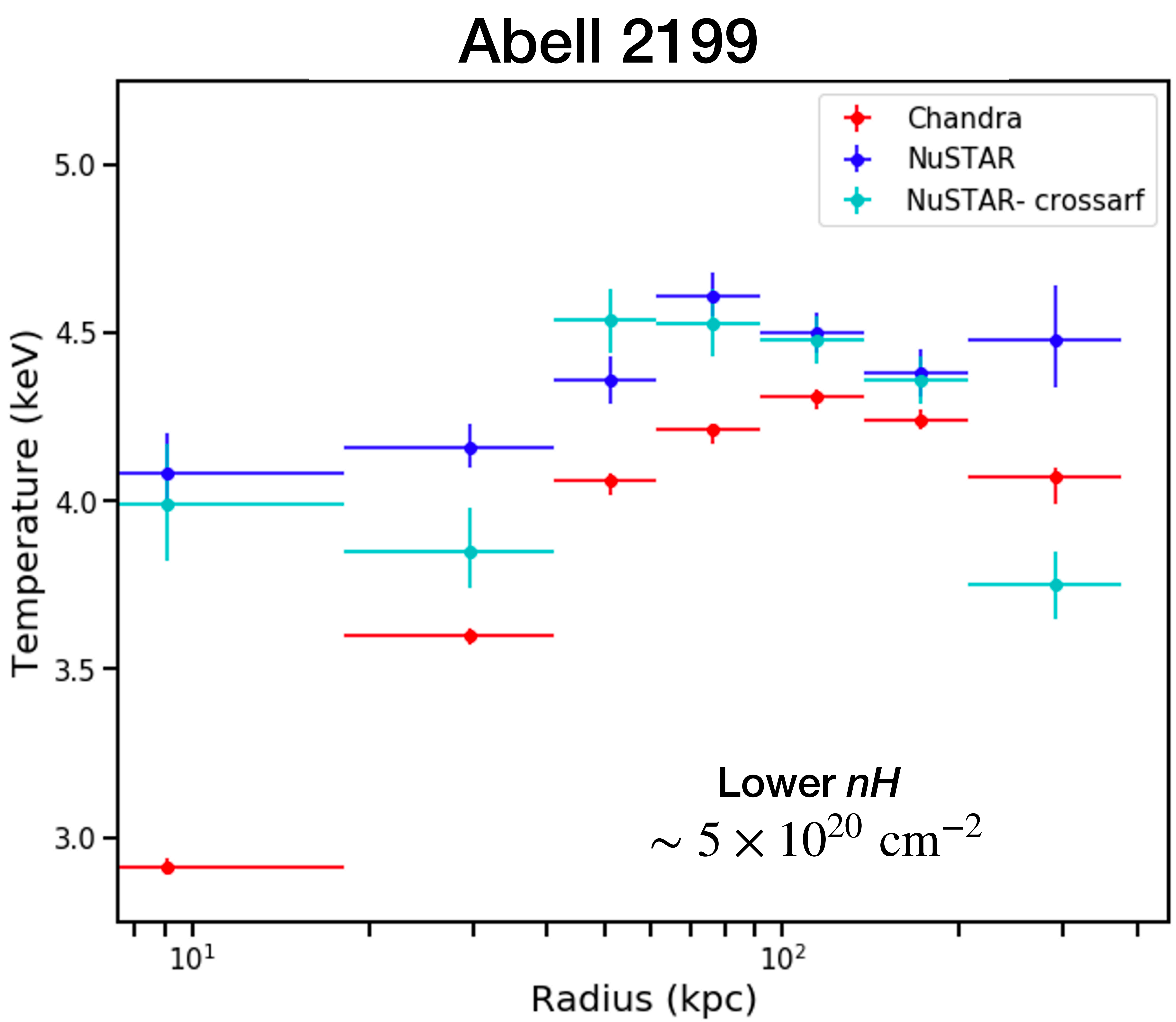

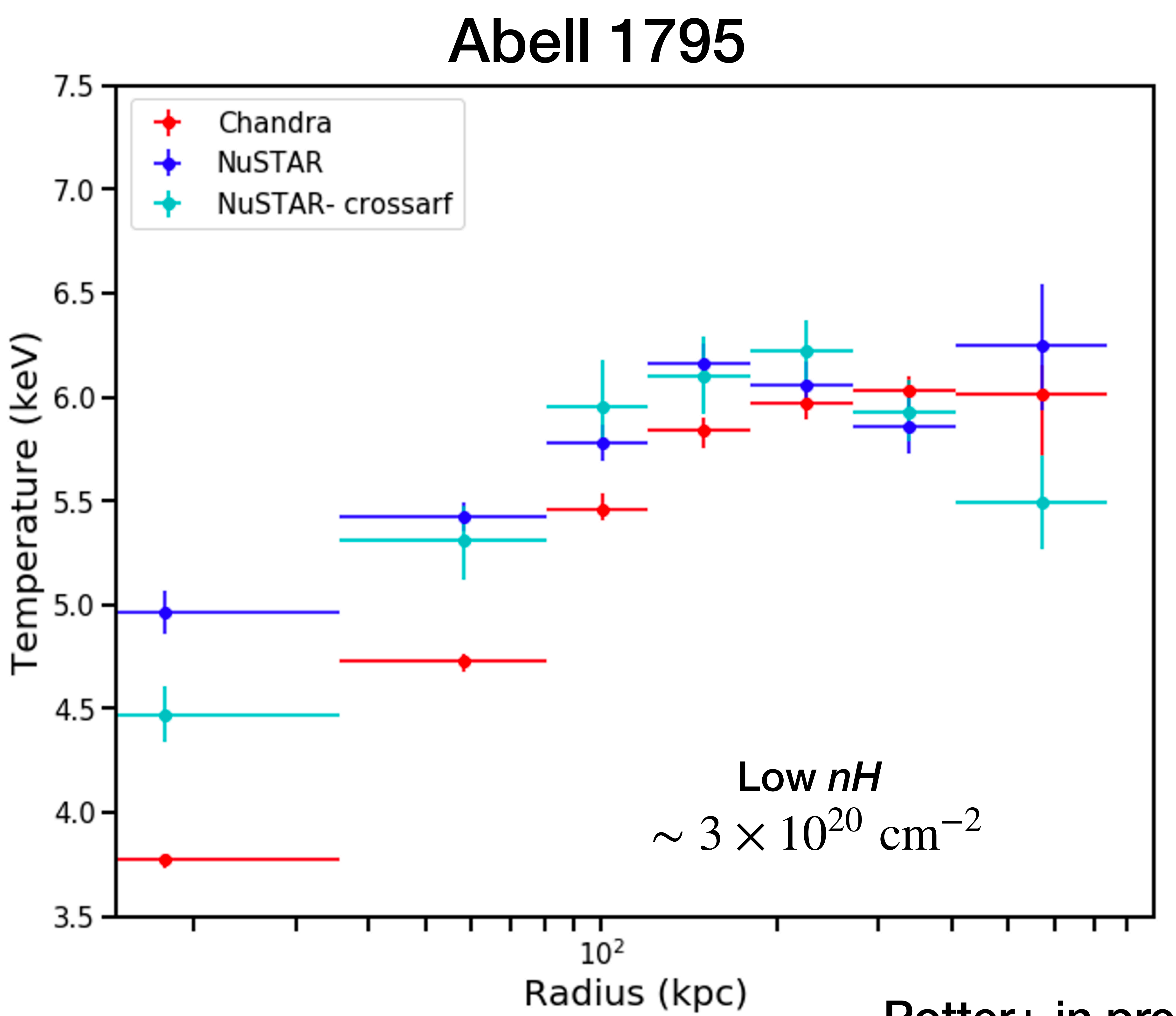

Potter+ in prep

Snapshot Cluster Temperatures

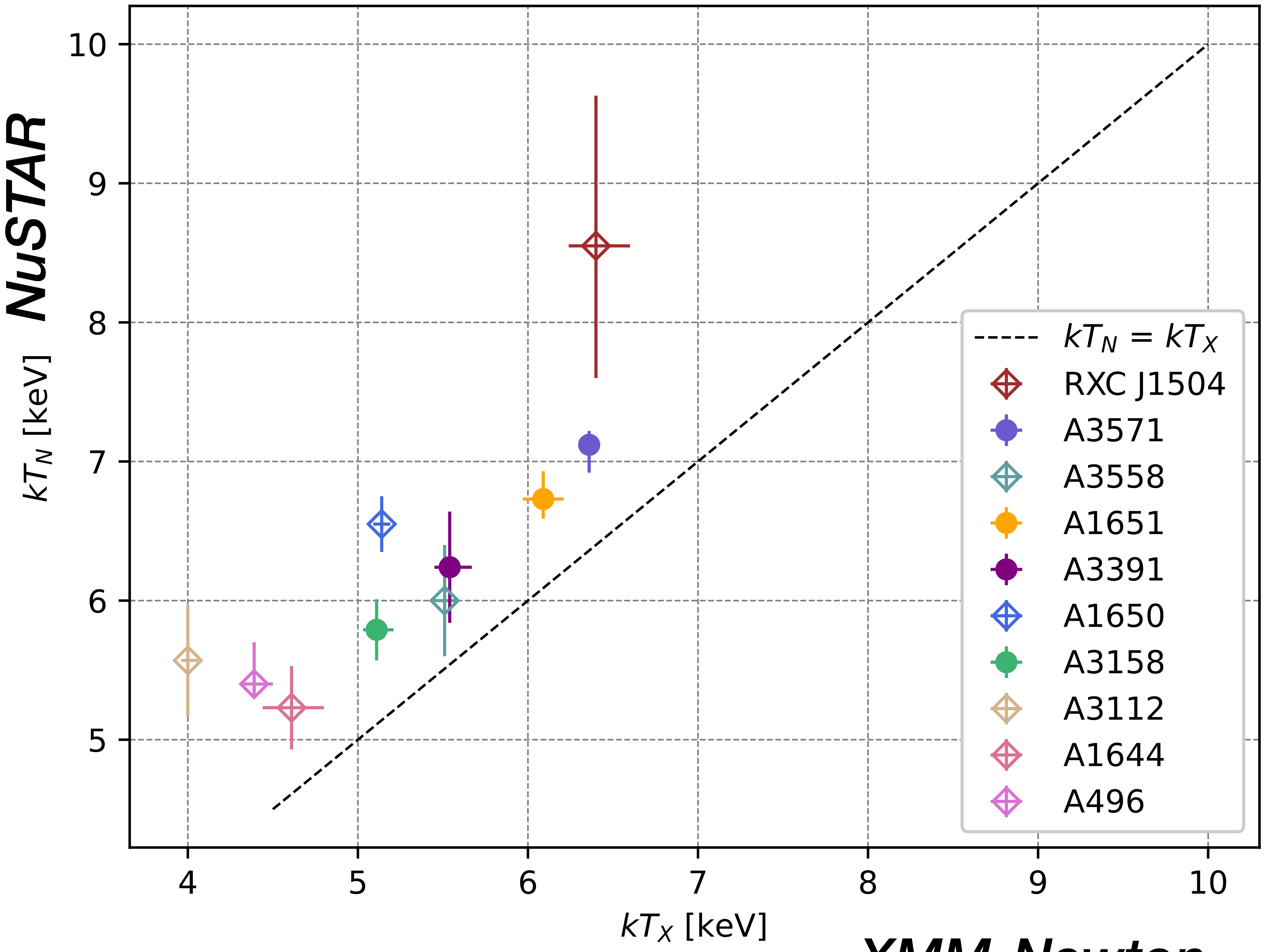

XMM-Newton

Lopez+ 2025 (*Chandra/XMM-Newton kT*s from Schellenberger+ 2015)

Snapshot Cluster Temperatures

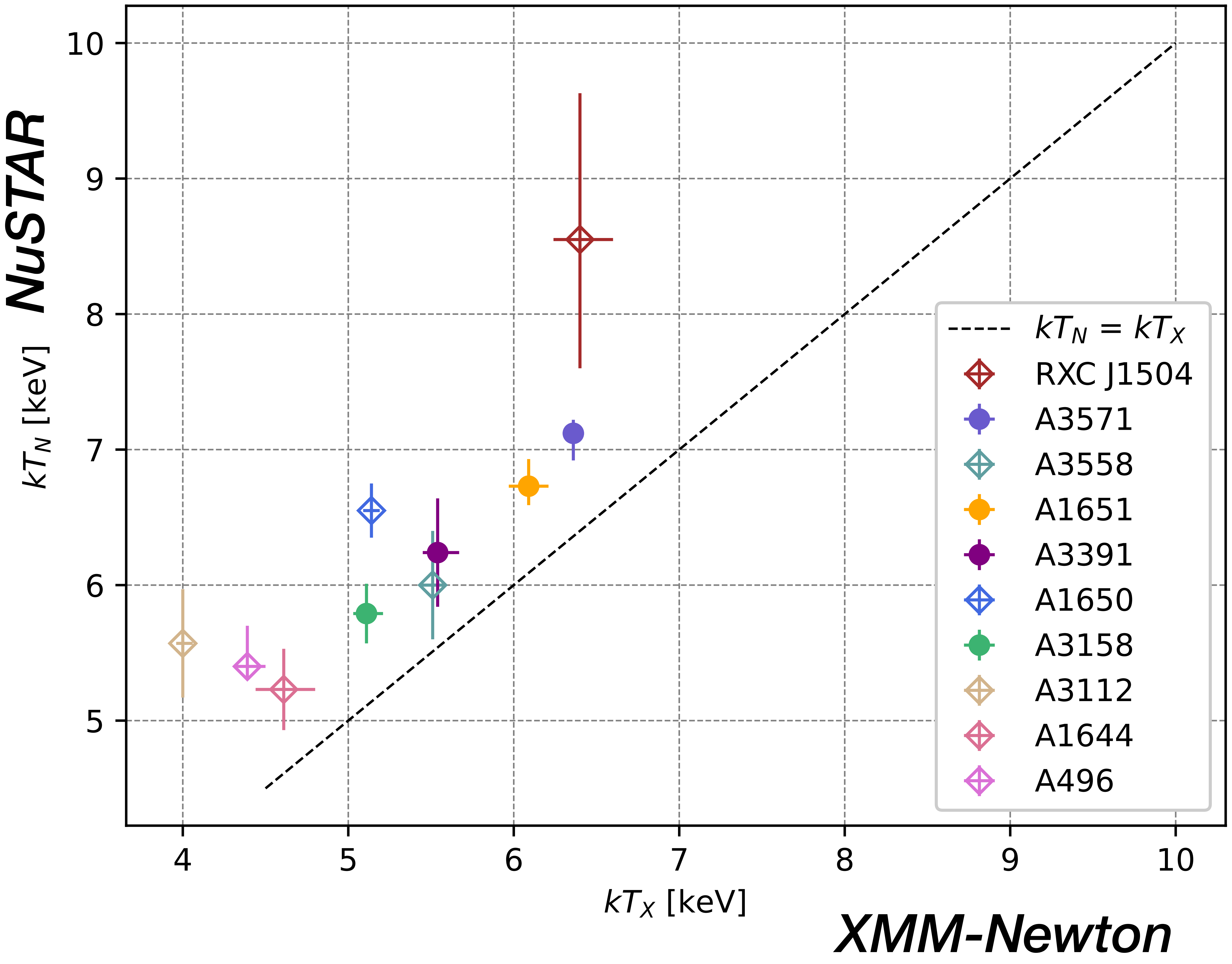

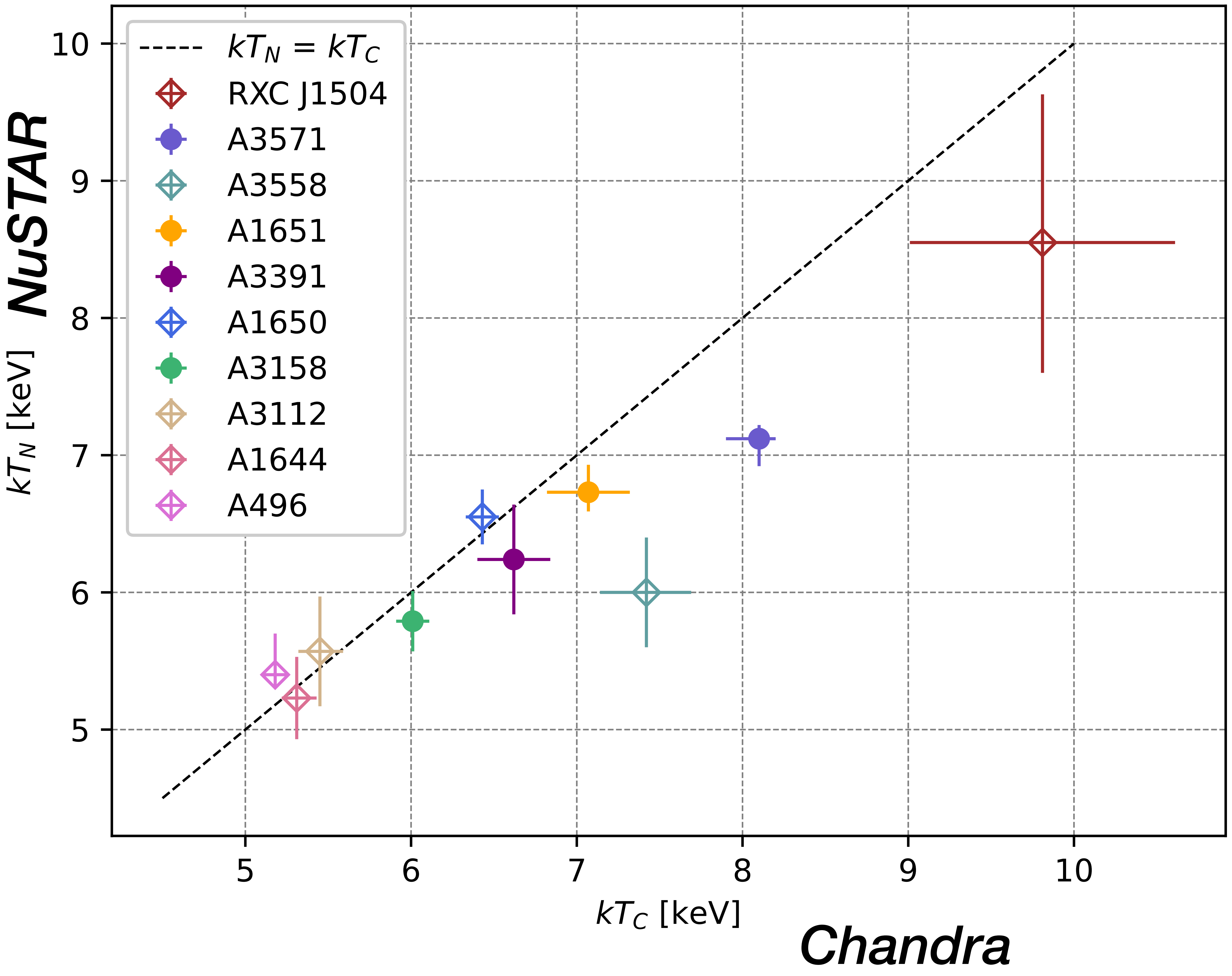

Lopez+ 2025 (*Chandra/XMM-Newton kT*s from Schellenberger+ 2015)

Snapshot Cluster Temperatures

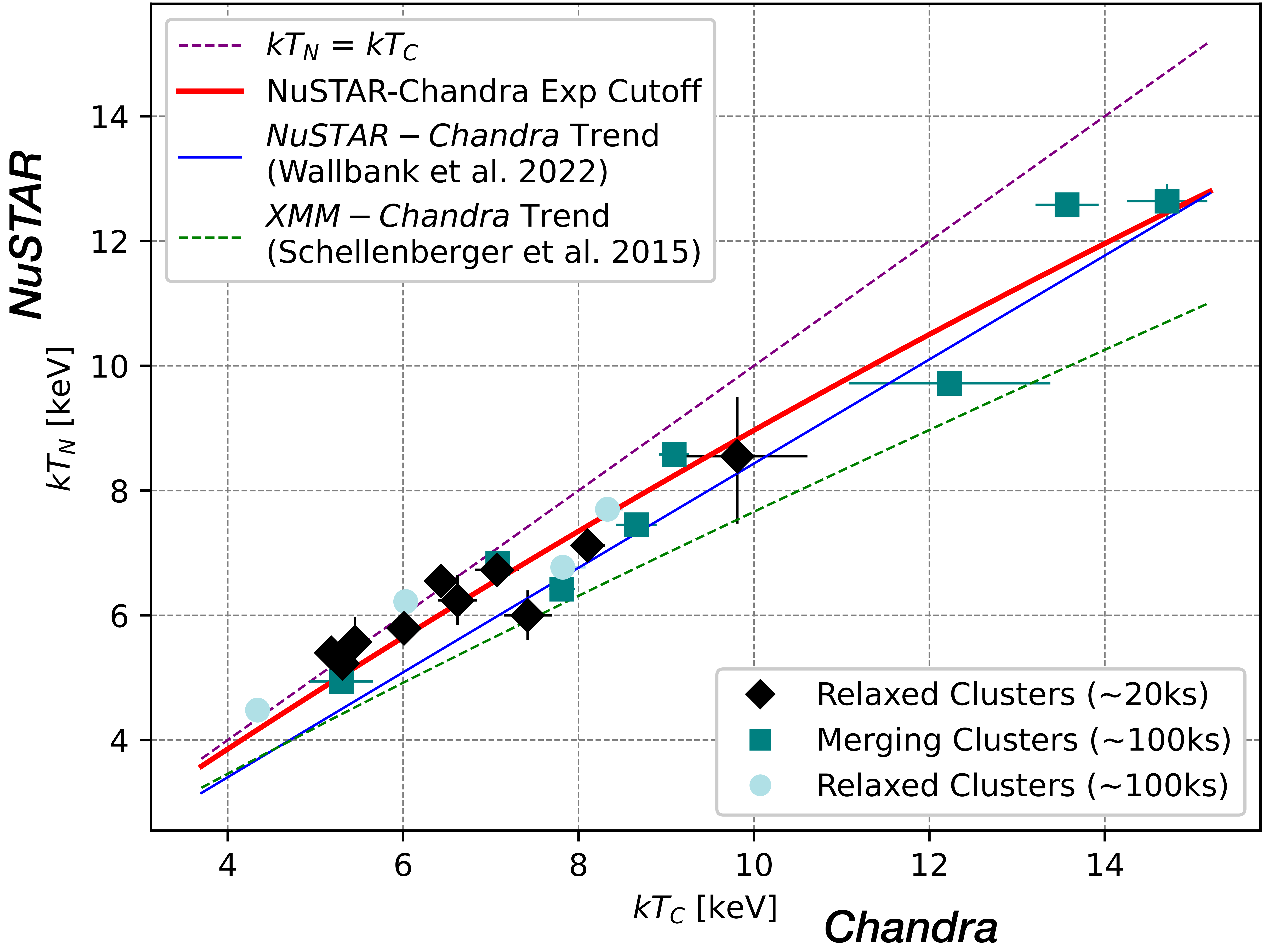

Lopez+ 2025 submitted

Snapshot Cluster Temperatures

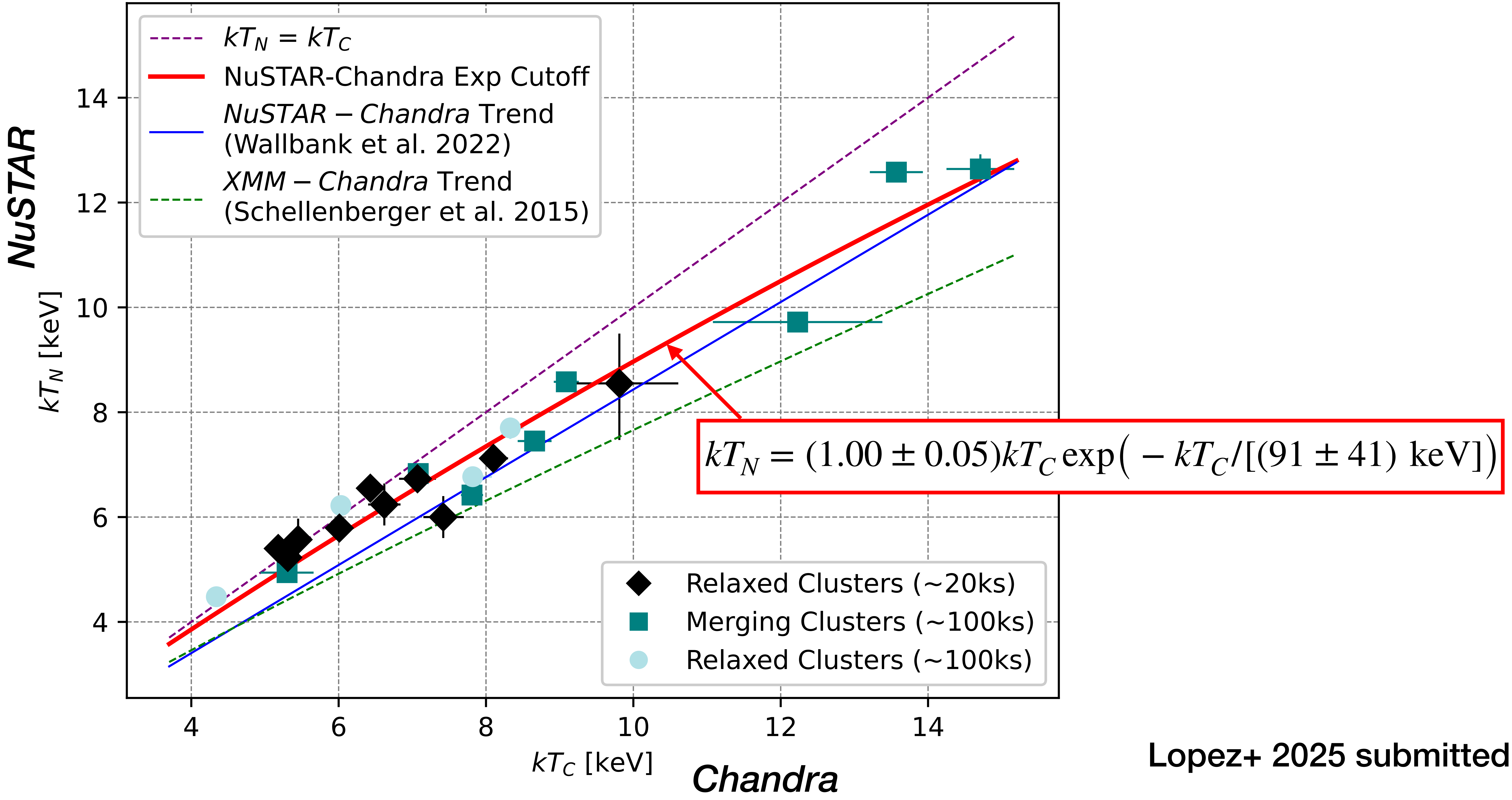

Lopez+ 2025 submitted

Snapshot Cluster Temperatures

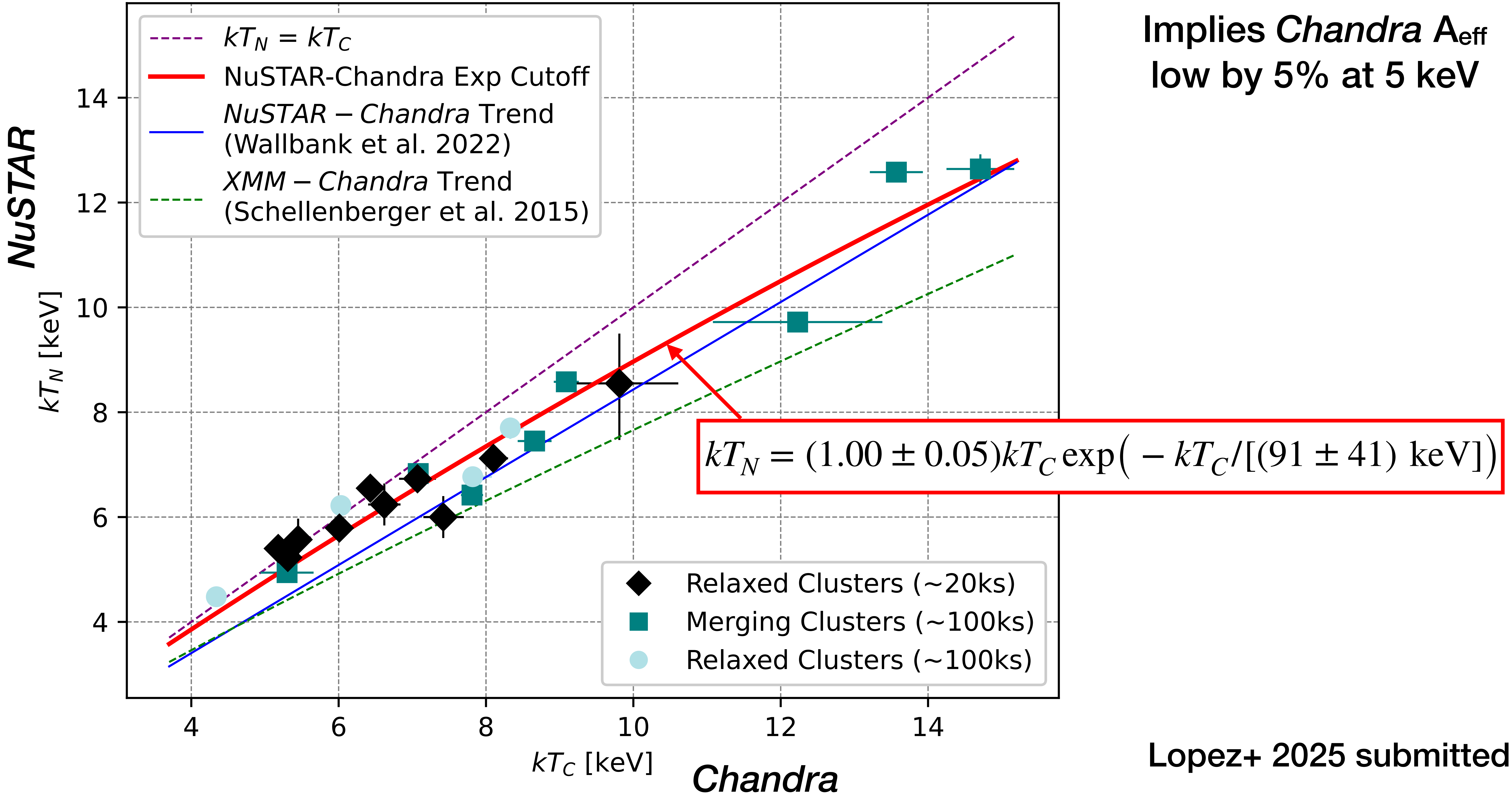

Implies *Chandra* A_{eff} low by 5% at 5 keV

Lopez+ 2025 submitted

Snapshot Cluster Temperatures

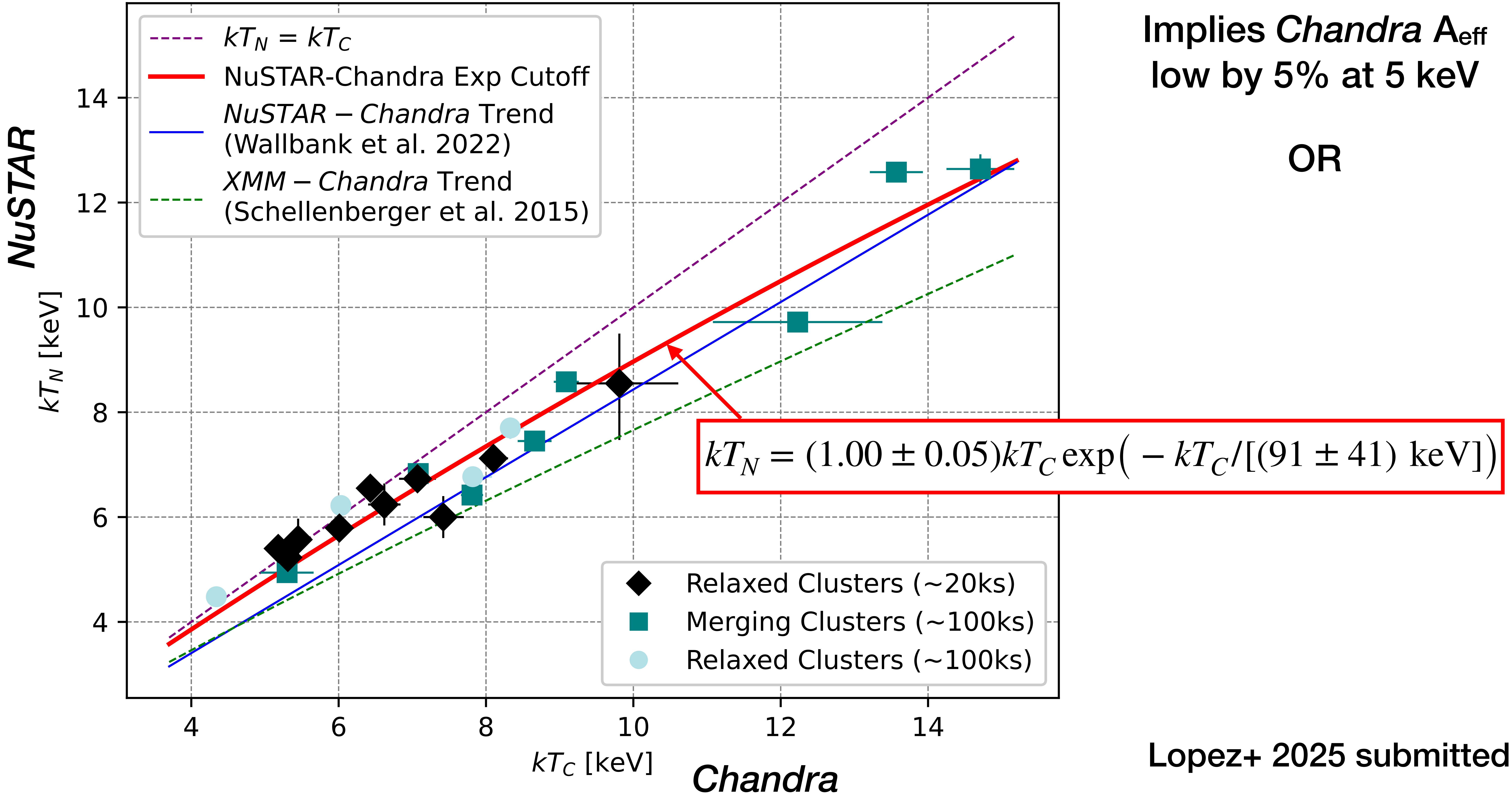

Implies *Chandra* A_{eff} low by 5% at 5 keV

OR

Lopez+ 2025 submitted

Snapshot Cluster Temperatures

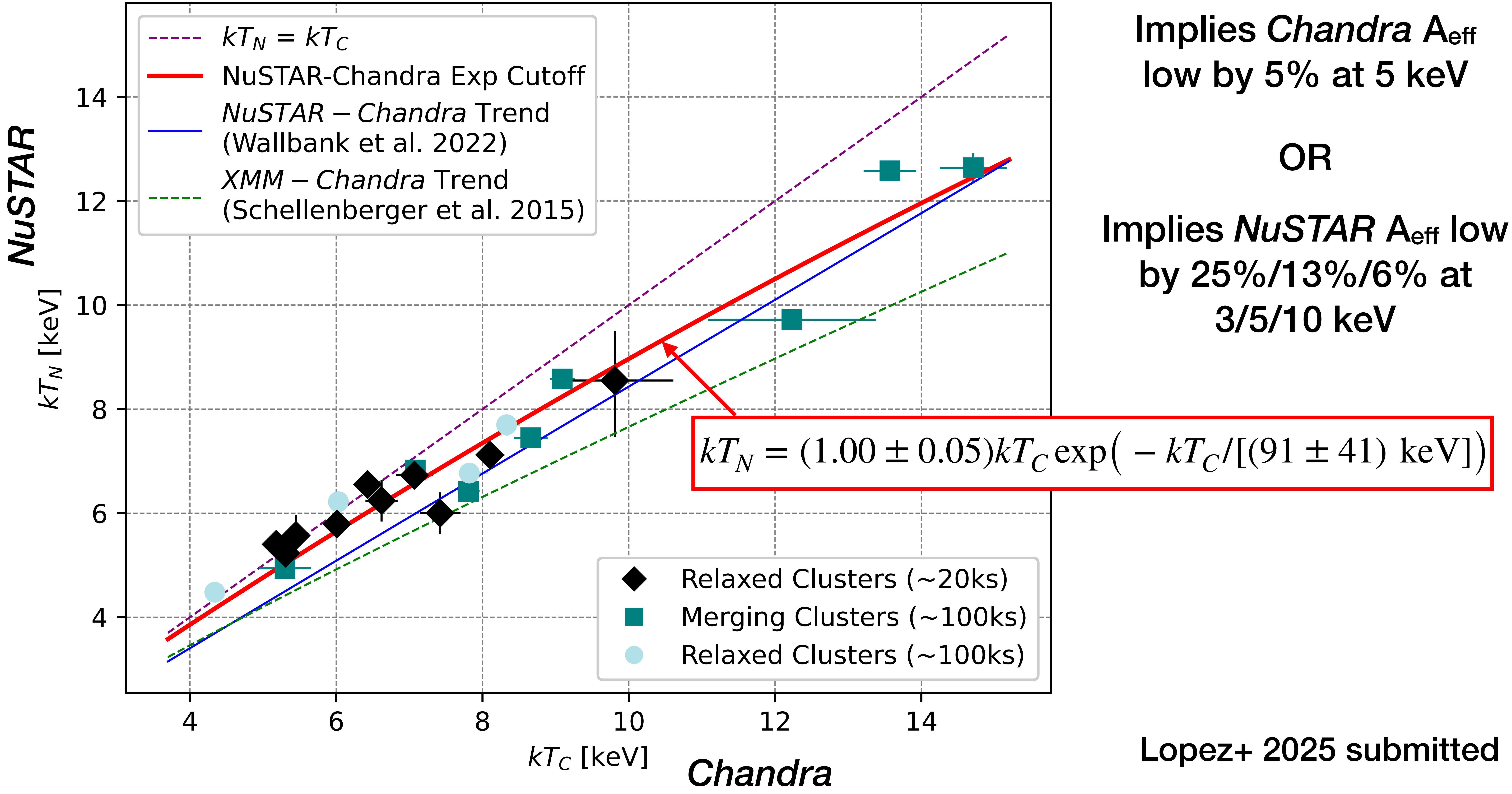

Implies *Chandra* A_{eff} low by 5% at 5 keV

OR

Implies *NuSTAR* A_{eff} low by 25%/13%/6% at 3/5/10 keV

Lopez+ 2025 submitted

XRISM Observations of the Coma Cluster

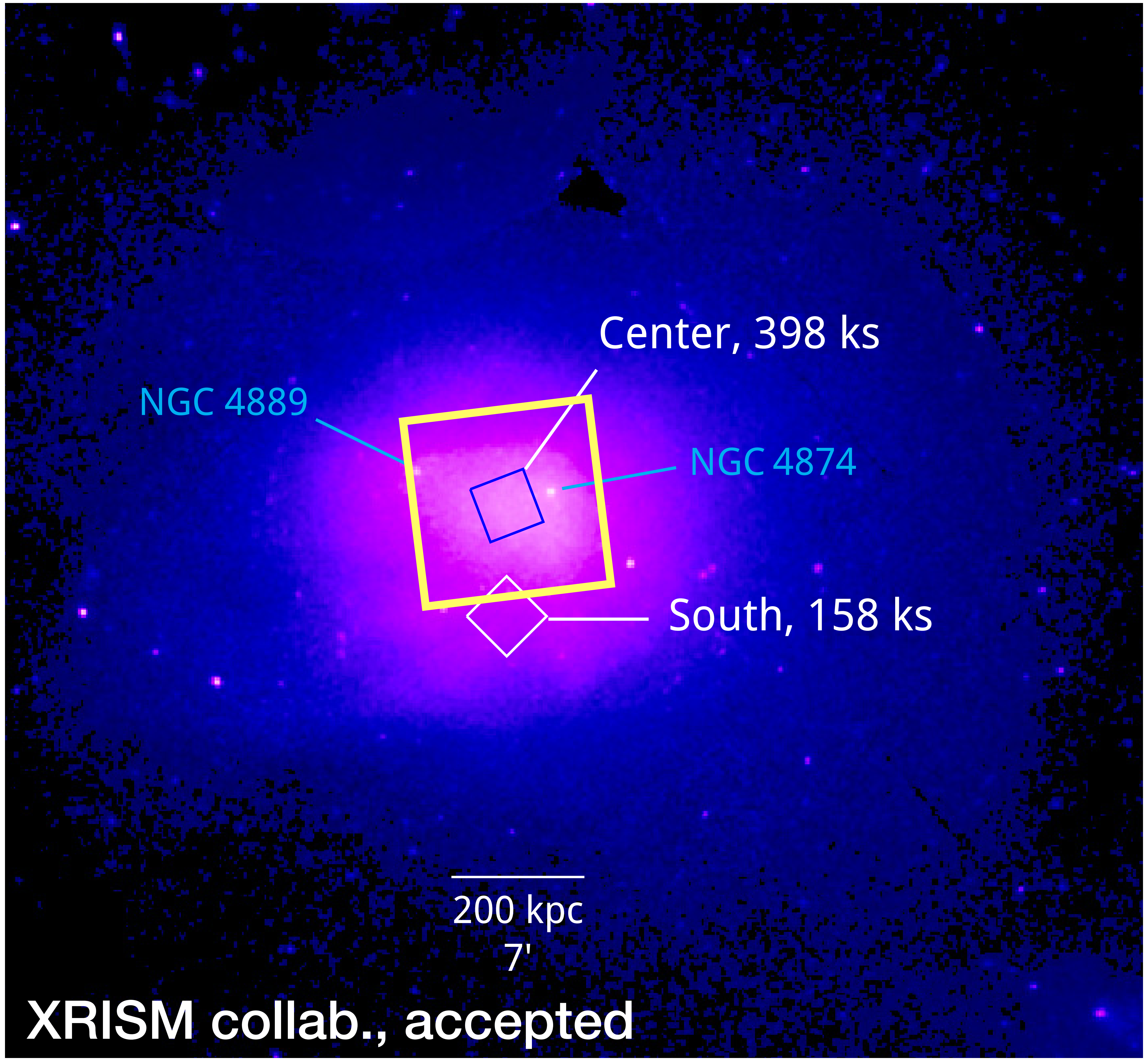

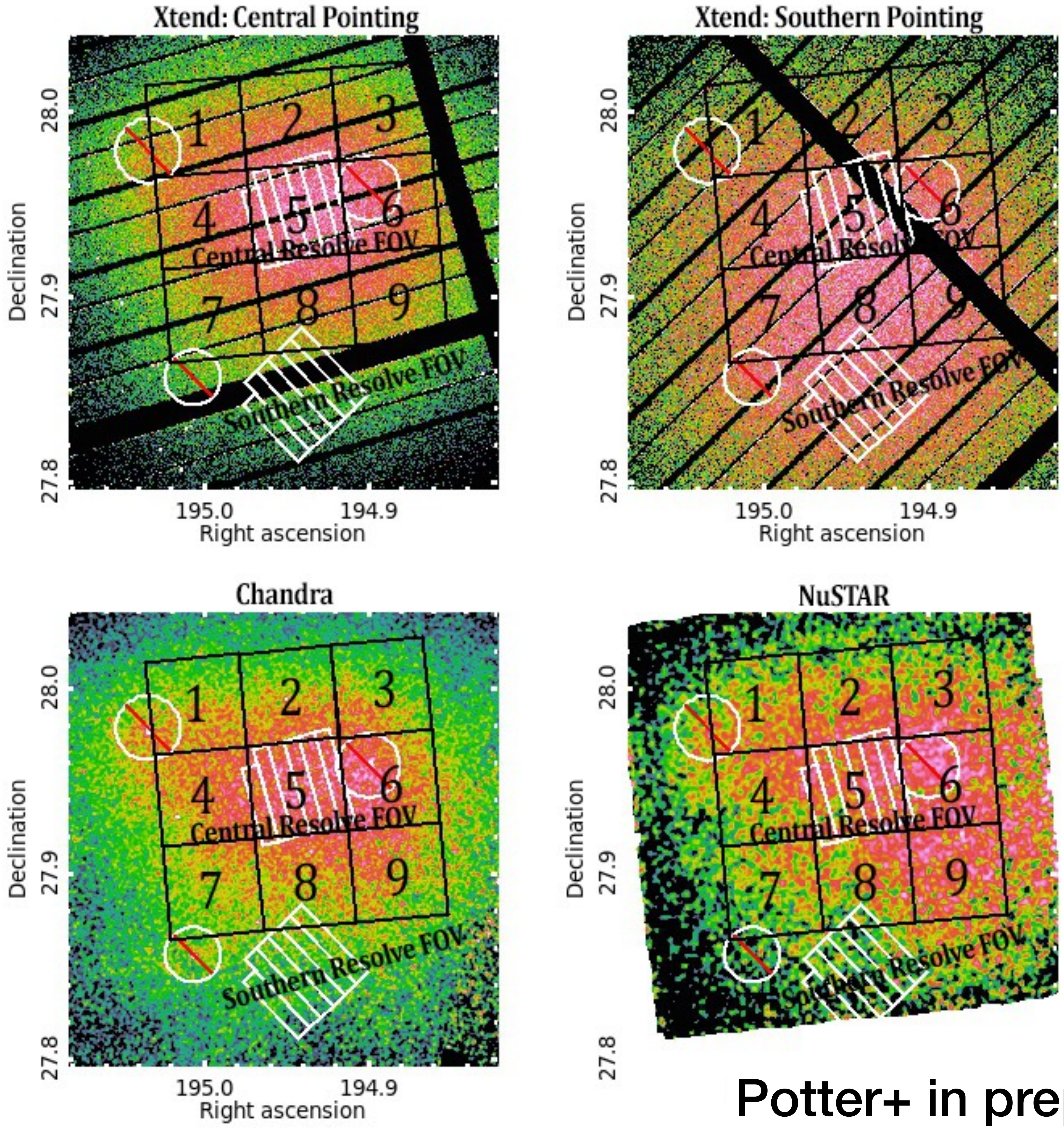

Potter+ in prep

Comparison using Resolve FOVs

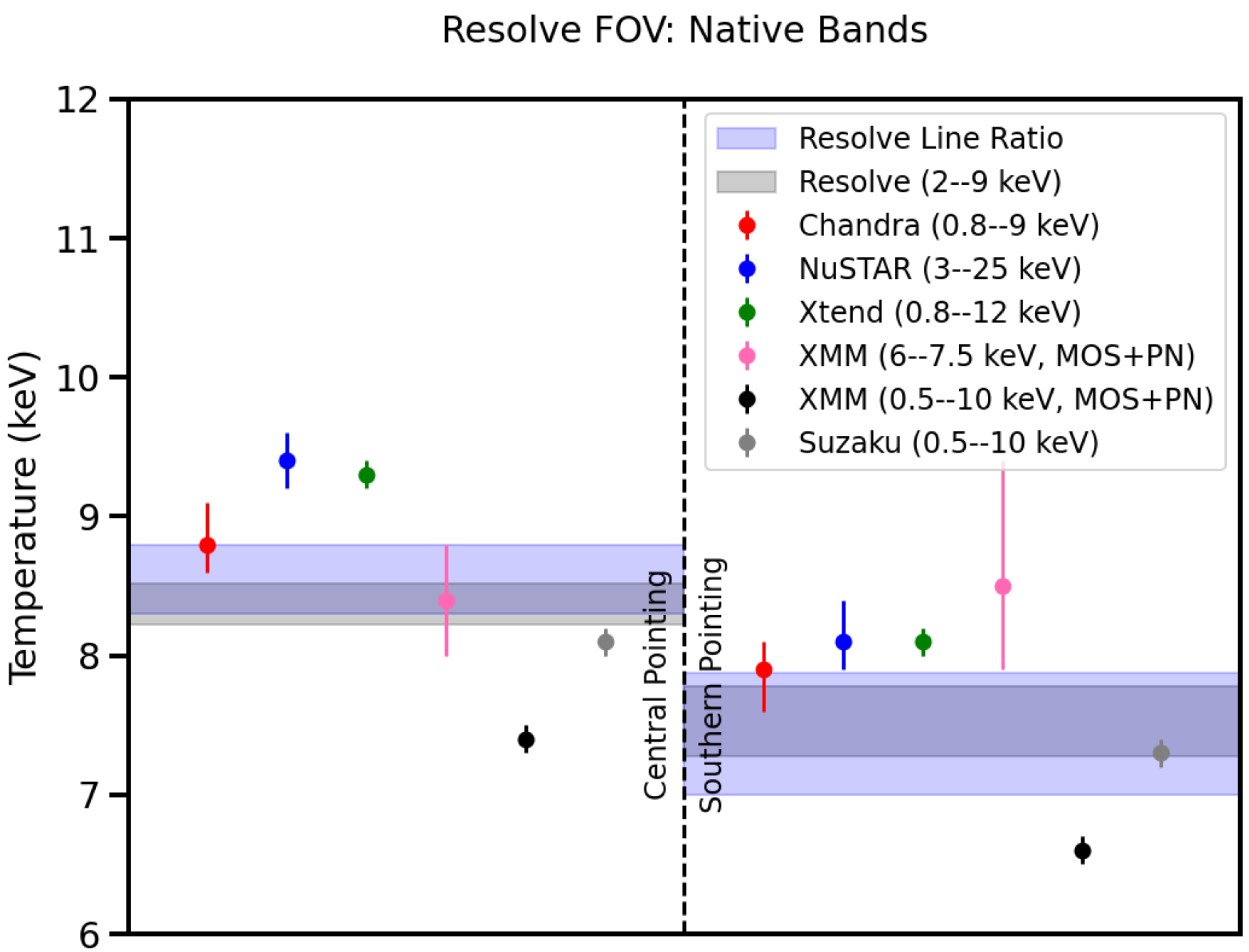

Same as Region 5 in the following slides

Potter+ in prep

Comparison using Resolve FOVs

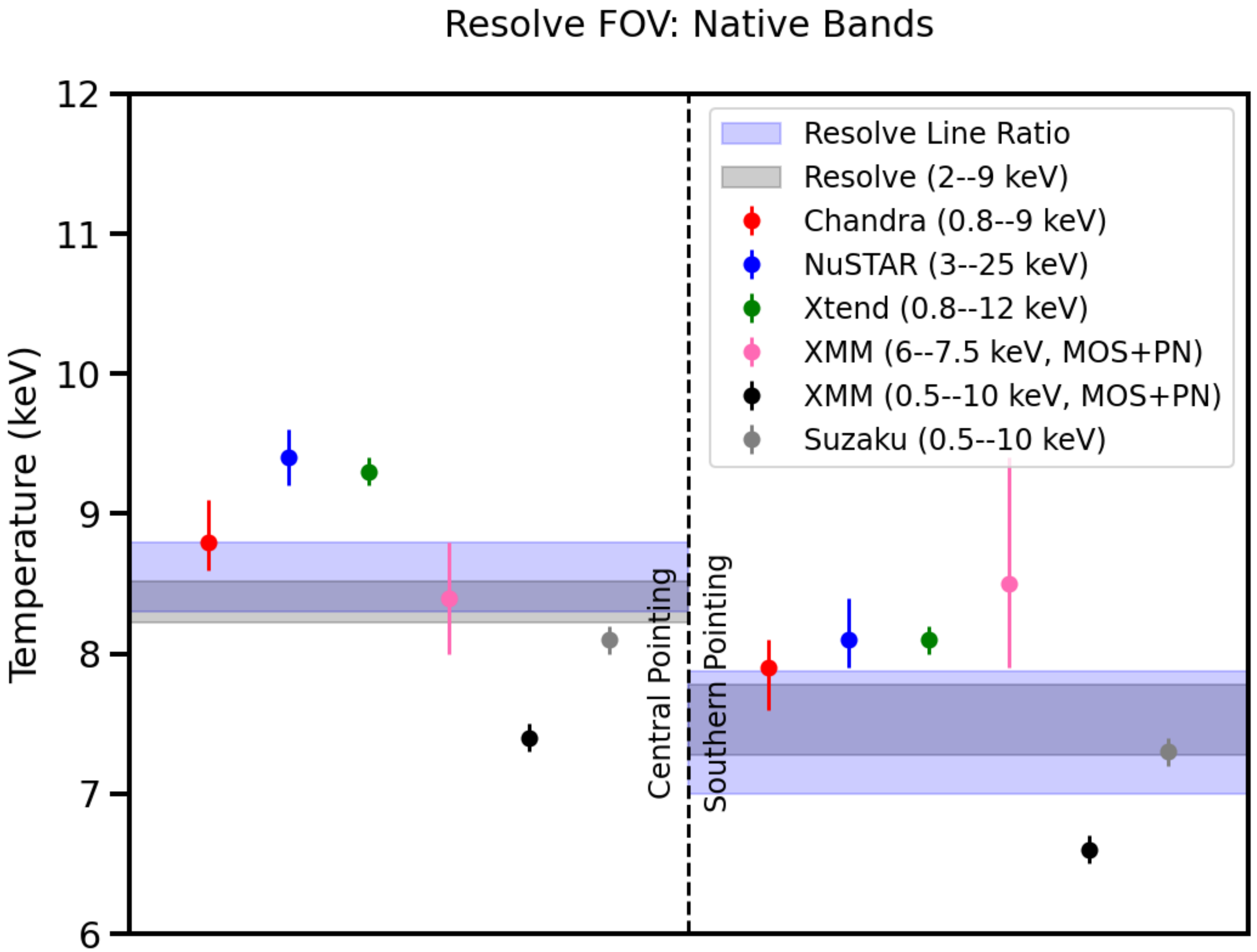

Same as Region 5 in the following slides

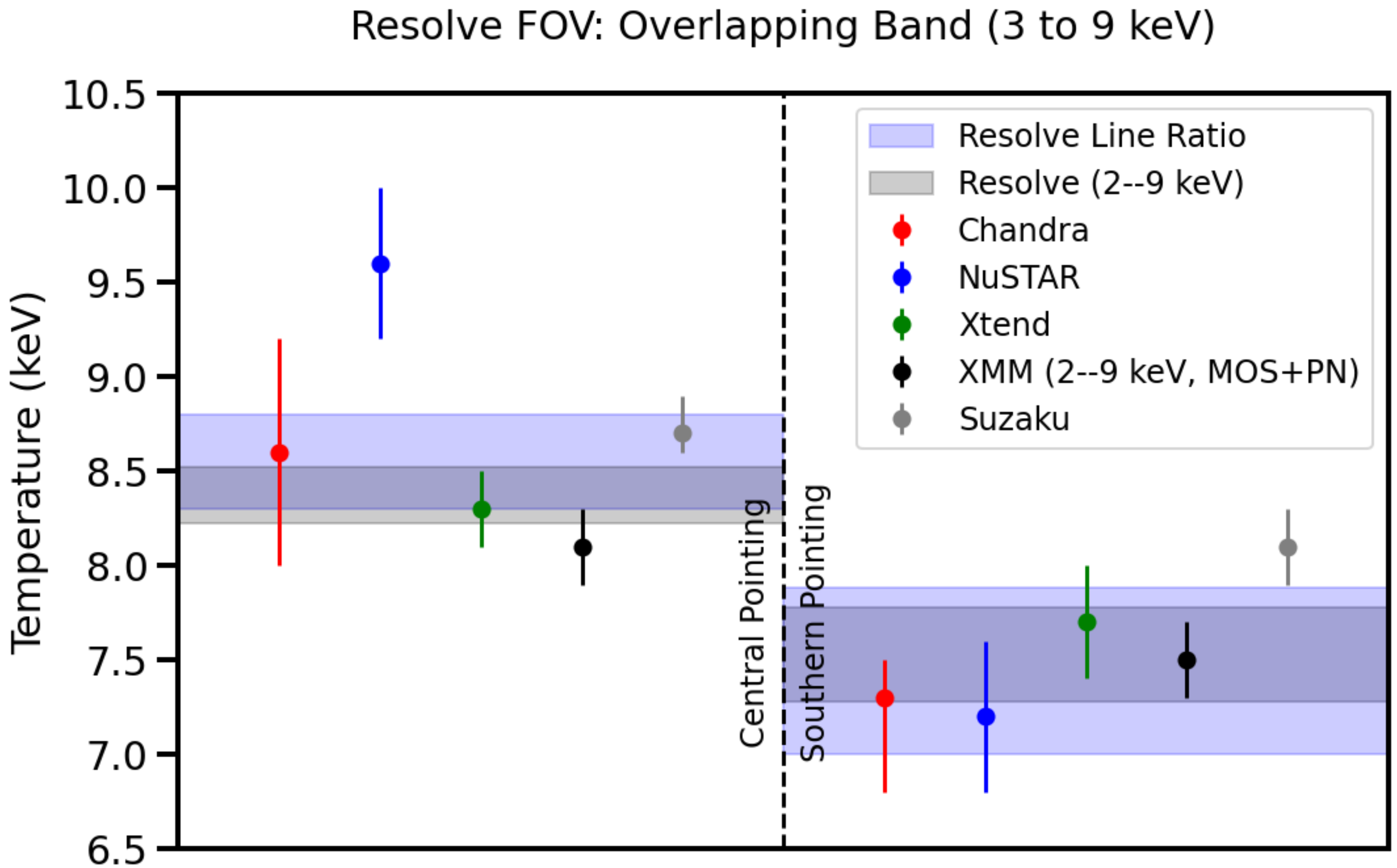

Same as Region 5 in the following slides

Potter+ in prep

Measurements in 9 Grid Regions

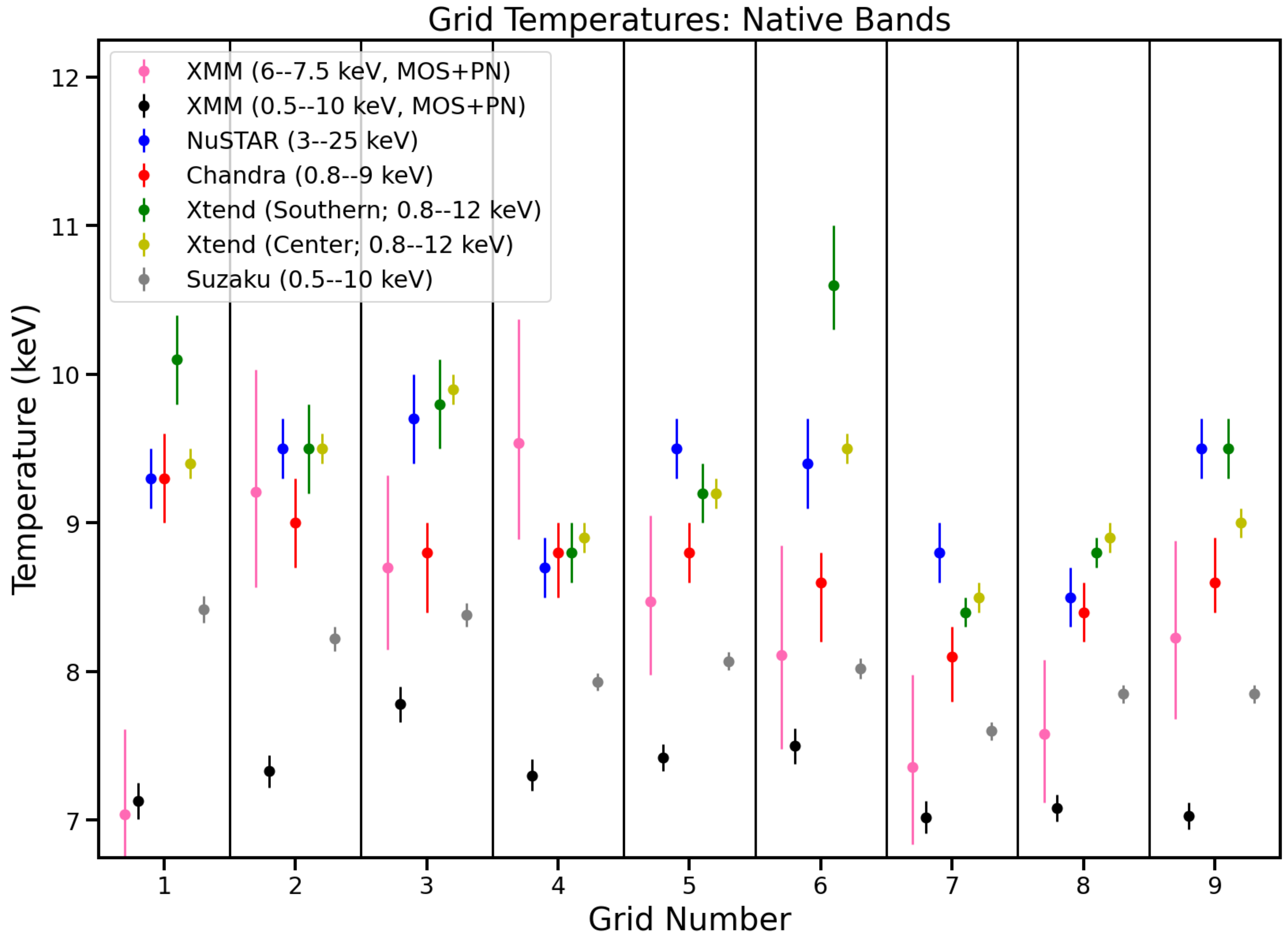

Potter+ in prep

Measurements in 9 Grid Regions

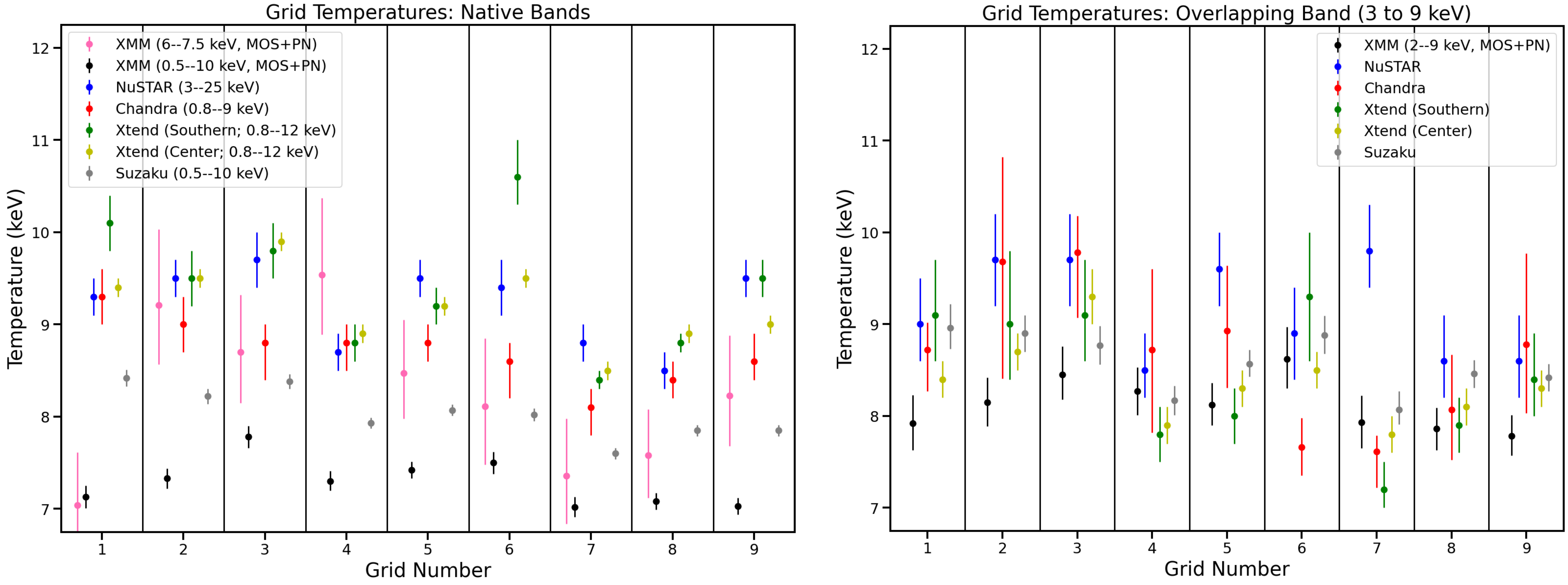

Potter+ in prep

Measurements in 9 Grid Regions

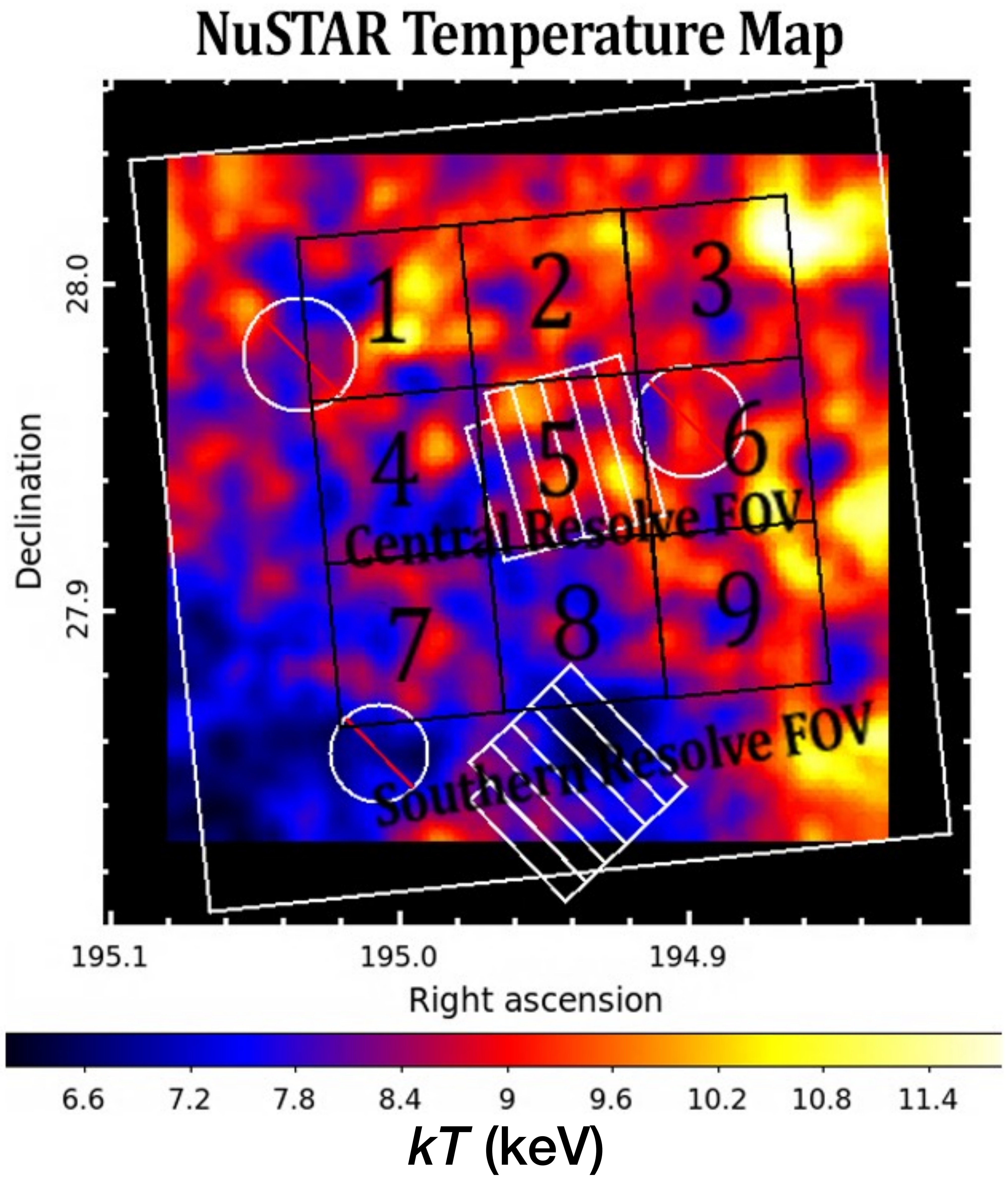

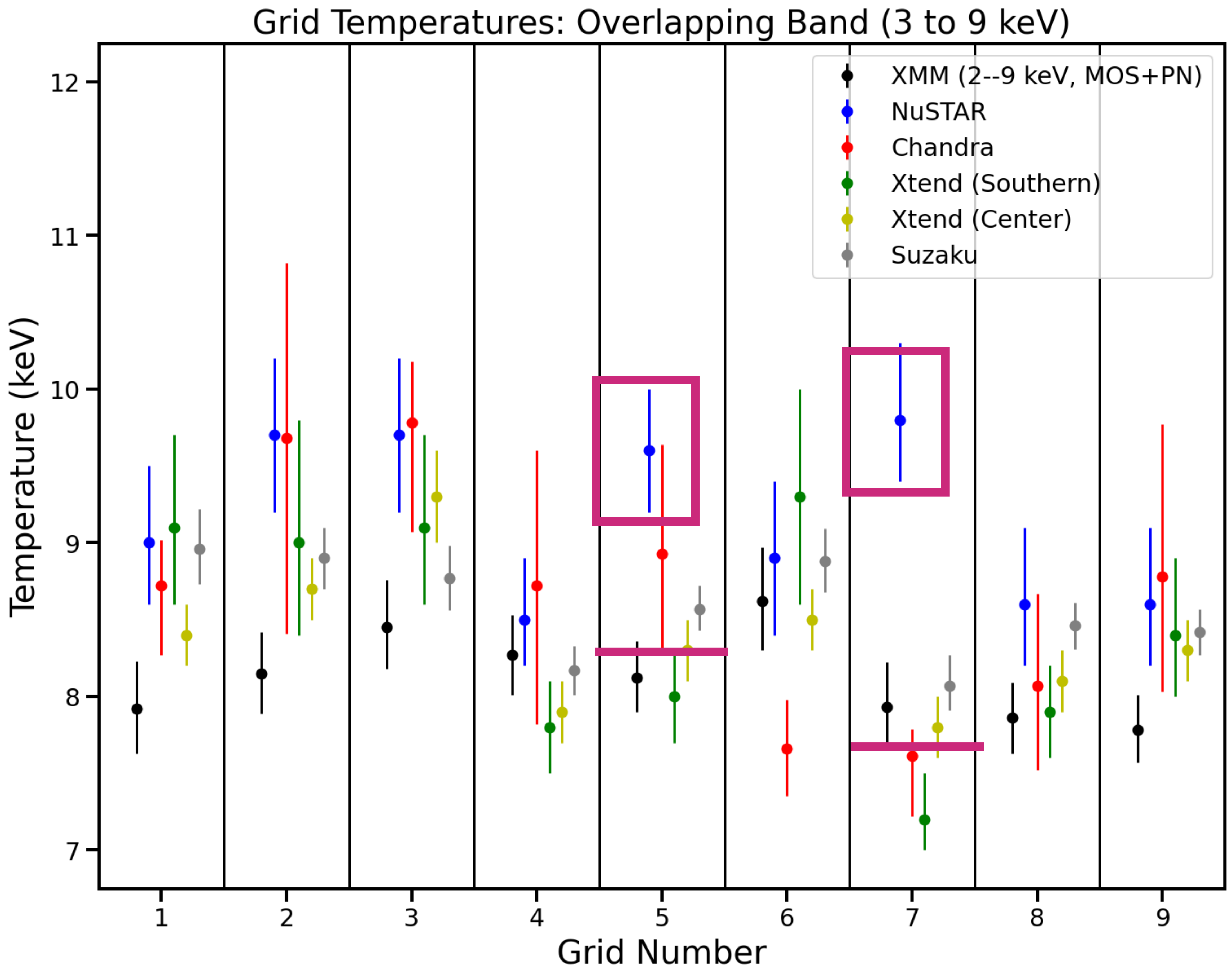

Potter+ in prep

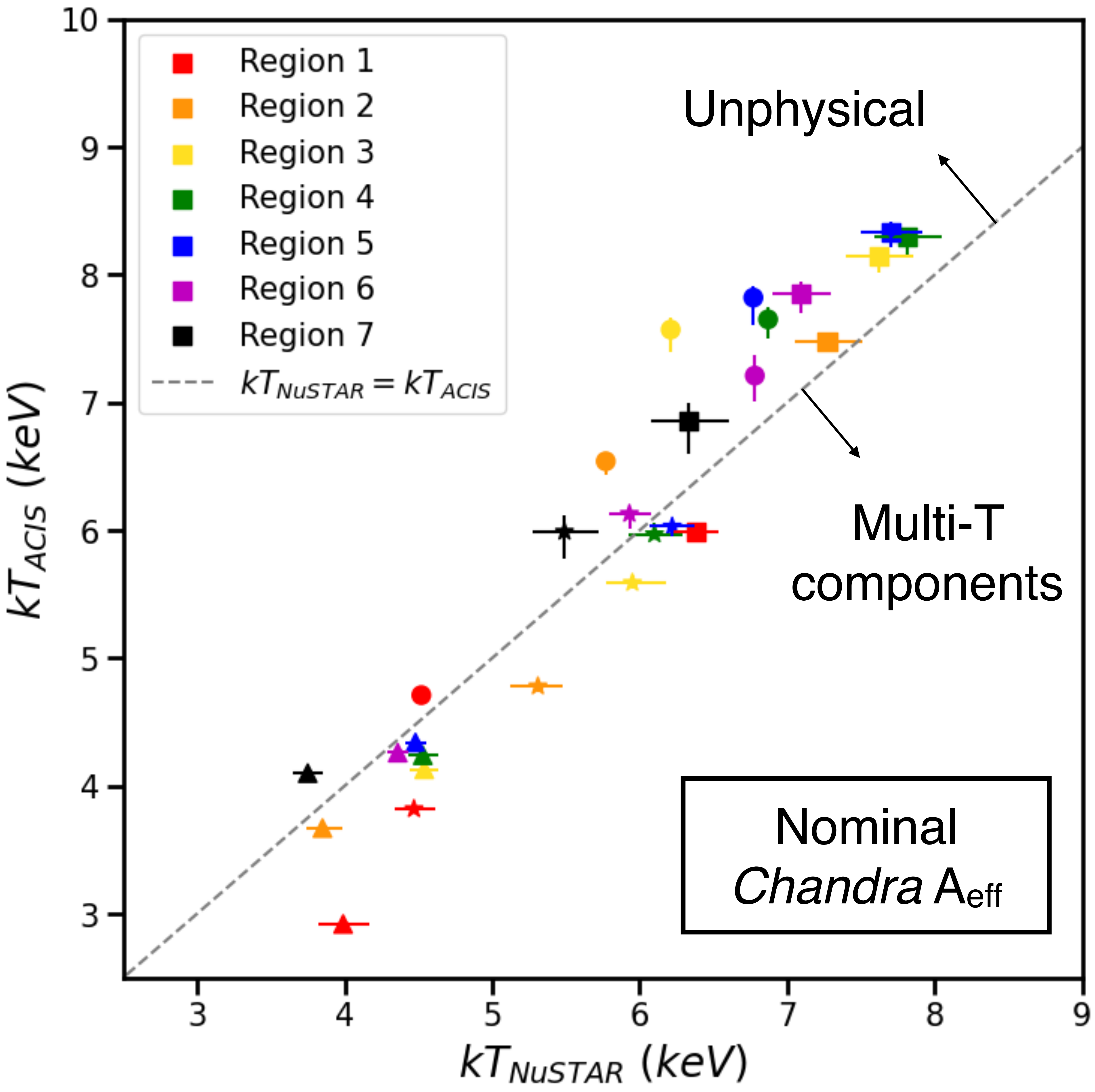

Region 1
Region 2
Region 3
Region 4
Region 5
Region 6
Region 7
$kT_{NuSTAR} = kT_{ACIS}$
Unphysical
Multi-T components
Nominal *Chandra* A_{eff}
kT_{ACIS} (keV)
kT_{NuSTAR} (keV)
10
9
8
7
6
5
4
3
3
4
5
6
7
8
9

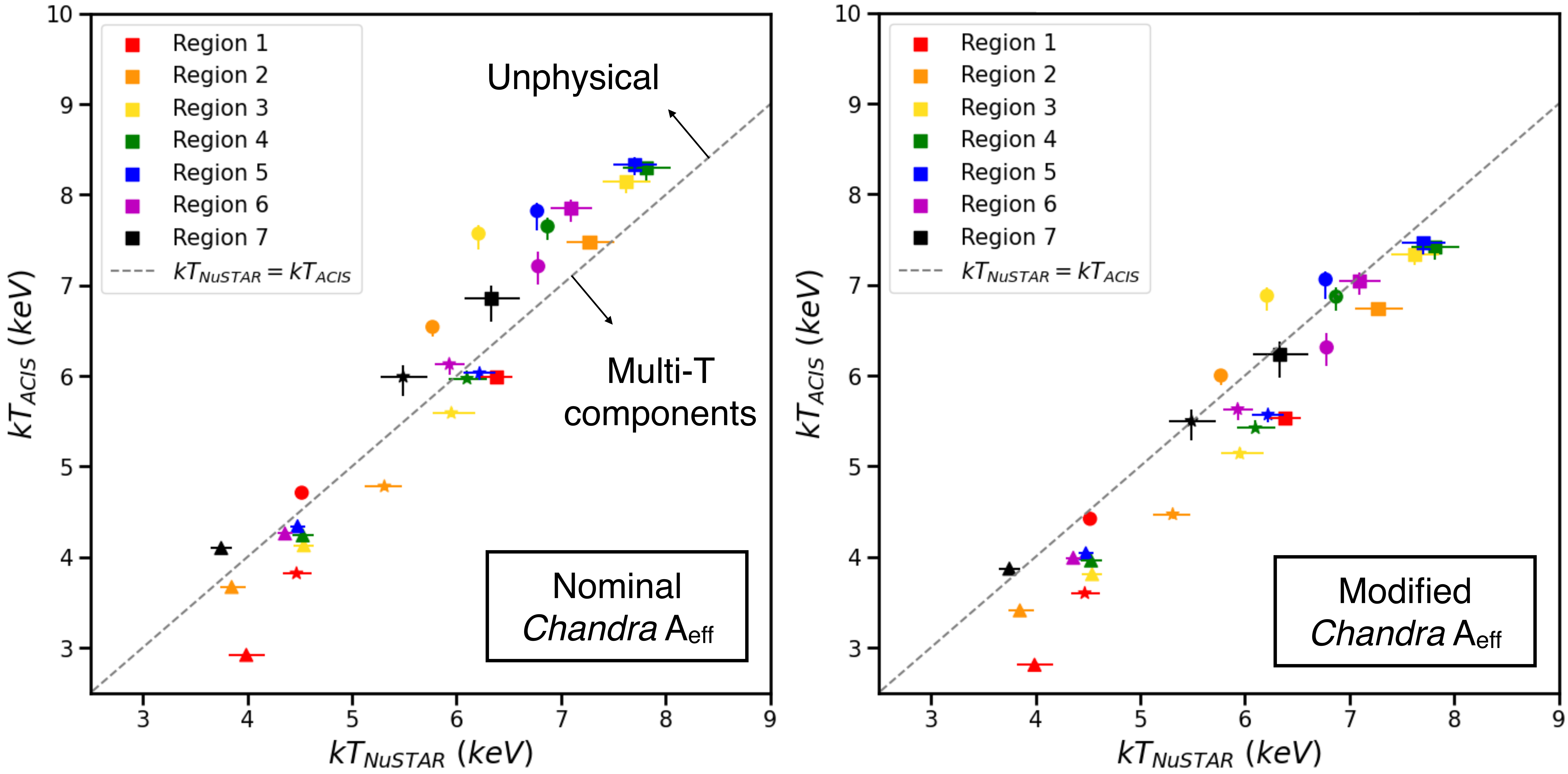

Region 1
Region 2
Region 3
Region 4
Region 5
Region 6
Region 7
$kT_{NuSTAR} = kT_{ACIS}$
Unphysical
Multi-T components
Nominal *Chandra* A_{eff}
Modified *Chandra* A_{eff}
kT_{ACIS} (keV)
kT_{NuSTAR} (keV)

Future Work (funded, for now…)

- A correction to *Chandra*'s hard band effective area similar to *XMM-Newton*'s achieves better agreement with *NuSTAR*, although it's not perfect
- The *XMM-Newton* effective area correction tends to exacerbate disagreement with *NuSTAR*; temperatures pushed even lower
- Need to do spatially resolved comparisons across the archives, find patterns to track down potential origins of discrepancies

Cluster	t_{Nu} (ks)	t_{Ch} (ks)	t_{XMM} (ks)	Cluster	t_{Nu} (ks)	t_{Ch} (ks)	t_{XMM} (ks)
Bullet	294	584	47	Abell 754	124	190	312
ZWCL 1856d8	268	43	13	Abell 2255	123	45	42
A2146	265	2386	-	Abell S753	121	87	133
SPT CLJ2031m4037	238	259	30	Abell 2163	117	90	153
Ophiuchus	232	283	230	Abell 2029	102	184	198
Abell 478	222	153	130	Coma	60	486	281
Abell 523	209	30	230	ZWCL 1856d8p6616	29	43	12
Abell 3266	208	35	187	RXC J1504	24	164	300
Abell 665	198	161	266	Abell 3112	22	152	228
CL 0217p70	177	25	-	Abell 3158	22	62	32
RX J1347d5m1145	172	331	38	Abell 1644S	21	71	34
Abell 2256	166	218	296	Abell 3558	21	15	68
MACS J0717d5p3745	163	247	195	Abell 496	20	105	291
CIZA 0107d7p5408	159	165	-	Abell 3391	20	68	69
Abell 1795	154	3552	137	Abell 1651	20	10	27
Abell 2199	138	160	180	Abell 3571	18	34	34
Abell 2319	134	91	92	Abell 1650	18	252	43
Abell 3395	129	120	30				

Future Work (funded, for now…)

- A correction to *Chandra*'s hard band effective area similar to *XMM-Newton*'s achieves better agreement with *NuSTAR*, although it's not perfect
- The *XMM-Newton* effective area correction tends to exacerbate disagreement with *NuSTAR*; temperatures pushed even lower
- Need to do spatially resolved comparisons across the archives, find patterns to track down potential origins of discrepancies

Cluster	t_{Nu} (ks)	t_{Ch} (ks)	t_{XMM} (ks)	Cluster	t_{Nu} (ks)	t_{Ch} (ks)	t_{XMM} (ks)
Bullet	294	584	47	Abell 754	124	190	312
ZWCL 1856d8	268	43	13	Abell 2255	123	45	42
A2146	265	2386	-	Abell S753	121	87	133
SPT CLJ2031m4037	238	259	30	Abell 2163	117	90	153
Ophiuchus	232	283	230	Abell 2029	102	184	198
Abell 478	222	153	130	Coma	60	486	281
Abell 523	209	30	230	ZWCL 1856d8p6616	29	43	12
Abell 3266	208	35	187	RXC J1504	24	164	300
Abell 665	198	161	266	Abell 3112	22	152	228
CL 0217p70	177	25	-	Abell 3158	22	62	32
RX J1347d5m1145	172	331	38	Abell 1644S	21	71	34
Abell 2256	166	218	296	Abell 3558	21	15	68
MACS J0717d5p3745	163	247	195	Abell 496	20	105	291
CIZA 0107d7p5408	159	165	-	Abell 3391	20	68	69
Abell 1795	154	3552	137	Abell 1651	20	10	27
Abell 2199	138	160	180	Abell 3571	18	34	34
Abell 2319	134	91	92	Abell 1650	18	252	43
Abell 3395	129	120	30				

Backup Slides

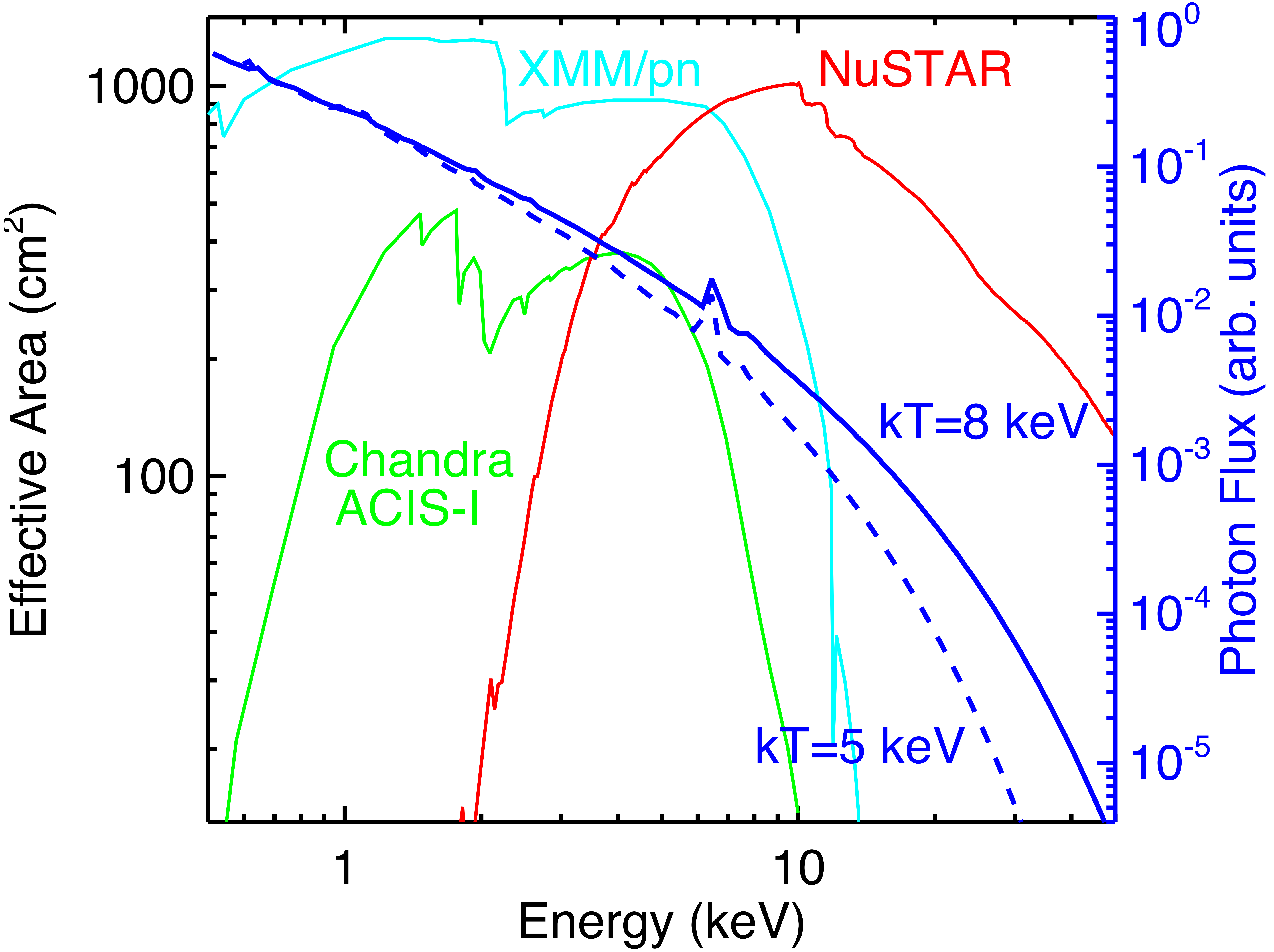

XMM/pn
NuSTAR
Chandra
ACIS-I
kT=8 keV
kT=5 keV
1000
100
1
10
Effective Area (cm^2)
Energy (keV)
10^0
10^{-1}
10^{-2}
10^{-3}
10^{-4}
10^{-5}
Photon Flux (arb. units)

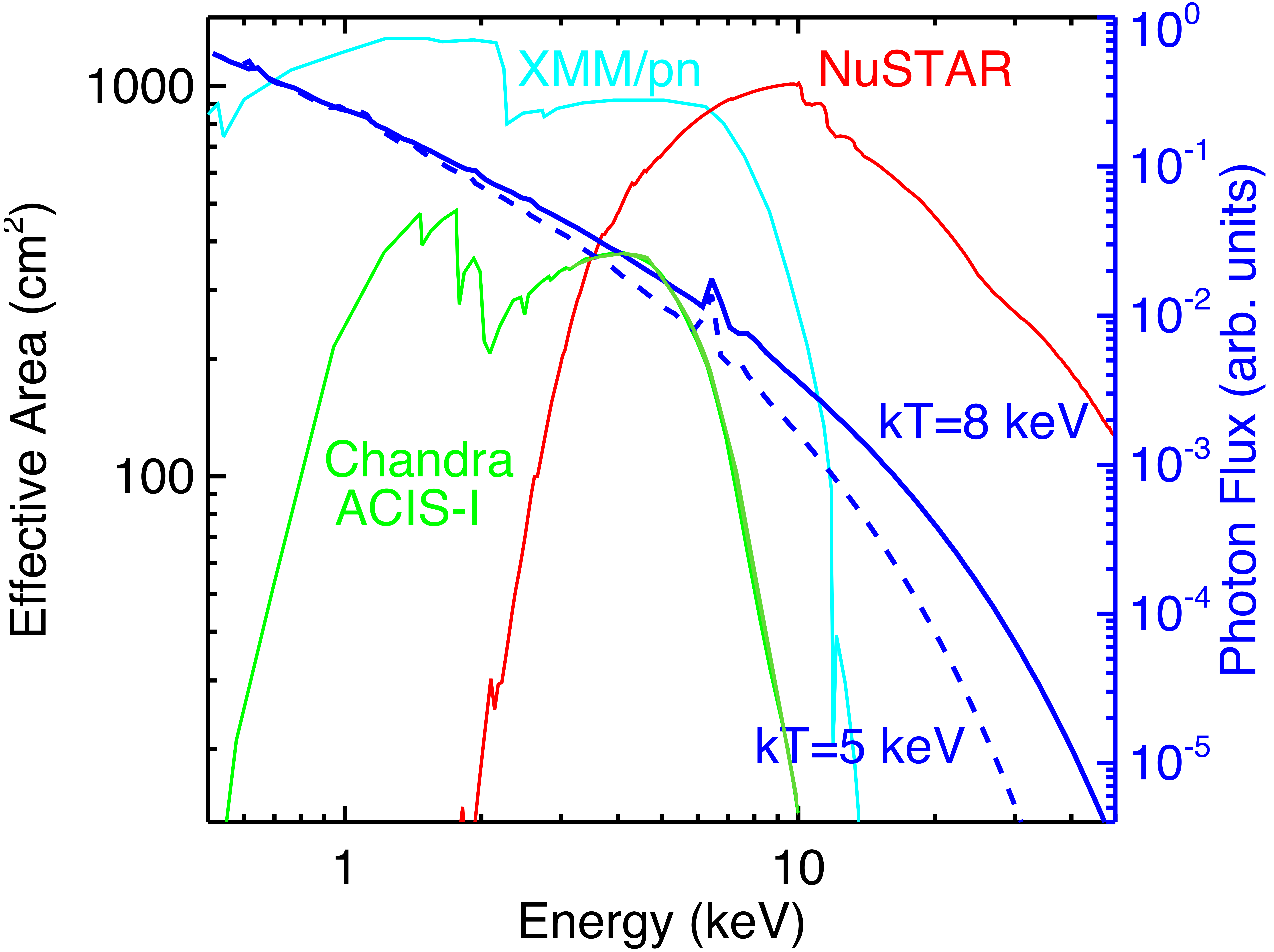

XMM/pn
NuSTAR
Chandra
ACIS-I
kT=8 keV
kT=5 keV
1000
100
1
10
10^0
10^{-1}
10^{-2}
10^{-3}
10^{-4}
10^{-5}
Effective Area (cm^2)
Photon Flux (arb. units)
Energy (keV)

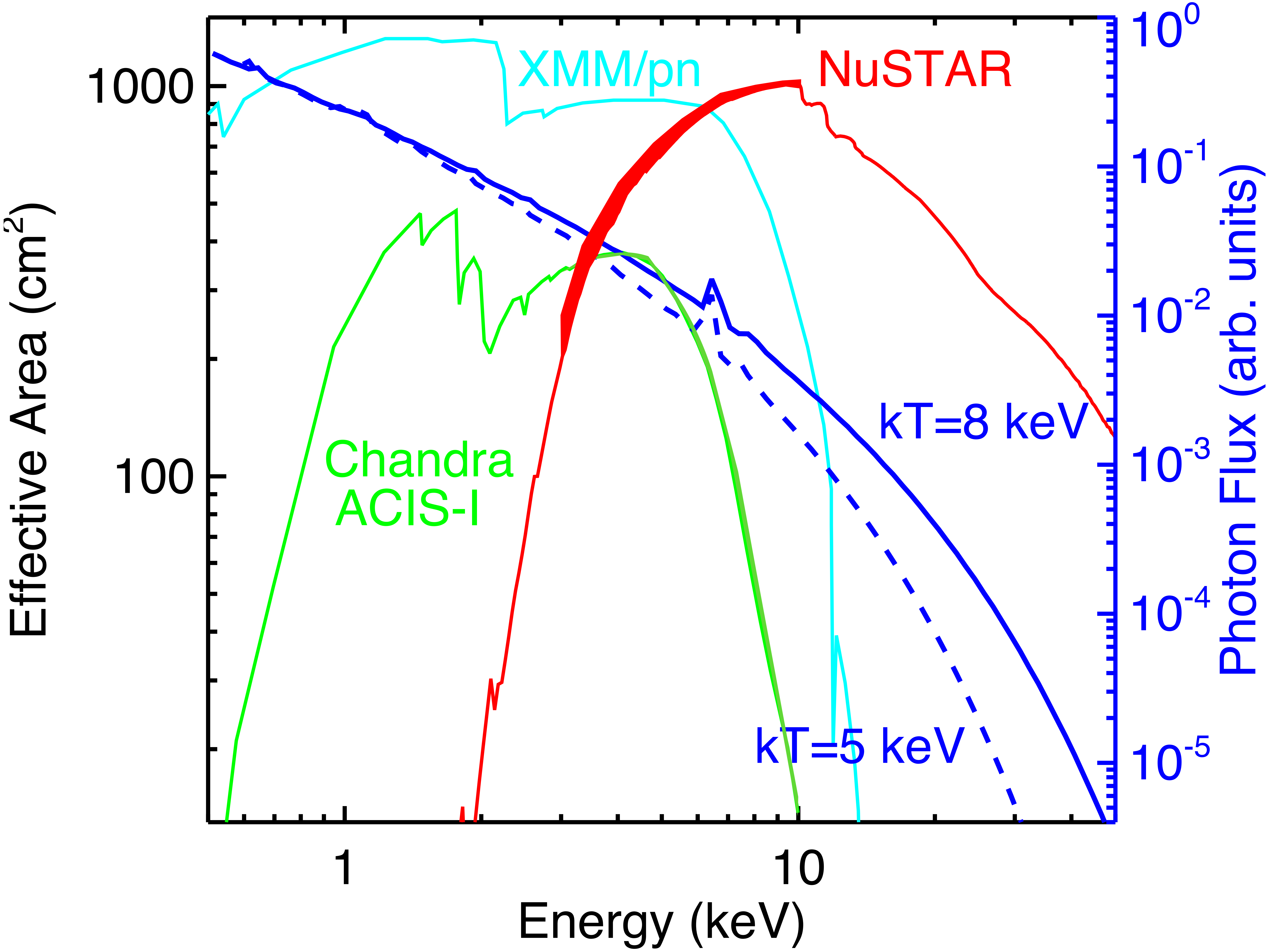

XMM/pn
NuSTAR
Chandra
ACIS-I
kT=8 keV
kT=5 keV
1000
100
1
10
Effective Area (cm^2)
Energy (keV)
Photon Flux (arb. units)
10^0
10^{-1}
10^{-2}
10^{-3}
10^{-4}
10^{-5}

Abell 2029, 5th Annulus

Nominal Chandra ARF

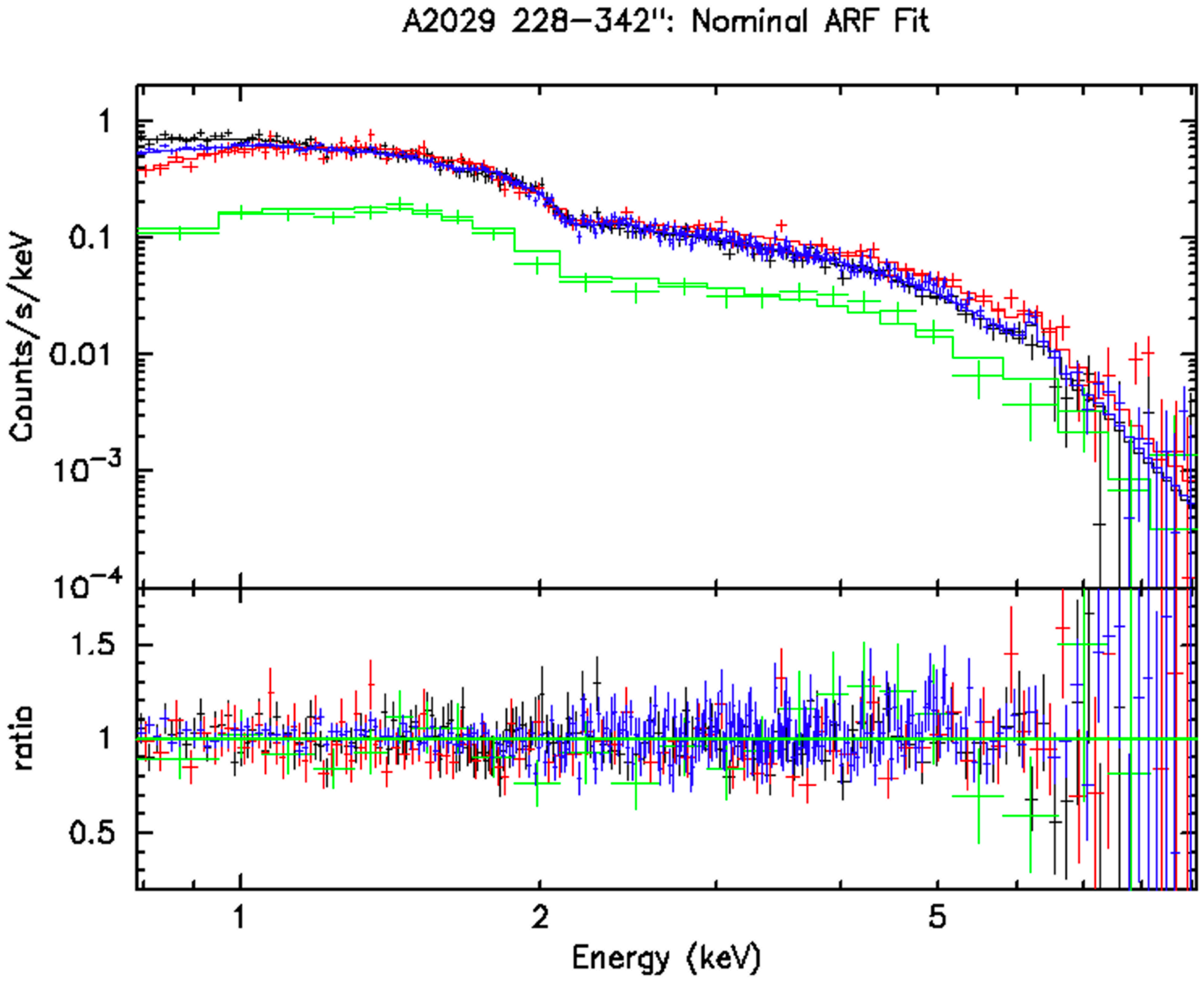

Modified Chandra ARF

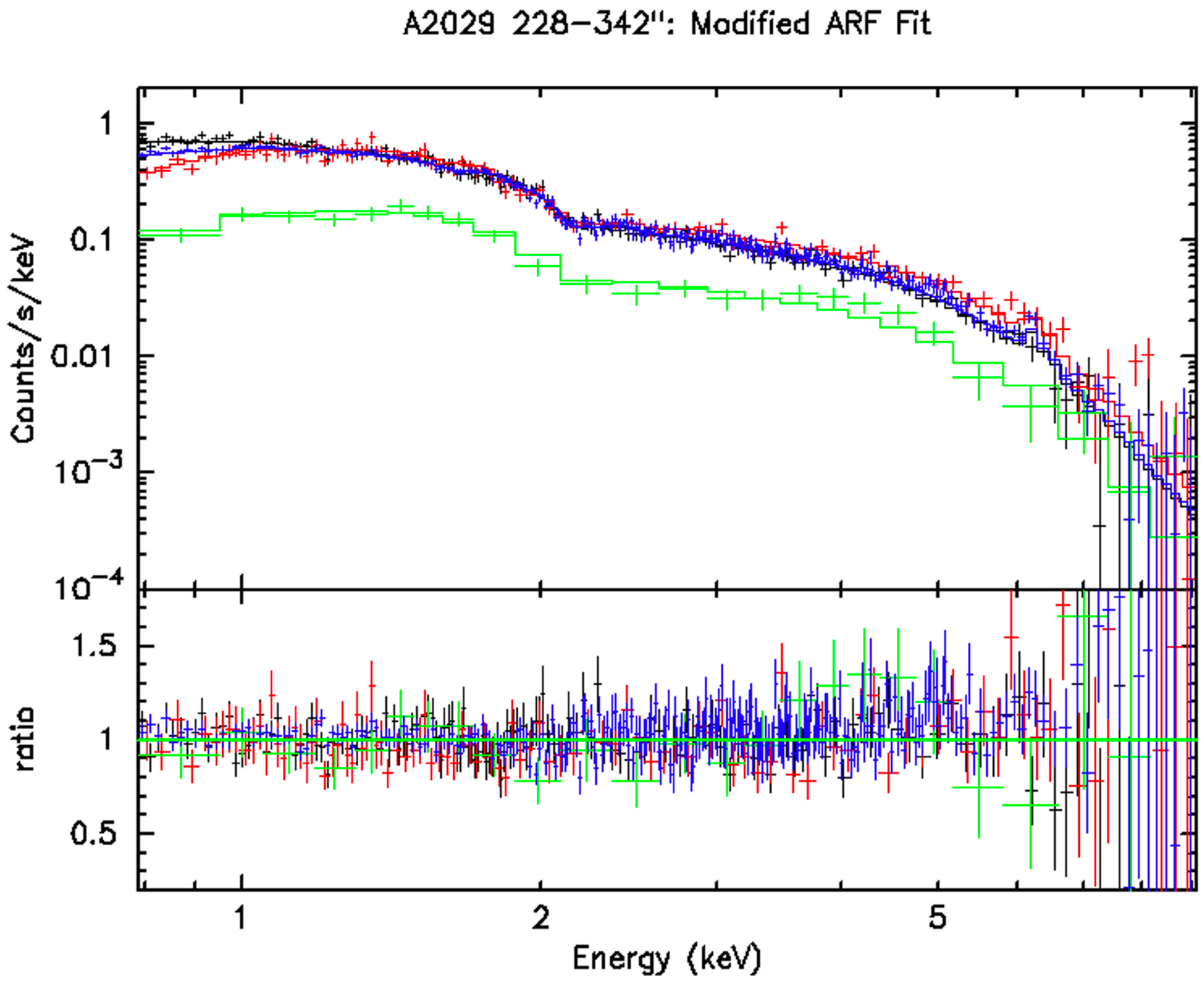

Abell 2199, 5th Annulus

Nominal Chandra ARF

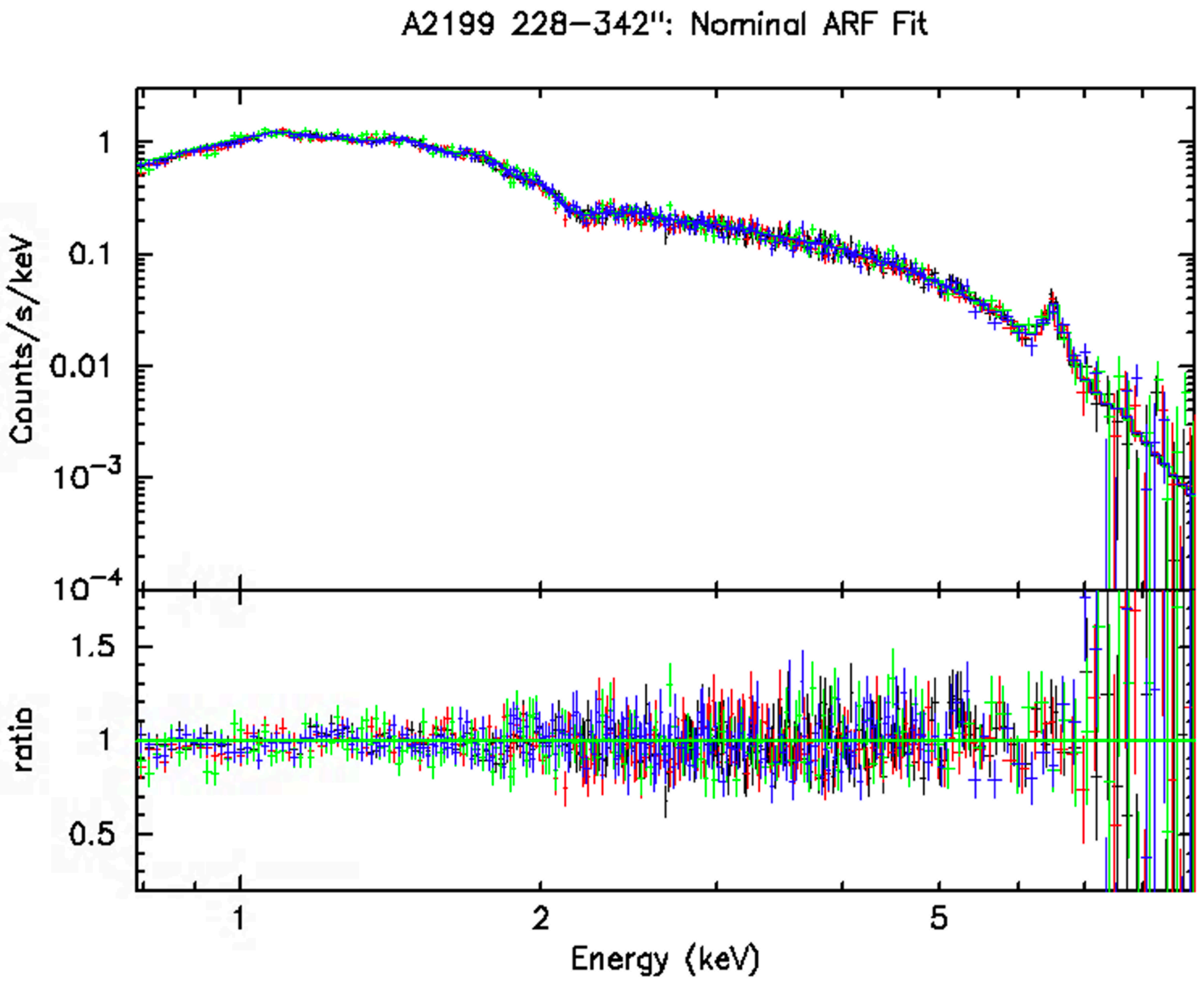

Modified Chandra ARF

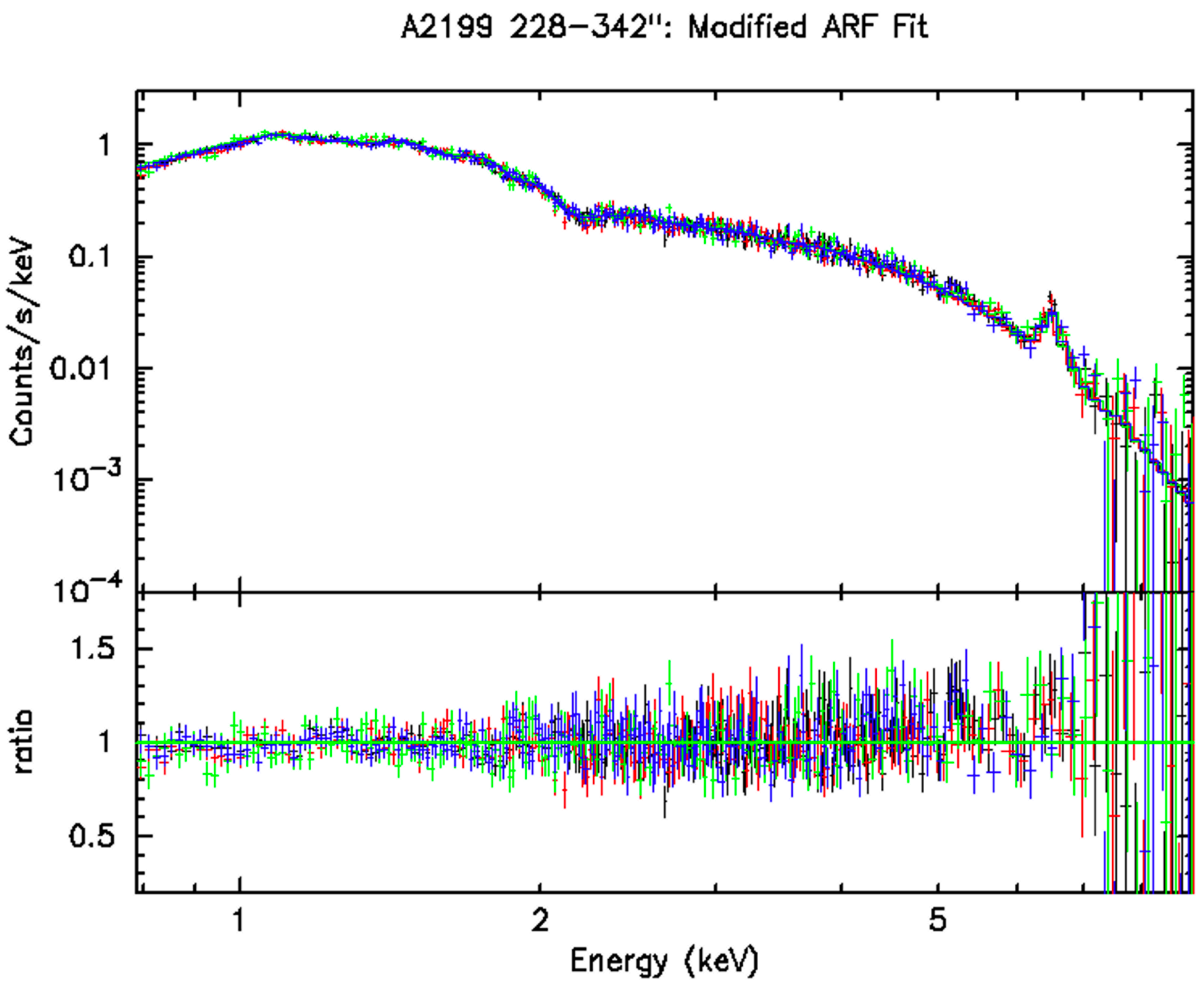

Deep observations of relaxed clusters
Nominal Chandra ARFs

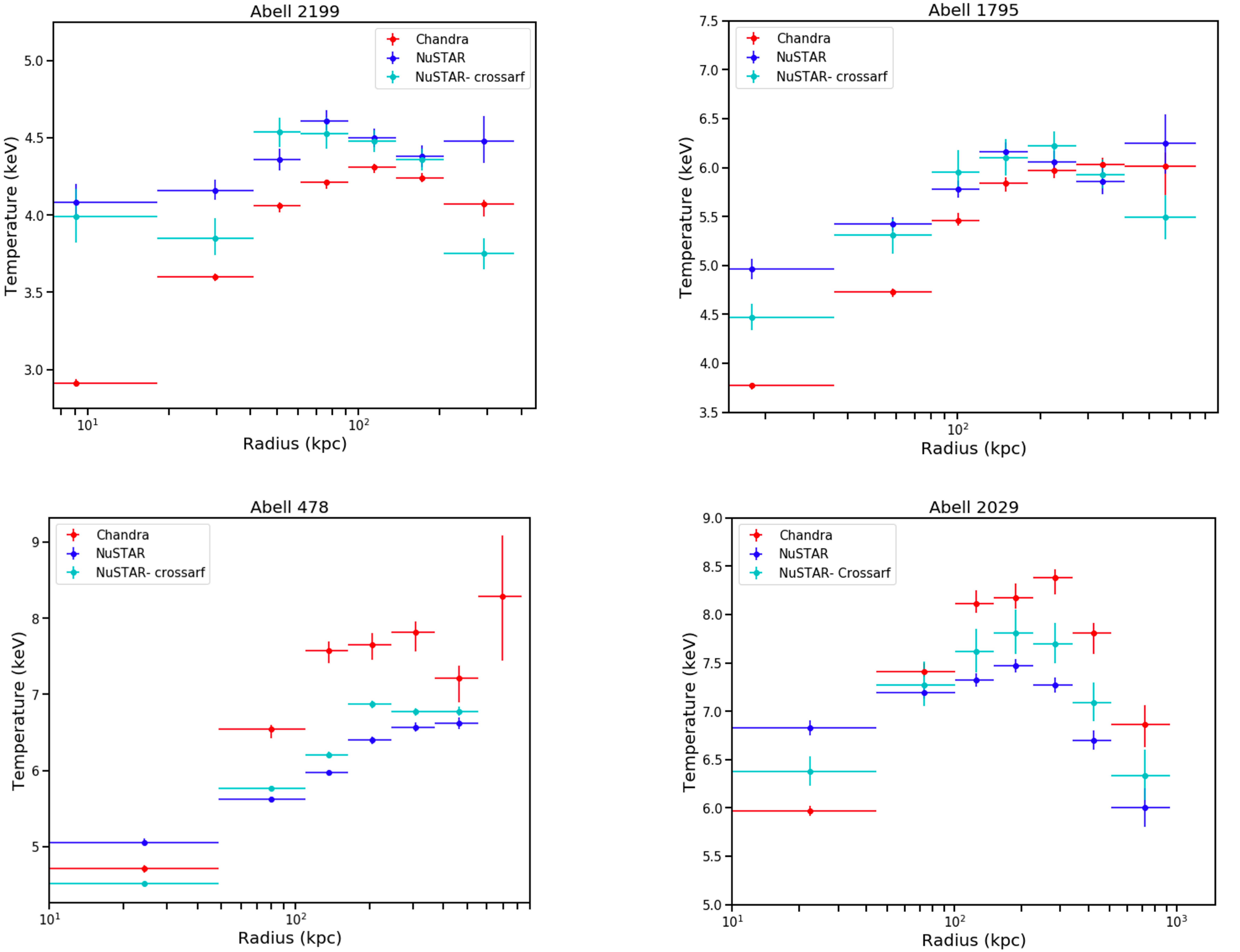

Potter+ in prep

Deep observations of relaxed clusters
Modified Chandra ARFs

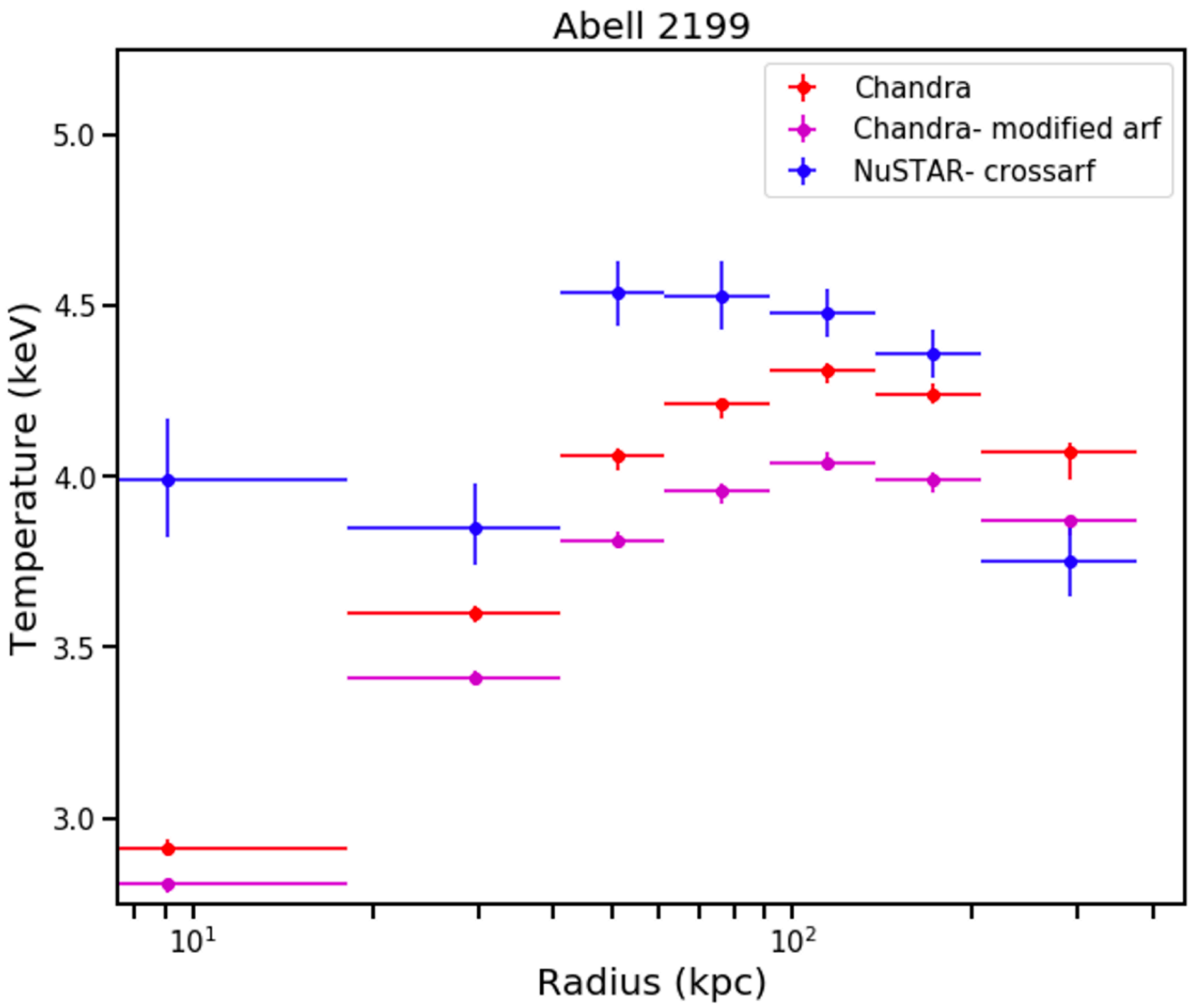

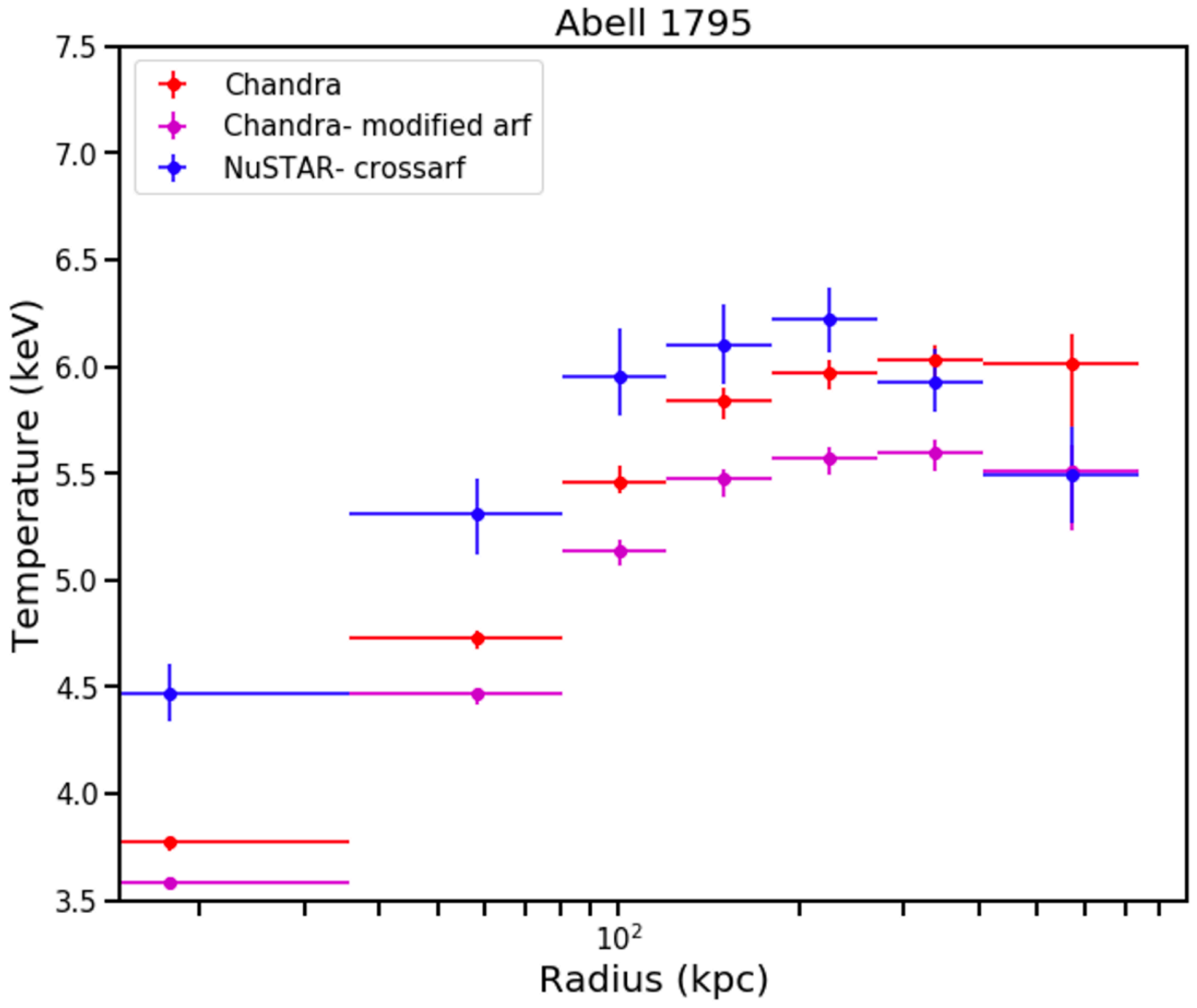

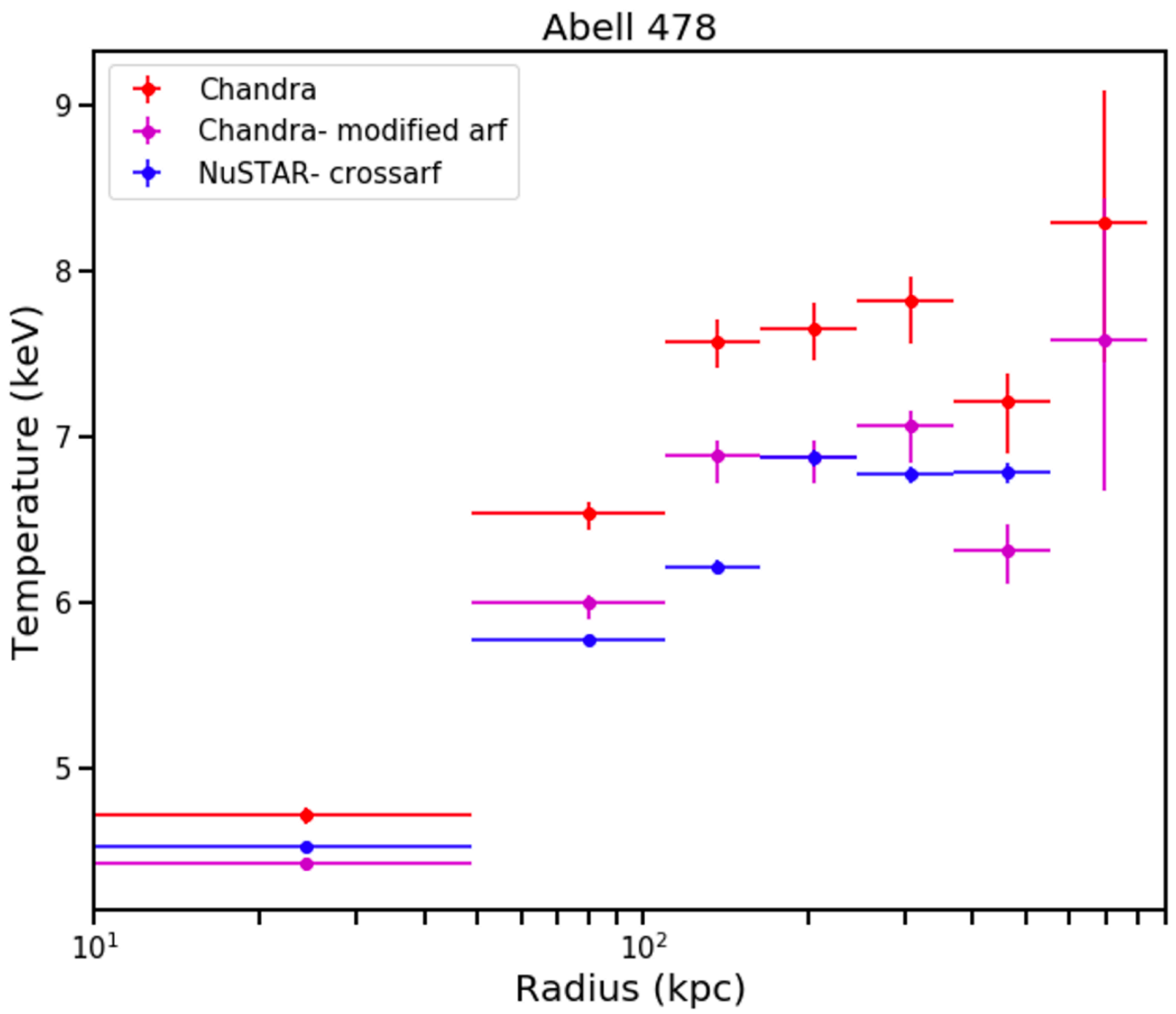

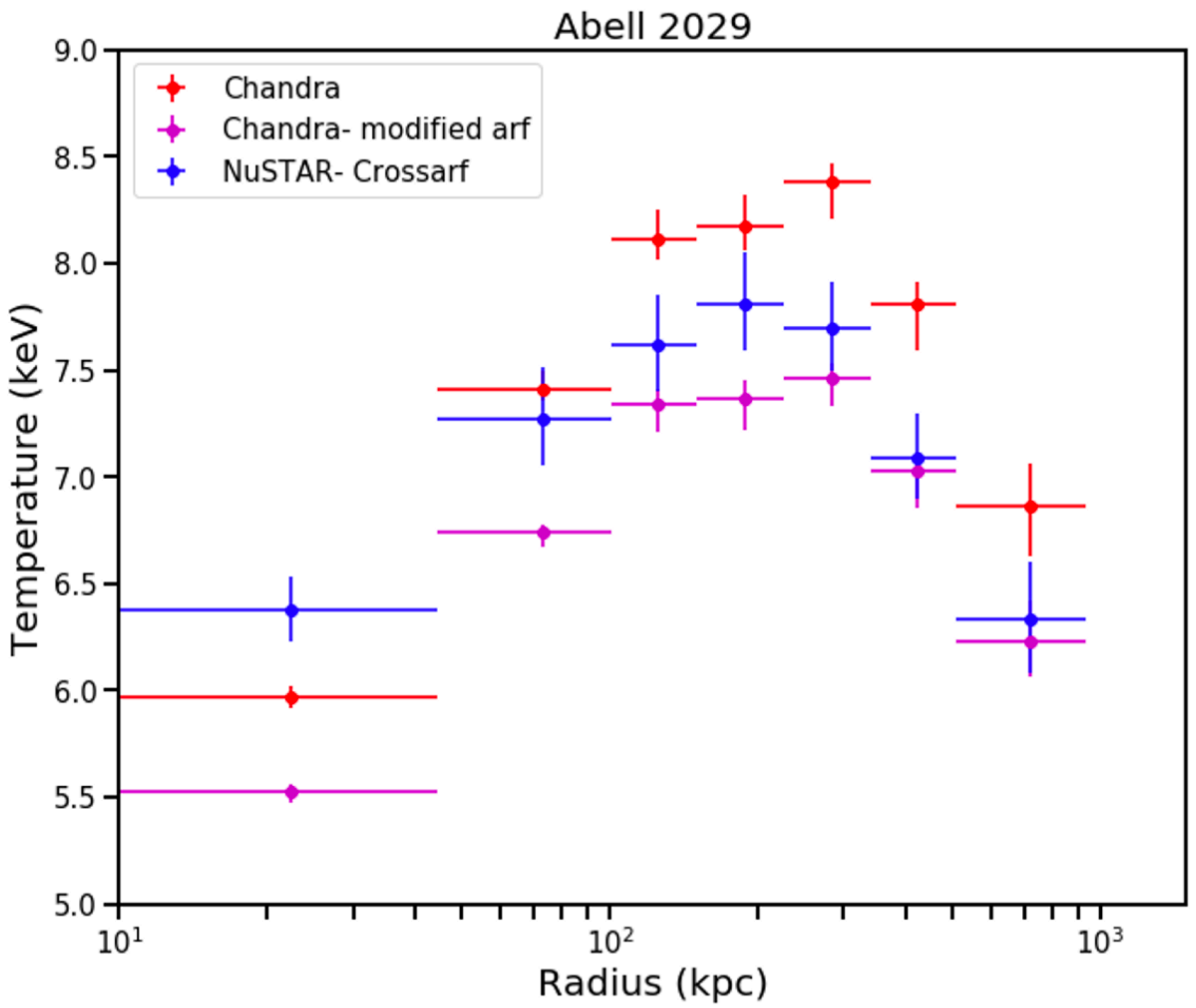

Potter+ in prep

Snapshot Cluster Temperatures

Lopez+ 2025 submitted

Cluster Name	Redshift z	Gain Offset keV	kT_c keV	kT_X keV	kT_N keV	kT_{Ni} keV
RXC J1504	0.2172	-0.10 ± 0.04	$9.81^{+0.80}_{-0.79}$	$6.40^{+0.20}_{-0.16}$	$8.55^{+1.09}_{-0.95}$	$5.93^{+0.18}_{-0.33}$
Abell 3571	0.0390	-0.09 ± 0.02	$8.10^{+0.08}_{-0.08}$	$6.36^{+0.06}_{-0.03}$	$7.12^{+0.10}_{-0.20}$	
Abell 3558	0.0484	-0.05 ± 0.03	$7.42^{+0.27}_{-0.28}$	$5.51^{+0.08}_{-0.08}$	$6.00^{+0.40}_{-0.40}$	$6.23^{+0.30}_{-0.30}$
Abell 1651	0.0850	-0.09 ± 0.04	$7.07^{+0.25}_{-0.25}$	$6.09^{+0.12}_{-0.12}$	$6.73^{+0.20}_{-0.14}$	
Abell 3391	0.0561	-0.10 ± 0.07	$6.62^{+0.22}_{-0.22}$	$5.54^{+0.13}_{-0.09}$	$6.24^{+0.40}_{-0.40}$	
Abell 1650	0.0838	-0.10 ± 0.04	$6.43^{+0.10}_{-0.10}$	$5.14^{+0.05}_{-0.05}$	$6.55^{+0.20}_{-0.20}$	$5.88^{+0.90}_{-0.30}$
Abell 3158	0.0592	-0.05 ± 0.05	$6.01^{+0.10}_{-0.10}$	$5.11^{+0.10}_{-0.08}$	$5.79^{+0.22}_{-0.22}$	
Abell 3112	0.0753	-0.10 ± 0.03	$5.45^{+0.12}_{-0.09}$	$4.00^{+0.06}_{-0.04}$	$5.57^{+0.40}_{-.040}$	$4.59^{+0.20}_{-0.20}$
Abell 1644	0.0474	-0.06 ± 0.05	$5.31^{+0.14}_{-0.13}$	$4.61^{+0.19}_{-0.17}$	$5.23^{+0.30}_{-0.30}$	$5.24^{+0.20}_{-0.20}$
Abell 496	0.0331	-0.07 ± 0.03	$5.18^{+0.07}_{-0.07}$	$4.39^{+0.11}_{-0.08}$	$5.40^{+0.30}_{-0.10}$	$3.82^{+0.10}_{-0.03}$

Schellenberger+ 2015

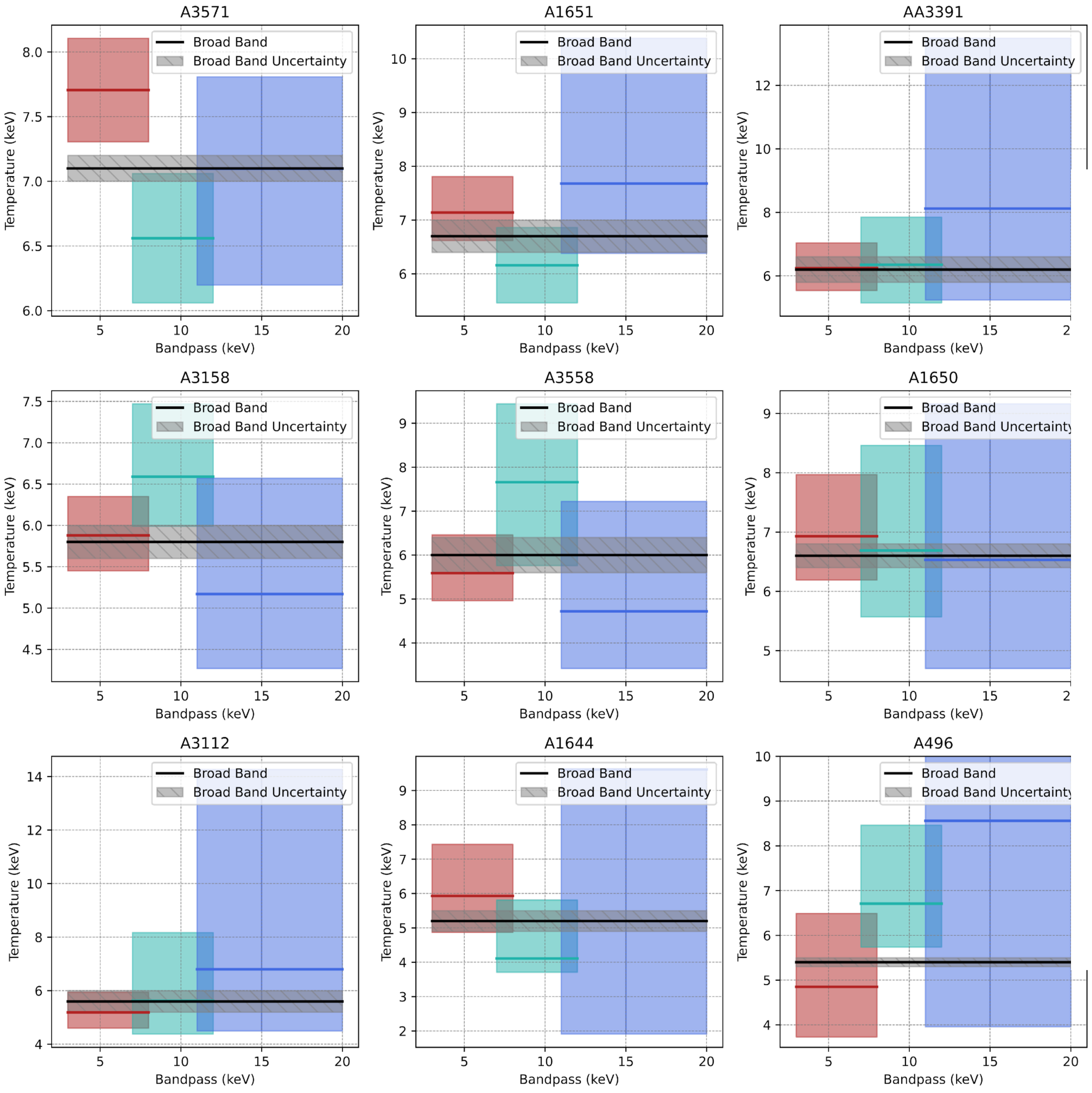
A3571
A1651
AA3391
A3158
A3558
A1650
A3112
A1644
A496
Broad Band
Broad Band Uncertainty
Temperature (keV)
Bandpass (keV)

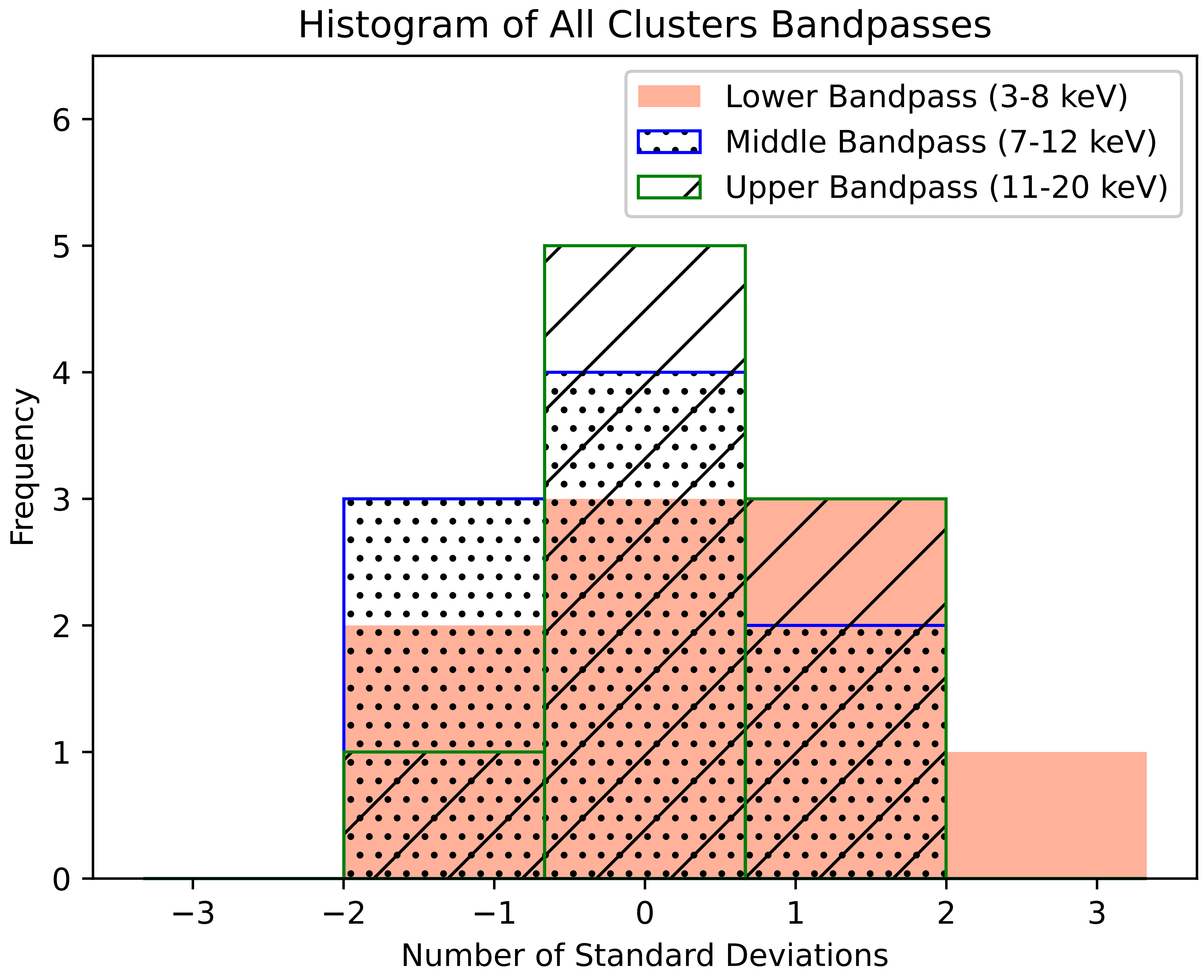
Histogram of All Clusters Bandpasses
Lower Bandpass (3-8 keV)
Middle Bandpass (7-12 keV)
Upper Bandpass (11-20 keV)
Frequency
Number of Standard Deviations

Snapshot Spectral Fits

Snapshot Spectral Fits

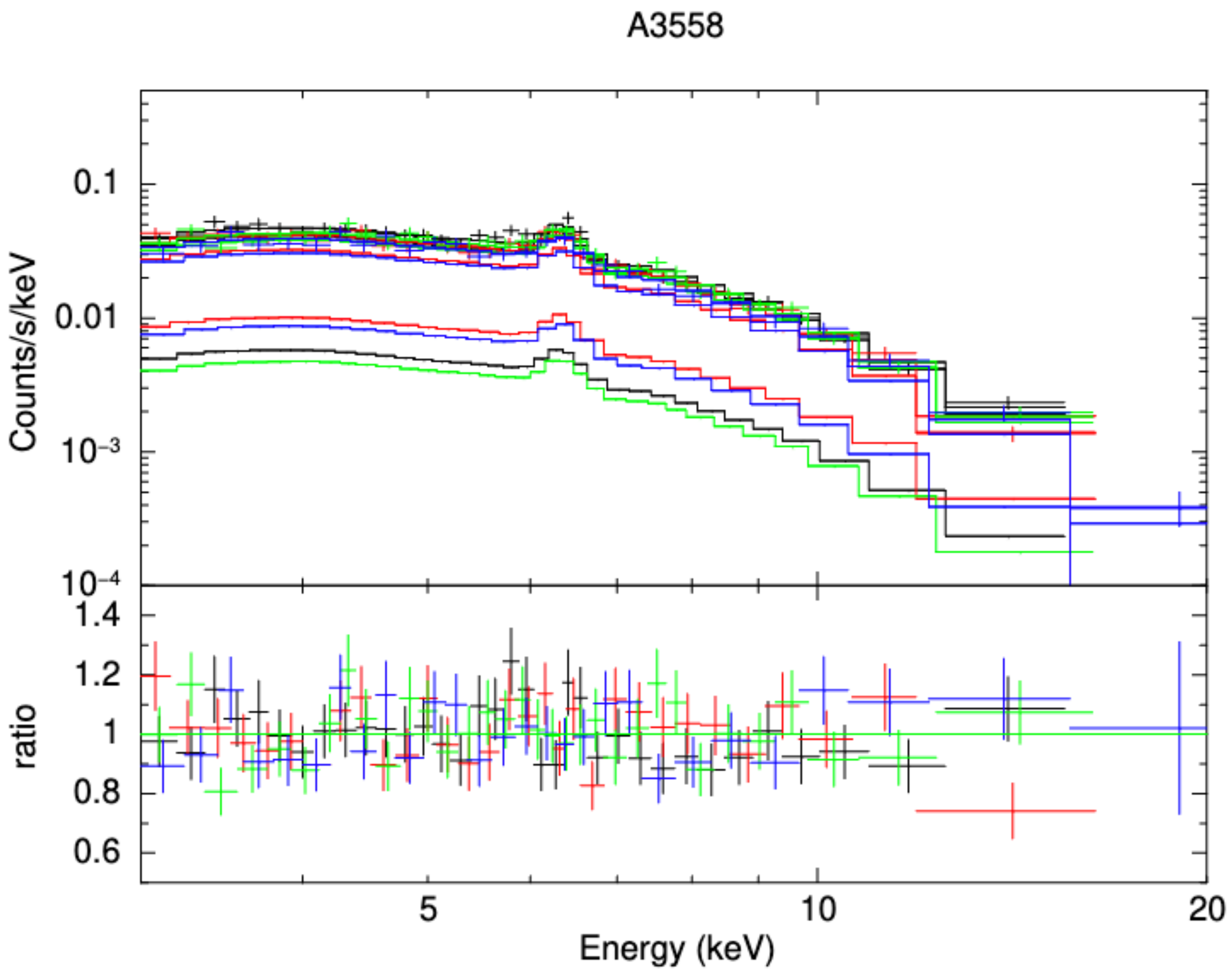

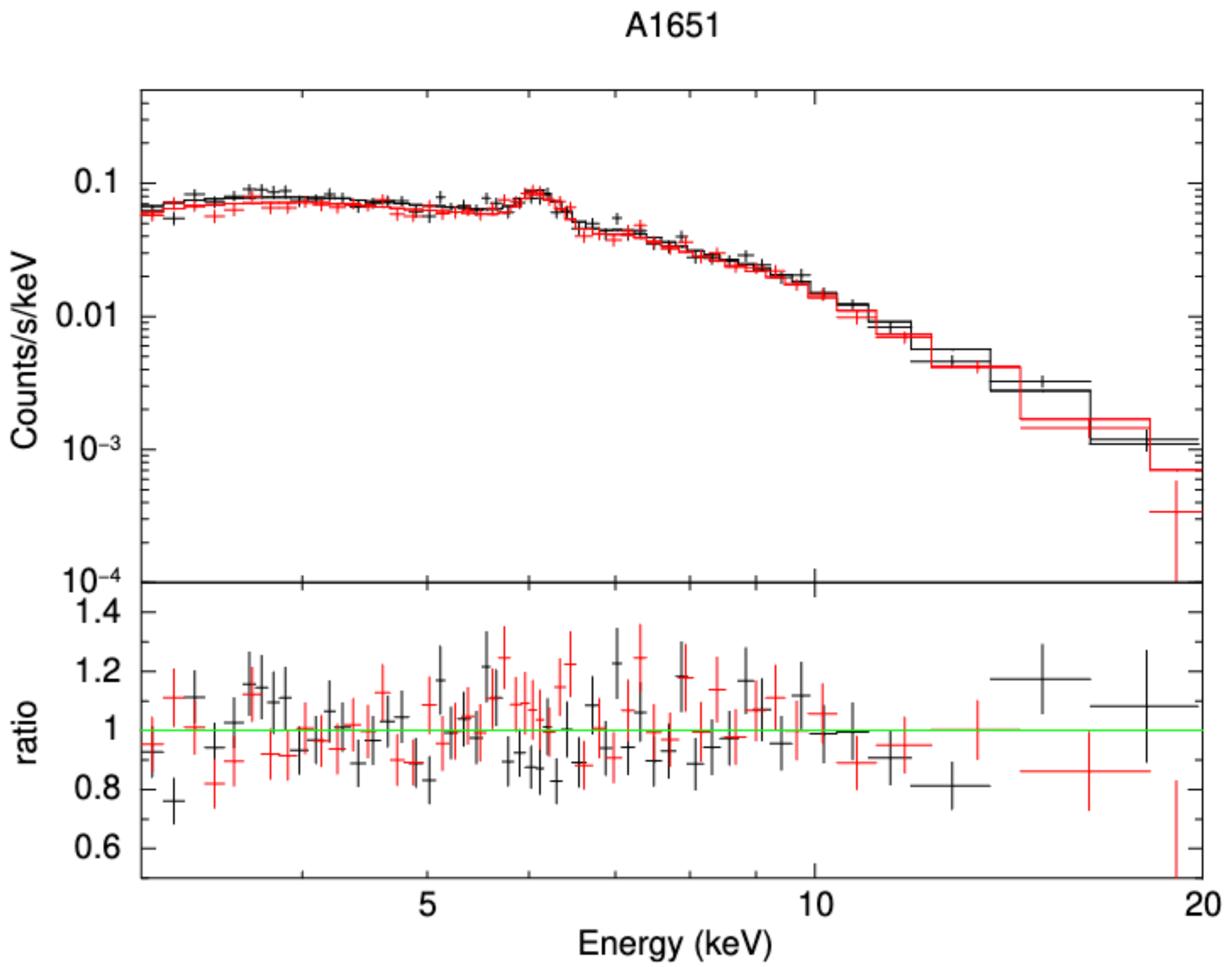

Snapshot Spectral Fits

Snapshot Spectral Fits

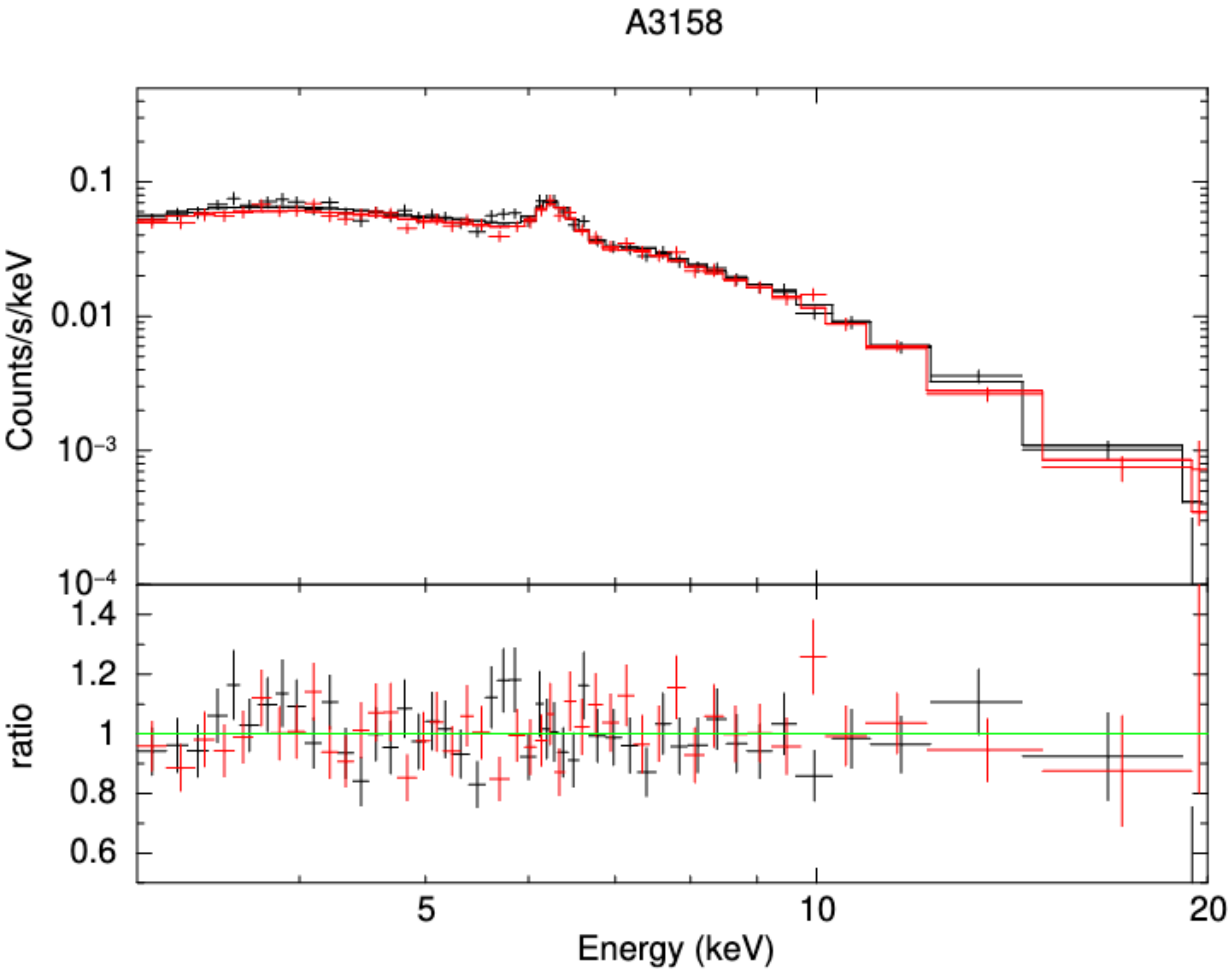

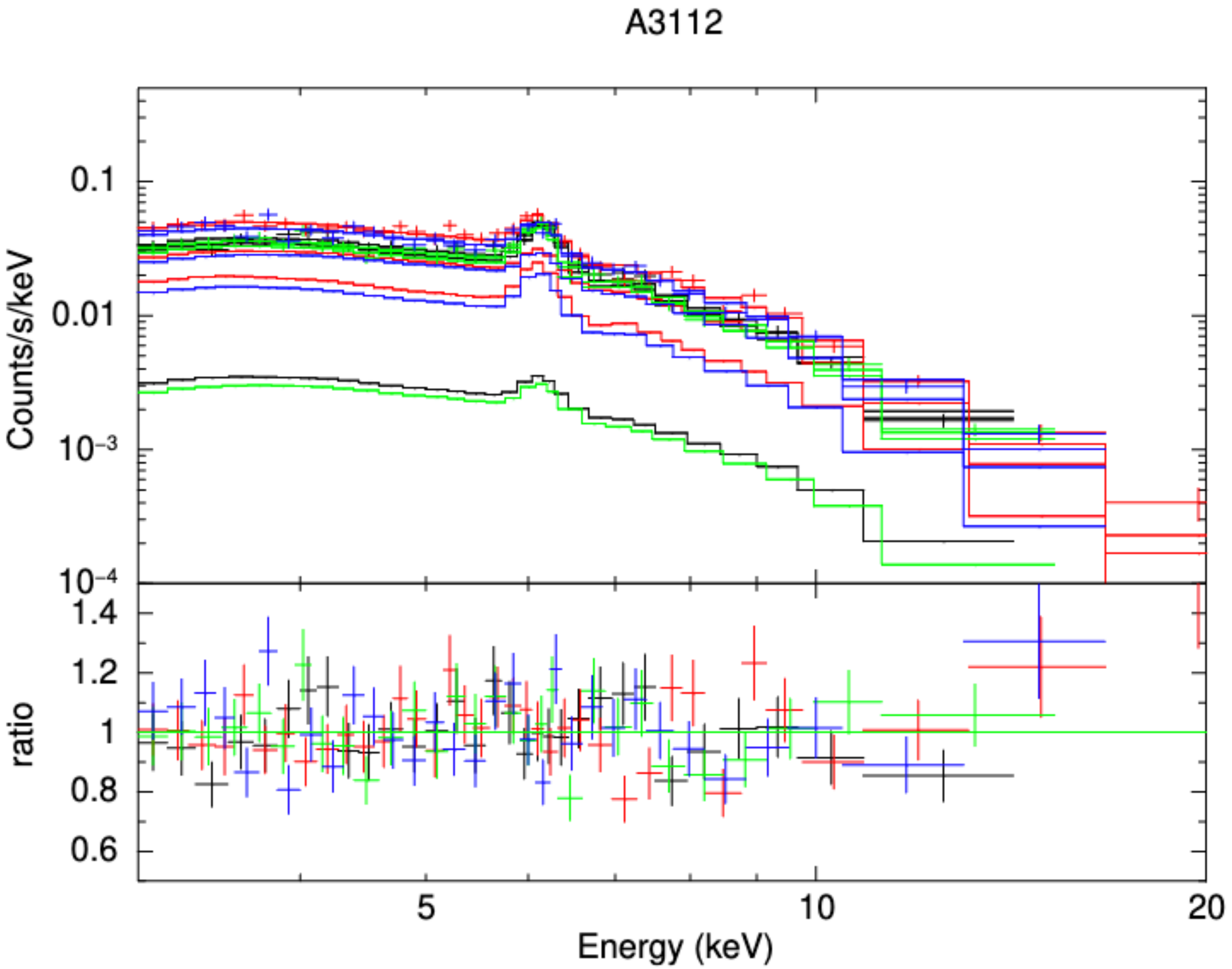

Snapshot Spectral Fits

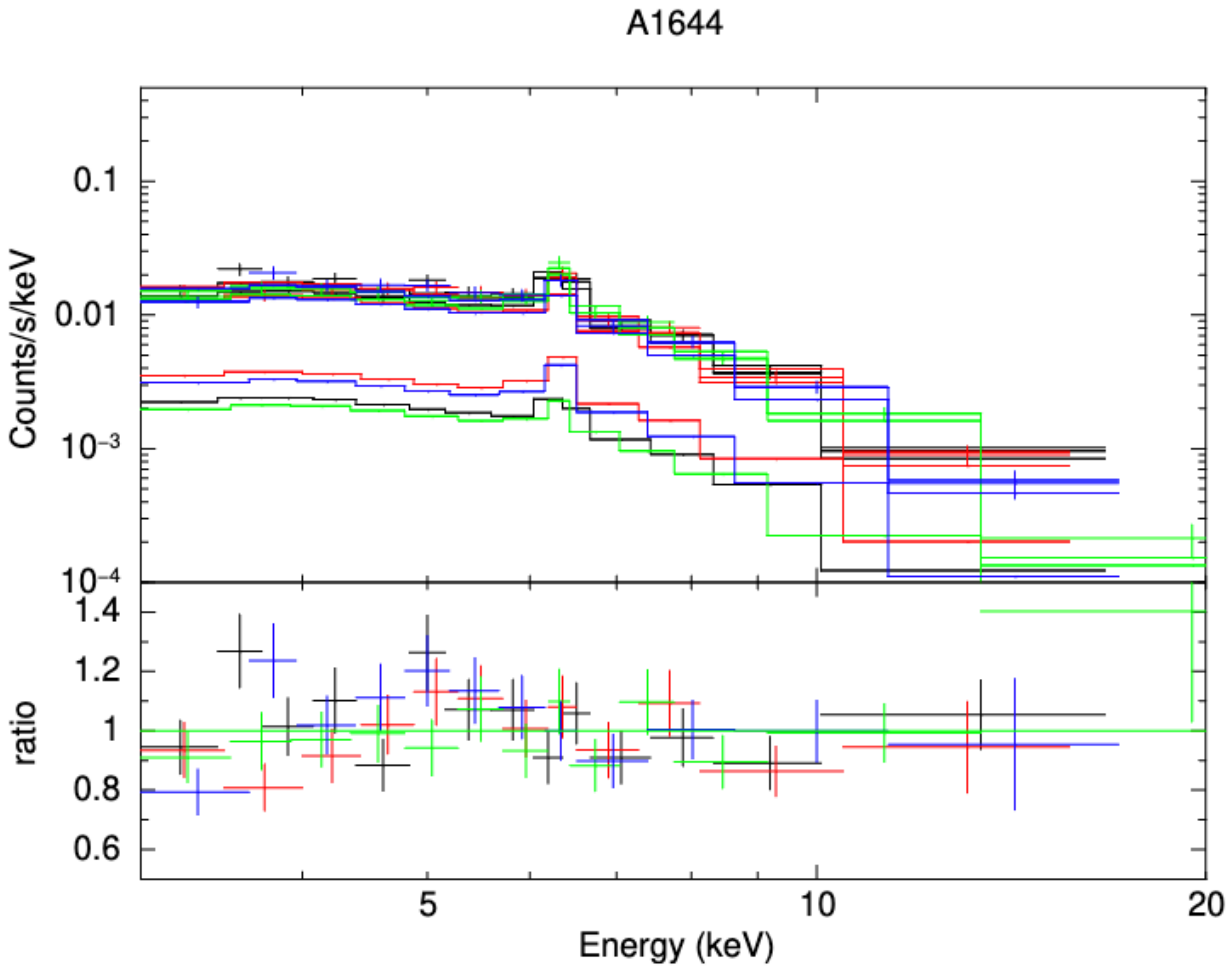

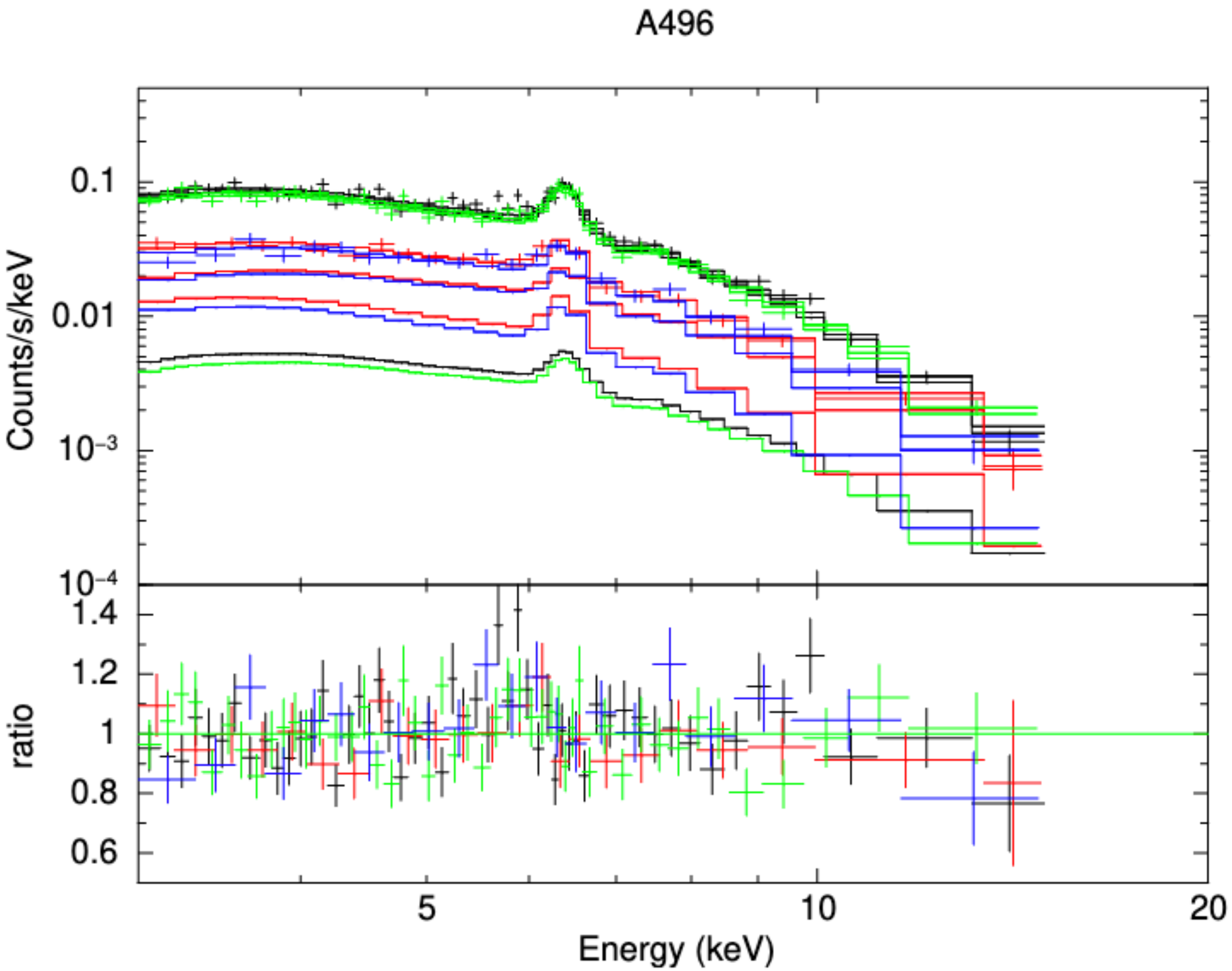

NuSTAR - XMM-Newton Comparison

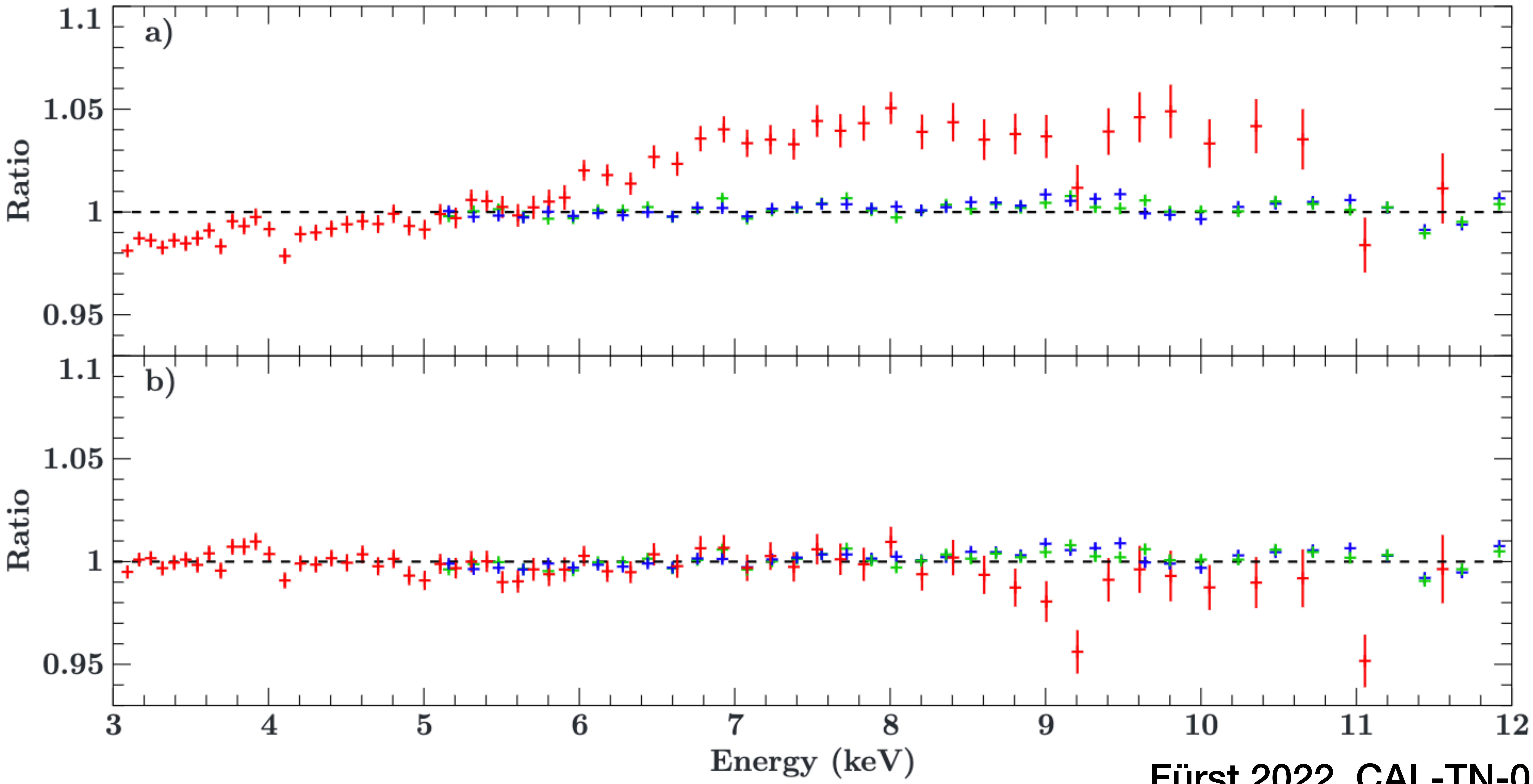

Fürst 2022, CAL-TN-0230-1-3

A478: XMM-Newton Fitting

Angr abund table, previous calibration

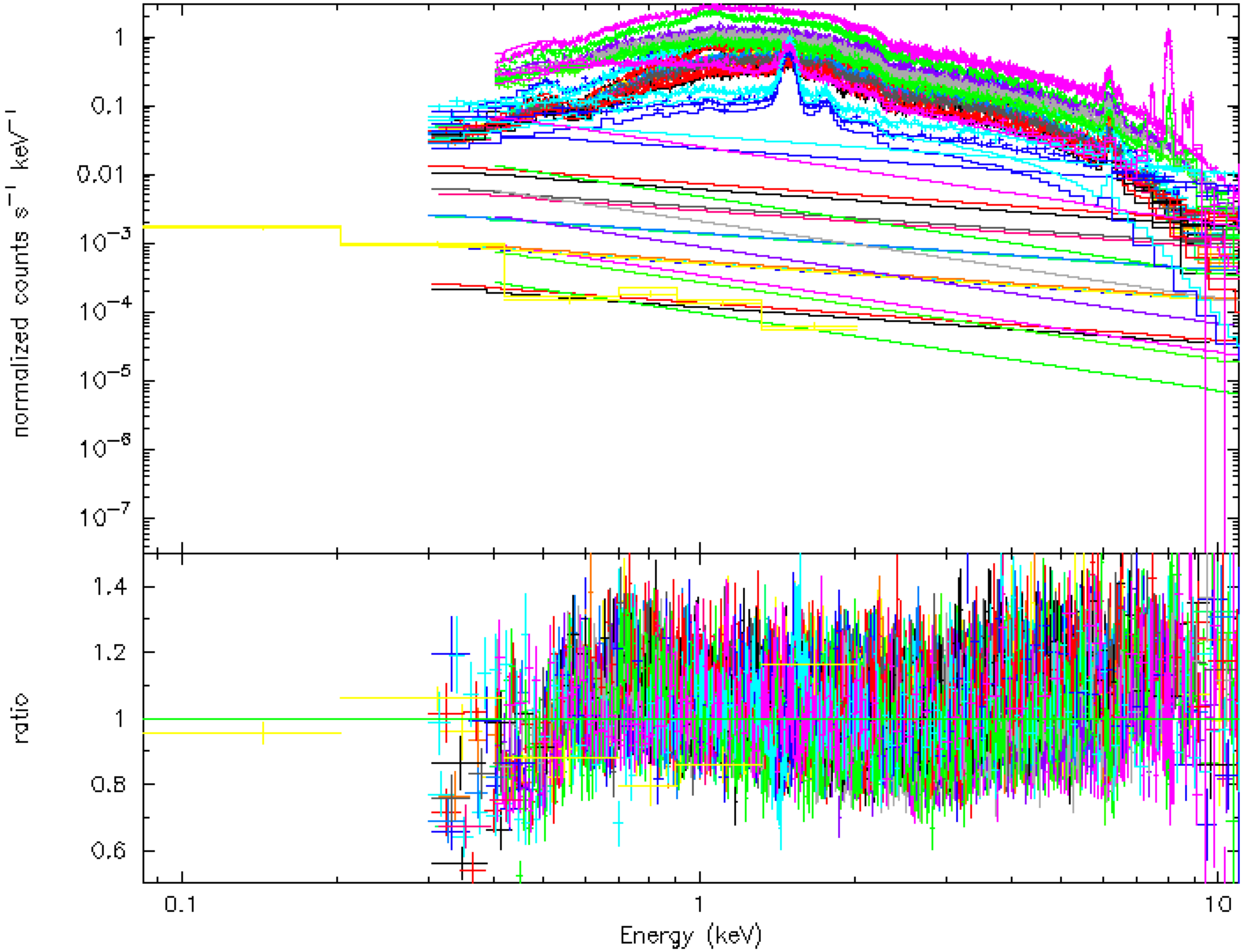

Wilm abund table (for abs modeling), with ARF corrections

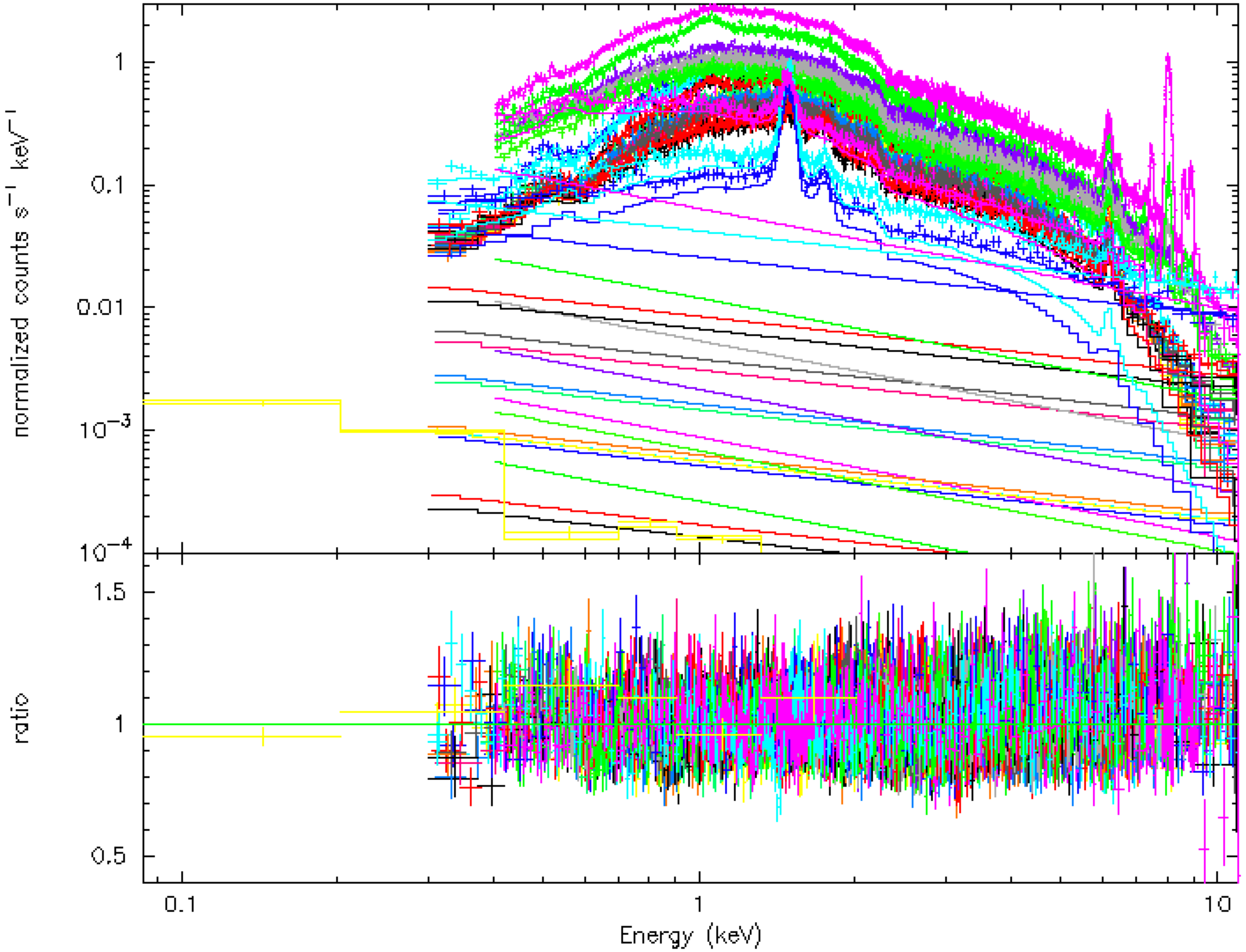

Scattered & Stray Light